

1 Dear Editor,  
2 thanks for these hints. In most cases it was possible to incorporate them.  
3 We changed the text regarding your suggestions on “on the other hand”.  
4 The units are always per kg. Only when we apply eq. (2), where we multiply a volume, we use  
5 volumetric concentrations. This also holds for table 1: These are the “wad\_sta” values of eq. (2).  
6 In the context of this manuscript TA is used as concentration. Nonetheless, it was possible to omit  
7 the term “TA concentration” in most cases. Only when the description appears technical (like for the  
8 description of the effect of river input on TA) we had to stay with “TA concentrations”.

9 Line 507 (old version):

10 Large parts of the produced organic matter are exported out of the validation area. This implies that  
11 uptake of nitrate would increase TA in this area. We changed this sentence: “Assuming large parts  
12 of organic matter exported out of the validation area this production compensates the  
13 missing TA generation by benthic denitrification. This amount of nitrate would not fully be  
14 available for primary production if parts of it would be consumed by denitrification.”

15 Line 528 (old version):

16 You are right, we changed this sentence: “Shallow oxidation of biogenic methane formed in  
17 deep or shallow tidal flat sediments (not modelled) (Höpner & Michaelis, 1994; Neira &  
18 Rackemann, 1996; Böttcher et al., 2007) has the potential both to lower or enhance the  
19 buffer capacity, thus counteracting or promoting the respective effect of carbonate  
20 dissolution.”

21 =====

22

23  
24 Dear Johannes Paetsch,

25  
26 We are pleased to inform you that the Associate Editor report for the  
27 following BG manuscript is now available:

28  
29 Title: The impact of intertidal areas on the carbonate system of the  
30 southern North Sea

31 Author(s): Fabian Schwichtenberg et al.

32 MS No.: bg-2020-24

33 MS Type: Research article

34 Iteration: Correction

35

36 The Associate Editor has decided that some corrections are necessary before  
37 the manuscript can be published. Please log in using your Copernicus Office  
38 user ID 133937 to find the Associate Editor report at:

39 [https://editor.copernicus.org/BG/ms\\_records/bg-2020-24](https://editor.copernicus.org/BG/ms_records/bg-2020-24)

40

41 We kindly ask you to upload the files required for the production process  
42 no later than 23 Jul 2020 at:

43 [https://editor.copernicus.org/BG/production\\_file\\_upload/bg-2020-24](https://editor.copernicus.org/BG/production_file_upload/bg-2020-24)

44

45 Please find all information on manuscript submission at:  
46 [https://www.biogeosciences.net/for\\_authors/submit\\_your\\_manuscript.html](https://www.biogeosciences.net/for_authors/submit_your_manuscript.html)  
47  
48 Please note that all Referee and editor reports, the author's response, as  
49 well as the different manuscript versions of the peer-review completion  
50 (post-discussion review of revised submission) will be published along with  
51 your final-revised paper in BG.  
52  
53 You are invited to monitor the processing of your manuscript via your MS  
54 overview at: [https://editor.copernicus.org/BG/my\\_manuscript\\_overview](https://editor.copernicus.org/BG/my_manuscript_overview)  
55  
56 In case any questions arise, please do not hesitate to contact me. Thank  
57 you very much for your cooperation.  
58  
59 Kind regards,  
60  
61 Natascha Töpfer  
62 Copernicus Publications  
63  
64  
65 Editorial Support  
66 [editorial@copernicus.org](mailto:editorial@copernicus.org)  
67

68

---

69 **Associate Editor Decision: Publish subject to technical corrections** (15 Jul 2020) by Jack Middelburg

70 Comments to the Author:

71 Dear Dr. Schwichtenberg and co-authors:

72

73 Thank you for submitting your second revision to Biogeosciences. I have read it, and although some  
74 alternative processes might be involved, I am happy to inform you that your paper is now accepted  
75 for publication.

76

77 While reading I identified the need for a few minor corrections:

78

79 All through, please only use “on the other hand” when it is following a ‘on the one hand’.

80

81 Please check your units again: sometimes you use micromole per liter sometimes per kg (e.g. see  
82 Table 1 vs. Table 2-4). Try to avoid use of TA concentrations if writing TA or TA level will do. See  
83 comment of one of the referees about TA equivalent vs. concentration (but this is discipline  
84 dependent).

85

86 Line 507: Logic. Nitrate uptake by phytoplankton only produces alkalinity if the organic matter is  
87 preserved. It was unclear from your text whether this is the case.

88

89 Line 528: specify aerobic oxidation here. Anaerobic oxidation may generate TA and thus enhance  
90 buffering.

91

92 With best regards

93

94 Jack Middelburg, Associate Editor

# The impact of intertidal areas on the carbonate system of the southern North Sea

Fabian Schwichtenberg<sup>1,6</sup>, Johannes Pätsch<sup>1,5</sup>, Michael Ernst Böttcher<sup>2,3,4</sup>, Helmuth Thomas<sup>5</sup>,  
Vera Winde<sup>2</sup>, Kay-Christian Emeis<sup>5</sup>

<sup>1</sup> Theoretical Oceanography, Universität Hamburg, Bundesstr. 53, D-20146 Hamburg, Germany

<sup>2</sup> Geochemistry & Isotope Biogeochemistry Group, Department of Marine Geology, Leibniz Institute of Baltic Sea Research (IOW), Seestr. 15, D-18119 Warnemünde, Germany

<sup>3</sup> Marine Geochemistry, University of Greifswald, Friedrich-Ludwig-Jahn Str. 17a, D-17489 Greifswald, Germany

<sup>4</sup> Department of Maritime Systems, Interdisciplinary Faculty, University of Rostock, Albert-Einstein-Str. 21, D-18059 Rostock, Germany

<sup>5</sup> Institute of Coastal Research, Helmholtz Zentrum Geesthacht (HZG), Max-Planck-Str. 1, D-21502 Geesthacht, Germany

<sup>6</sup> Present Address: German Federal Maritime and Hydrographic Agency, Bernhard-Nocht-Str. 78, D-20359 Hamburg, Germany

Correspondence to Johannes Pätsch ([johannes.paetsch@uni-hamburg.de](mailto:johannes.paetsch@uni-hamburg.de))

## Abstract

The coastal ocean is strongly affected by ocean acidification because of its shallow water depths, low volume, and the closeness to terrestrial dynamics. Earlier observations of dissolved inorganic carbon (DIC) and total alkalinity (TA) in the southern part of the North Sea, a Northwest-European shelf sea, revealed lower acidification effects than expected. It has been assumed that anaerobic degradation and subsequent TA release in the adjacent back-barrier tidal areas ('Wadden Sea') in summer time is responsible for this phenomenon. In this study the exchange rates of TA and DIC between the Wadden Sea tidal basins and the North Sea and the consequences for the carbonate system in the German Bight are estimated using a 3-D ecosystem model. The aim of this study is to differentiate the various sources contributing to observed high summer TA in the southern North Sea. Measured TA

30 and DIC in the Wadden Sea are considered as model boundary conditions. This procedure  
31 acknowledges the dynamic behaviour of the Wadden Sea as an area of effective production  
32 and decomposition of organic material. According to the modelling results, 39 Gmol TA yr<sup>-1</sup>  
33 were exported from the Wadden Sea into the North Sea, which is less than a previous  
34 estimate, but within a comparable range. The interannual variabilities of TA and DIC, mainly  
35 driven by hydrodynamic conditions, were examined for the years 2001 – 2009. Dynamics in  
36 the carbonate system is found to be related to specific weather conditions. The results  
37 suggest that the Wadden Sea is an important driver for the carbonate system in the  
38 southern North Sea. On average 41 % of TA inventory changes in the German Bight were  
39 caused by riverine input, 37 % by net transport from adjacent North Sea sectors, 16 % by  
40 Wadden Sea export, and 6 % are caused by internal net production of TA. The dominant role  
41 of river input for the TA inventory disappears when focussing on TA concentration changes  
42 due to the corresponding freshwater fluxes diluting the marine TA concentrations. The ratio  
43 of exported TA versus DIC reflects the dominant underlying biogeochemical processes in the  
44 Wadden Sea. Whereas, aerobic degradation of organic matter plays a key role in the North  
45 Frisian Wadden Sea during all seasons of the year, anaerobic degradation of organic matter  
46 dominated in the East Frisian Wadden Sea. Despite of the scarcity of high-resolution field  
47 data it is shown that anaerobic degradation in the Wadden Sea is one of the main  
48 contributors of elevated summer TA values in the southern North Sea.

49

## 50 **1. Introduction**

51 Shelf seas are highly productive areas constituting the interface between the inhabited  
52 coastal areas and the global ocean. Although they represent only 7.6 % of the world ocean's  
53 area, current estimates assume that they contribute approximately 21 % to total global  
54 ocean CO<sub>2</sub> sequestration (Borges, 2011). At the global scale the uncertainties of these  
55 estimates are significant due to the lack of spatially and temporally resolved field data. Some  
56 studies investigated regional carbon cycles in detail (e.g., Kempe & Pegler, 1991; Brasse et  
57 al., 1999; Reimer et al., 1999; Thomas et al., 2004; 2009; Artioli et al., 2012; Lorkowski et al.,  
58 2012; Burt et al., 2016; Shadwick et al., 2011; Laruelle et al., 2014; Carvalho et al., 2017) and  
59 pointed out sources of uncertainties specifically for coastal settings.

60 However, natural pH dynamics in coastal- and shelf- regions, for example, have been shown  
61 to be up to an order of magnitude higher than in the open ocean (Provoost et al, 2010).

62 Also, the nearshore effects of CO<sub>2</sub> uptake and acidification are difficult to determine,  
63 because of the shallow water depth and a possible superposition by benthic-pelagic  
64 coupling, and strong variations in fluxes of TA are associated with inflow of nutrients from  
65 rivers, pelagic nutrient driven production and respiration (Provoost et al., 2010), submarine  
66 groundwater discharge (SGD; Winde et al., 2014), and from benthic-pelagic pore water  
67 exchange (e.g., Billerbeck et al., 2006; Riedel et al., 2010; Moore et al., 2011; Winde et al.,  
68 2014; Santos et al., 2012; 2015; Brenner et al., 2016; Burt et al., 2014; 2016; Seibert et al.,  
69 2019). Finally, shifts within the carbonate system are driven by impacts from watershed  
70 processes and modulated by changes in ecosystem structure and metabolism (Duarte et al.,  
71 2013).

72 Berner et al. (1970) and Ben-Yakoov (1973) were among the first who investigated elevated  
73 TA and pH variations caused by microbial dissimilatory sulphate reduction in the anoxic pore  
74 water of sediments. At the Californian coast, the observed enhanced TA export from  
75 sediments was related to the burial of reduced sulphur compounds (pyrite) (Dollar et al.,  
76 1991; Smith & Hollibaugh, 1993; Chambers et al., 1994). Other studies conducted in the  
77 Satilla and Altamaha estuaries and the adjacent continental shelf found non-conservative  
78 mixing lines of TA versus salinity, which was attributed to anaerobic TA production in  
79 nearshore sediments (Wang & Cai, 2004; Cai et al., 2010). Iron dynamics and pyrite  
80 formation in the Baltic Sea were found to impact benthic TA generation from the sediments  
81 (Gustafsson et al., 2019; Łukawska-Matuszewska and Graca, 2017).

82 The focus of the present study is the southern part of the North Sea, located on the  
83 Northwest-European Shelf. This shallow part of the North Sea is connected with the tidal  
84 basins of the Wadden Sea via channels between barrier islands enabling an exchange of  
85 water, and dissolved and suspended material (Rullkötter, 2009; Lettmann et al., 2009;  
86 Kohlmeier and Ebenhöf, 2009). The Wadden Sea extends from Den Helder (The  
87 Netherlands) in the west to Esbjerg (Denmark) in the north and covers an area of about  
88 9500 km<sup>2</sup> (Ehlers, 1994). The entire system is characterised by semidiurnal tides with a tidal  
89 range between 1.5 m in the westernmost part and 4 m in the estuaries of the rivers Weser  
90 and Elbe (Streif, 1990). During low tide about 50 % of the area are falling dry (van Beusekom

91 et al., 2019). Large rivers discharge nutrients into the Wadden Sea, which in turn shows a  
92 high degree of eutrophication, aggravated by mineralisation of organic material imported  
93 into the Wadden Sea from the open North Sea (van Beusekom et al., 2012).

94 In comparison to the central and northern part of the North Sea, TA levels in the southern  
95 part are significantly elevated during summer (Salt et al., 2013; Thomas et al., 2009; Brenner  
96 et al., 2016; Burt et al., 2016). The observed high TA levels have been attributed to an impact  
97 from the adjacent tidal areas (Hoppema, 1990; Kempe & Pegler, 1991; Brasse et al., 1999;  
98 Reimer et al., 1999; Thomas et al., 2009; Winde et al., 2014), but this impact has not been  
99 rigorously quantified. Using several assumptions, Thomas et al. (2009) calculated an annual  
100 TA export from the Wadden Sea / Southern Bight of 73 Gmol TA yr<sup>-1</sup> to close the TA budget  
101 for the southern North Sea.

102 The aim of this study is to reproduce the elevated summer levels of TA in the southern North  
103 Sea with a 3D biogeochemical model that has TA as prognostic variable. With this tool at  
104 hand, we balance the budget TA in the relevant area on an annual basis. Quantifying the  
105 different budget terms, like river input, Wadden Sea export, internal pelagic and benthic  
106 production, degradation and respiration allows us to determine the most important  
107 contributors to TA variations. In this way we refine the budget terms by Thomas et al. (2009)  
108 and replace the original closing term by data. The new results are discussed on the  
109 background of the budget approach proposed by Thomas et al. (2009).

## 110 **2. Methods**

### 111 **2.1. Model specifications**

#### 112 ***2.1.1. Model domain and validation area***

113 The ECOHAM model domain for this study (Fig. 1) was first applied by Pätsch et al. (2010).  
114 For model validations (magenta: validation area, Fig. 1), an area was chosen that includes  
115 the German Bight as well as parts along the Danish and the Dutch coast. The western  
116 boundary of the validation area is situated at 4.5° E. The southern and northern boundaries  
117 are at 53.5° and 55.5° N, respectively. The validation area is divided by the magenta dashed  
118 line at 7° E into the western and eastern part. For the calculation of box averages of DIC and  
119 TA a bias towards the deeper areas with more volume and more data should be avoided.  
120 Therefore, each water column covered with data within the validation area delivered one

121 mean value, which is calculated by vertical averaging. These mean water column averages  
122 were horizontally interpolated onto the model grid. After this procedure average box values  
123 were calculated. In case of box-averaging model output, the same procedure was applied,  
124 but without horizontal interpolation.

### 125 ***2.1.2. The hydrodynamic module***

126 The physical parameters temperature, salinity, horizontal and vertical advection as well as  
127 turbulent mixing were calculated by the submodule HAMSOM (Backhaus, 1985), which was  
128 integrated in the ECOHAM model. It is a baroclinic primitive equation model using the  
129 hydrostatic and Boussinesq approximation. It is applied to several regional sea areas  
130 worldwide (Mayer et al., 2018; Su & Pohlmann, 2009). Details are described by Backhaus &  
131 Hainbucher (1987) and Pohlmann (1996). The hydrodynamic model ran prior to the  
132 biogeochemical part. Daily result fields were stored for driving the biogeochemical model in  
133 offline mode. Surface elevation, temperature and salinity resulting from the Northwest-  
134 European Shelf model application (Lorkowski et al., 2012) were used as boundary conditions  
135 at the southern and northern boundaries. The temperature of the shelf run by Lorkowski et  
136 al. (2012) showed a constant offset compared with observations (their Fig. 3), because  
137 incoming solar radiation was calculated too high. For the present simulations the shelf run  
138 has been repeated with adequate solar radiation forcing.

139 River-induced horizontal transport due to the hydraulic gradient is incorporated (Große et  
140 al., 2017; Kerimoglu et al., 2018). This component of the hydrodynamic horizontal transport  
141 corresponds to the amount of freshwater discharge.

142 Within this study we use the term flushing time. It is the average time when a basin is filled  
143 with laterally advected water. The flushing time depends on the specific basin: large basins  
144 have usually higher flushing times than smaller basins. High flushing times correspond with  
145 low water renewal times.

### 146 ***2.1.3. The biogeochemical module***

147 The relevant biogeochemical processes and their parameterisations have been detailed in  
148 Lorkowski et al. (2012). In former model setups TA was restored to prescribed values derived  
149 from observations (Thomas et al., 2009) with a relaxation time of two weeks (Kühn et al.,  
150 2010; Lorkowski et al., 2012). The changes in TA treatment for the study at hand is described



151 below. Results from the Northwest-European Shelf model application (Lorkowski et al.,  
152 2012) were used as boundary conditions for the recent biogeochemical simulations at the  
153 southern and northern boundaries (Fig. 1).

154 The main model extension was the introduction of a prognostic treatment of TA in order to  
155 study the impact of biogeochemical and physical driven changes of TA onto the carbonate  
156 system and especially on acidification (Pätsch et al., 2018). The physical part contains  
157 advective and mixing processes as well as dilution by riverine freshwater input. The pelagic  
158 biogeochemical part is driven by planktonic production and respiration, formation and  
159 dissolution of calcite, pelagic and benthic degradation and remineralisation, and also by  
160 atmospheric deposition of reduced and oxidised nitrogen. All these processes impact TA. In  
161 this model version benthic denitrification has no impact on pelagic TA. Other benthic  
162 anaerobic processes are not considered. Only the carbonate ions from benthic calcite  
163 dilution increase pelagic TA. Aerobic remineralisation releases ammonium and phosphate,  
164 which enter the pelagic system across the benthic-pelagic interface and alter the pelagic TA.  
165 The theoretical background to this has been outlined by Wolf-Gladrow et al. (2007).

166 The years 2001 to 2009 were simulated with 3 spin up years in 2000. Two different scenarios  
167 (A and B) were conducted. Scenario A is the reference scenario without implementation of  
168 any Wadden Sea processes. For scenario B we used the same model configuration as for  
169 scenario A and additionally implemented Wadden Sea export rates of TA and DIC as  
170 described in section 2.3.1. The respective Wadden Sea export rates (Fig. 2) are calculated by  
171 the temporal integration of the product of `wad_sta` and `wad_exc` over one month (see  
172 section 2.3.1, equation 2).

## 173 **2.2. External sources and boundary conditions**

### 174 **2.2.1. Freshwater discharge**

175 Daily data of freshwater fluxes from 16 rivers were used (Fig. 1). For the German Bight and  
176 the other continental rivers daily observations of runoff provided by Pätsch & Lenhart (2008)  
177 were incorporated. The discharges of the rivers Elbe, Weser and Ems were increased by  
178 21 %, 19 % and 30 % in order to take additional drainage into account that originated from  
179 the area downstream of the respective points of observation (Radach and Pätsch, 2007). The  
180 respective tracer loads were increased accordingly. The data of Neal (2002) were

181 implemented for the British rivers for all years with daily values for freshwater. The annual  
182 amounts of freshwater of the different rivers are shown in the appendix (Table A1). Riverine  
183 freshwater discharge was also considered for the calculation of the concentrations of all  
184 biogeochemical tracers in the model.

### 185 **2.2.2. River input**

#### 186 **Data sources**

187 River load data for the main continental rivers were taken from the report by Pätsch &  
188 Lenhart (2008) that was kept up to date continuously so that data for the years 2007 – 2009  
189 were also available ([https://wiki.cen.uni-hamburg.de/ifm/ECOHAM/DATA\\_RIVER](https://wiki.cen.uni-hamburg.de/ifm/ECOHAM/DATA_RIVER)). They  
190 calculated daily loads of nutrients and organic matter based on data provided by the  
191 different river authorities. Additionally, loads of the River Eider were calculated according to  
192 Johannsen et al. (2008).

193 Up to now, all ECOHAM applications used constant riverine DIC concentrations. TA was not  
194 used. For the study at hand we introduced time varying riverine TA and DIC values. New data  
195 of freshwater discharge were introduced, as well as TA and DIC loads for the British rivers  
196 (Neal, 2002). Monthly mean concentrations of nitrate, TA and DIC were added for the Dutch  
197 rivers ([www.waterbase.nl](http://www.waterbase.nl)) and for the German river Elbe (Amann et al., 2015). The Dutch  
198 river data were observed in the years 2007 – 2009. The river Elbe data were taken in the  
199 years 2009 – 2011. These concentration data were prescribed for all simulation years as  
200 mean annual cycle.

201 The data sources and positions of the river mouths of all 16 rivers are shown in Table A2 and  
202 in Fig. 1. The respective riverine concentrations of TA and DIC are given in Table A3.  
203 Schwichtenberg (2013) describes the river data in detail.

204 A few small flood gates (“Siel”) and rivers transport fresh water from the recharge areas into  
205 the intertidal areas (Streif, 1990). The recharge areas for these inlets differ considerably  
206 from each other, leading to different relative contributions for the fresh water input.  
207 Whereas the catchments of Schweiburger Siel (22.2 km<sup>2</sup>) and the Hooksier Binnentief are  
208 only of minor importance, the Vareler Siel, the Eckenwarder Siel, and the Maade Siel are of  
209 medium importance, and the highest contribution may originate from the Wangersiel, the  
210 Dangaster Siel, and the Jade-Wapeler Siel (Lipinski, 1999).

211

## 212 **Effective river input**

213 In order to analyse the net effect on concentrations in the sea due to river input, the  
214 effective river input ( $Riv_{eff}$  [Gmol yr<sup>-1</sup>]) is introduced:

215

$$Riv_{eff} = \frac{\Delta C|_{riv}}{\rho \cdot yr} \cdot V \cdot C \quad (1)$$

216

217 with  $\Delta C|_{riv}$  [ $\mu\text{mol kg}^{-1}$ ]: the concentration change in the river mouth cell due to river load  $riv$   
218 and the freshwater flux from the river.  $V$  [l] is the volume of the river mouth cell,  $\rho$  [ $\text{kg l}^{-1}$ ]  
219 density of water,  $yr$  is one year,  $C$  [ $10^{-15} \text{l}^{-1}$ ] is a constant.

220 Bulk alkalinity discharged by rivers is quite large but most of the rivers entering the North  
221 Sea (here the German Bight) have lower TA concentrations than the sea water. In case of  
222 identical concentrations, the effective river load  $Riv_{eff}$  is zero. The TA related molecules enter  
223 the sea, and in most cases, they are leaving it via transport. In case of tracing or budgeting  
224 both the real TA river discharge and the transport must be recognized. In order to  
225 understand TA concentration changes in the sea  $Riv_{eff}$  is appropriate.

226

### 227 **2.2.3. Meteorological forcing**

228 The meteorological forcing was provided by NCEP Reanalysis (Kalnay et al., 1996) and  
229 interpolated on the model grid field. It consisted of six-hourly fields of air temperature,  
230 relative humidity, cloud coverage, wind speed, atmospheric pressure, and wind stress for  
231 every year. 2-hourly and daily mean short wave radiation were calculated from astronomic  
232 insolation and cloudiness with an improved formula (Lorkowski et al., 2012).

## 233 **2.3. The Wadden Sea**

### 234 **2.3.1. Implementation of Wadden Sea dynamics**

235 For the present study the exchange of TA and DIC between North Sea and Wadden Sea was  
236 implemented into the model by defining sinks and sources of TA and DIC for some of the  
237 south-eastern cells of the North Sea grid (Fig. 1). The cells with adjacent Wadden Sea were

238 separated into three exchange areas: The East Frisian, the North Frisian Wadden Sea and the  
239 Jade Bay, marked by “E”, “N” and “J” (Fig. 1, right side).

240 Two parameters were determined in order to quantify the TA and DIC exchange between  
241 the Wadden Sea and the North Sea.

- 242 1. Concentration changes of pelagic TA and DIC in the Wadden Sea during one tide, and
- 243 2. Water mass exchange between the back-barrier islands and the open sea during one  
244 tide

245 Measured concentrations of TA and DIC (Winde, 2013; Winde et al., 2014) as well as  
246 modelled water mass exchange rates of the export areas by Grashorn (2015) served as bases  
247 for the calculated exchange. Details on flux calculations and measurements are described  
248 below. The daily Wadden Sea exchange of TA and DIC was calculated as:

$$wad\_flu = \frac{wad\_sta * wad\_exc}{vol} \quad (2)$$

249 Differences in measured concentrations in the Wadden Sea during rising and falling water  
250 levels, as described in section 2.3.2, were temporally interpolated and summarized as  
251  $wad\_sta$  [mmol m<sup>-3</sup>]. Modelled daily Wadden Sea exchange rates of water masses (tidal  
252 prisms during falling water level) were defined as  $wad\_exc$  [m<sup>3</sup> d<sup>-1</sup>], and the volume of the  
253 corresponding North Sea grid cell was  $vol$  [m<sup>3</sup>].  $wad\_flu$  [mmol m<sup>-3</sup> d<sup>-1</sup>] were the daily  
254 concentration changes of TA and DIC in the respective North Sea grid cells.

255 In fact, some amounts of the tidal prisms return without mixing with North Sea water, and  
256 calculations of Wadden Sea – North Sea exchange should therefore consider flushing times  
257 in the respective back-barrier areas. Since differences in measured concentrations between  
258 rising and falling water levels were used, this effect is already assumed to be represented in  
259 the data. This approach enabled the use of tidal prisms without consideration of any flushing  
260 times.

### 261 **2.3.2. Wadden Sea - measurements**

262 The flux calculations for the Wadden Sea – North Sea exchange were carried out in tidal  
263 basins of the East and North Frisian Wadden Sea (Spiekeroog Island, Sylt-Rømø) as well as in  
264 the Jade Bay. For the present study seawater samples representing tidal cycles during

265 different seasons (Winde, 2013). The mean concentrations of TA and DIC during rising and  
266 falling water levels and the respective differences ( $\Delta$ TA and  $\Delta$ DIC) are given in Table 1.  
267 Measurements in August 2002 were taken from Moore et al. (2011). The  $\Delta$ -values were used  
268 as *wad\_sta* and were linearly interpolated between the times of observations for the  
269 simulations. In this procedure, the linear progress of the  $\Delta$ -values does not represent the  
270 natural behaviour perfectly, especially if only few data are available. As a consequence,  
271 possible short events of high TA and DIC export rates that occurred in periods outside the  
272 observation periods may have been missed.

273 Due to the low number of concentration measurements a statistical analysis of uncertainties  
274 of  $\Delta$ TA and  $\Delta$ DIC was not possible. They were measured with a lag of 2 hours after low tide  
275 and high tide. This was done in order to obtain representative concentrations of rising and  
276 falling water levels. As a consequence, only 2 - 3 measurements for each location and season  
277 were considered for calculations of  $\Delta$ TA and  $\Delta$ DIC.

### 278 **2.3.3. Wadden Sea – modelling the exchange rates**

279 Grashorn (2015) performed the hydrodynamic computations of exchanged water masses  
280 (*wad\_exc*) with the model FVCOM (Chen et al., 2003) by adding up the cumulative seaward  
281 transport during falling water level (tidal prisms) between the back-barrier islands that were  
282 located near the respective ECOHAM cells with adjacent Wadden Sea area. These values are  
283 given in Table 2 for each ECOHAM cell in the respective export areas. The definition of the  
284 first cell N1 and the last cell E4 is in accordance to the clockwise order in Fig. 1 (right side).  
285 The mean daily runoff of all N-, J- and E-positions was  $8.1 \text{ km}^3 \text{ d}^{-1}$ ,  $0.8 \text{ km}^3 \text{ d}^{-1}$  and  $2.3 \text{ km}^3 \text{ d}^{-1}$   
286 respectively.

### 287 **2.3.4. Additional Sampling of DIC and TA**

288 DIC and TA for selected freshwater inlets sampled in October 2010 and May 2011 are  
289 presented in Table 3. Sampling and analyses took place as described by Winde et al. (2014)  
290 and are here reported for completeness and input for discussion only. The autumn data are  
291 deposited under doi:10.1594/PANGEA.841976. The samples for TA measurements were  
292 filled without headspace into pre-cleaned 12 ccm Exetainer<sup>®</sup>, filled with 0.1 ml saturated  
293  $\text{HgCl}_2$  solution. The samples for DIC analysis were completely filled into 250 ccm ground-  
294 glass-stoppered bottles, and then poisoned with 100  $\mu\text{l}$  of a saturated  $\text{HgCl}_2$  solution. The  
295 DIC concentrations were determined at IOW by coulometric titration according to Johnson

296 et al. (1993), using reference material provided by A. Dickson (University of California, San  
297 Diego; Dickson et al., 2003) for the calibration (batch 102). TA was measured by  
298 potentiometric titration using HCl using a Schott titri plus equipped with an IOLine electrode  
299 A157. Standard deviations for DIC and TA measurements were better than +/-2 and +/-  
300 10  $\mu\text{mol kg}^{-1}$ , respectively.

301

#### 302 **2.4. Statistical analysis**

303 A statistical overview of the simulation results in comparison to the observations (Salt et al.,  
304 2013) is given in Table 4 and 5. In the validation area (magenta box in Fig. 1) observations of  
305 10 different stations were available, each with four to six measurements at different depths  
306 (51 measured points). Measured TA and DIC of each point were compared with modelled TA  
307 and DIC in the respective grid cells, respectively. The standard deviations (Stdv), the root  
308 means square errors (RMSE), and correlation coefficients ( $r$ ) were calculated for each  
309 simulation. In addition to the year 2008, which we focus on in this study, observations were  
310 performed at the same positions in summer 2005 and 2001. These data are also statistically  
311 compared with the model results.

### 312 **3. Results**

#### 313 **3.1. Model validation - TA in summer 2008**

314 The results of scenarios A and B were compared with observations of TA in August 2008 (Salt  
315 et al., 2013) for surface water. The observations revealed high TA levels in the German Bight  
316 (east of  $7^\circ$  E and south of  $55^\circ$  N) and around the Danish coast (around  $56^\circ$  N) as shown in  
317 Fig. 3a. The observed concentrations in these areas ranged between 2350 and  
318 2387  $\mu\text{mol TA kg}^{-1}$ . These findings were in accordance with observed TA in August /  
319 September 2001 (Thomas et al., 2009). TA in other parts of the observation domain ranged  
320 between 2270  $\mu\text{mol TA kg}^{-1}$  near the British coast ( $53^\circ$  N –  $56^\circ$  N) and 2330  $\mu\text{mol TA kg}^{-1}$  near  
321 the Dutch coast and the Channel. In the validation box the overall average and the standard  
322 deviation of all observed TA concentrations (Stdv) was 2334 and 33  $\mu\text{mol TA kg}^{-1}$ ,  
323 respectively.

324 In scenario A the simulated surface TA showed a more homogeneous pattern than  
325 observations with maximum values of 2396  $\mu\text{mol TA kg}^{-1}$  at the western part of the Dutch

326 coast and even higher ( $2450 \mu\text{mol TA kg}^{-1}$ ) in the river mouth of the Wash estuary at the  
327 British coast. Minimum values of  $2235$  and  $2274 \mu\text{mol TA kg}^{-1}$  were simulated at the mouths  
328 of the rivers Elbe and Firth of Forth. The modelled TA ranged from  $2332$  to  $2351 \mu\text{mol TA kg}^{-1}$   
329 in the German Bight and in the Jade Bay. Strongest underestimations in relation to  
330 observations are located in a band close to the coast stretching from the East Frisian Islands  
331 to  $57^\circ \text{N}$  at the Danish coast (Fig. 4a). The deviation of simulation results of scenario A from  
332 observations in the validation box was represented by a RMSE of  $28 \mu\text{mol TA kg}^{-1}$ . The  
333 standard deviation was  $7 \mu\text{mol TA kg}^{-1}$  and the correlation amounted to  $r = 0.77$  (Table 4). In  
334 the years 2005 and 2001 similar statistical values are found, but the correlation coefficient  
335 was smaller.

336 The scenario B was based on a Wadden Sea export of TA and DIC as described above. The  
337 major difference in TA of this scenario compared to A occurred east of  $6.5^\circ \text{E}$ . Surface TA  
338 there peaked in the Jade Bay ( $2769 \mu\text{mol TA kg}^{-1}$ ) and were elevated off the North Frisian  
339 and Danish coasts from  $54.2^\circ$  to  $56^\circ \text{N}$  ( $> 2400 \mu\text{mol TA kg}^{-1}$ ). Strongest underestimations in  
340 relation to observations are noted off the Danish coast between  $56^\circ$  and  $57^\circ \text{N}$  (Fig. 4b). In  
341 the German Bight the model overestimated the observations slightly, while at the East  
342 Frisian Islands the model underestimates TA. When approaching the Dutch Frisian Islands  
343 the simulation overestimates TA compared to observations and strongest overestimations  
344 can be seen near the river mouth of River Rhine. Compared to scenario A the simulation of  
345 scenario B was closer to the observations in terms of RMSE ( $18 \mu\text{mol TA kg}^{-1}$ ) and the  
346 standard deviation ( $\text{Stdv} = 22 \mu\text{mol TA kg}^{-1}$ ). Also, the correlation ( $r = 0.86$ ) improved  
347 (Table 4). In the years 2001 and 2005 the observed mean values are slightly overestimated  
348 by the model. The statistical values for 2001 are better than for 2005, where scenario A  
349 better compares with the observations.

350

### 351 **3.2. Model validation - DIC concentrations in summer 2008**

352 Analogously to TA the simulation results were compared with surface observations of DIC in  
353 summer 2008 (Salt et al., 2013). They also revealed high values in the German Bight (east of  
354  $7^\circ \text{E}$  and south of  $55^\circ \text{N}$ ) and around the Danish coast (near  $56^\circ \text{N}$ ) which is shown in Fig. 5.  
355 The observed DIC concentrations in these areas ranged between  $2110$  and  $2173 \mu\text{mol DIC kg}^{-1}$   
356 <sup>1</sup>. Observed DIC concentrations in other parts of the model domain ranged between  $2030$

357 and 2070  $\mu\text{mol DIC kg}^{-1}$  in the north western part and 2080 - 2117  $\mu\text{mol DIC kg}^{-1}$  at the Dutch  
358 coast. In the validation box the overall average and the standard deviation of all observed  
359 DIC concentrations were 2108 and 25.09  $\mu\text{mol DIC kg}^{-1}$ , respectively.

360 The DIC concentrations in scenario A ranged between 1935 and 1977  $\mu\text{mol DIC kg}^{-1}$  at the  
361 North Frisian and Danish coast (54.5° N - 55.5° N) and 1965  $\mu\text{mol DIC kg}^{-1}$  in the Jade Bay.  
362 Maxima of up to 2164  $\mu\text{mol DIC kg}^{-1}$  were modelled at the western part of the Dutch coast  
363 north of the mouth of River Rhine (Fig. 5). The DIC concentrations in the German Bight  
364 showed a heterogeneous pattern in the model, and sometimes values decreased from west  
365 to east, which contrasts the observations (Fig. 5a). This may be the reason for the negative  
366 correlation coefficient  $r = -0.64$  between model and observations (Table 5). The significant  
367 deviation from observation of results from scenario A is also indicated by the RMSE of  
368 43  $\mu\text{mol DIC kg}^{-1}$ , and a standard deviation of 14  $\mu\text{mol DIC kg}^{-1}$ . In 2001 and 2005 the  
369 simulation results of this scenario A are better, which is expressed in positive correlation  
370 coefficients and small RMSE values.

371 In scenario B the surface DIC concentrations at the Wadden Sea coasts increased: The North  
372 Frisian coast shows concentrations of up to 2200  $\mu\text{mol DIC kg}^{-1}$  while the German Bight has  
373 values of 2100 – 2160  $\mu\text{mol DIC kg}^{-1}$ , and Jade Bay concentrations were higher than  
374 2250  $\mu\text{mol DIC kg}^{-1}$ . The other areas are comparable to scenario A. In scenario B the RMSE in  
375 the validation box decreased to 26  $\mu\text{mol DIC kg}^{-1}$  in comparison to scenario A. The standard  
376 deviation decreased to 9.1  $\mu\text{mol DIC kg}^{-1}$ , and the correlation improved to  $r = 0.55$  (Table 5).  
377 The average values are close to the observed ones for all years, even though in 2005 a large  
378 RMSE was found.

379 The comparison between observations and simulation results of scenario A (Fig. 4c) clearly  
380 show model underestimations in the south-eastern area and are strongest in the inner  
381 German Bight towards the North Frisian coast ( $> 120 \mu\text{mol DIC kg}^{-1}$ ). Scenario B also models  
382 values lower than observations in the south-eastern area (Fig. 4d), but the agreement  
383 between observation and model results is reasonable. Only off the Danish coast near 6.5° E,  
384 56° N the model underestimates DIC by 93  $\mu\text{mol DIC kg}^{-1}$ .



### 385 **3.3. Hydrodynamic conditions and flushing times**

386 The calculations of Wadden Sea TA export in Thomas et al. (2009) were based on several  
387 assumptions concerning riverine input of bulk TA and nitrate, atmospheric deposition of  
388 NO<sub>x</sub>, water column inventories of nitrate and the exchange between the Southern Bight and  
389 the adjacent North Sea (Lenhart et al., 1995). The latter was computed by considering that  
390 the water in the Southern Bight is flushed with water of the adjacent open North Sea at time  
391 scales of six weeks. For the study at hand, flushing times in the validation area in summer  
392 and winter are presented for the years 2001 to 2009 in Fig. 6. Additionally, monthly mean  
393 flow patterns of the model area are presented for June, July and August for the years 2003  
394 and 2008, respectively (Fig. 7). They were chosen to highlight the pattern in summer 2003  
395 with one of the highest flushing times (lowest water renewal times), and that in 2008  
396 corresponding to one of the lowest flushing times (highest water renewal times).

397 The flushing times were determined for the three areas 1 – validation area, 2 – western part  
398 of the validation area, 3 – eastern part of the validation area. They were calculated by  
399 dividing the total volume of the respective areas 1 – 3 by the total inflow into the areas  
400 m<sup>3</sup> (m<sup>3</sup> s<sup>-1</sup>)<sup>-1</sup>. Flushing times (rounded to integer values) were consistently higher in summer  
401 than in winter, meaning that highest inflow occurred in winter. Summer flushing times in the  
402 whole validation area ranged from 54 days in 2008 to 81 days in 2003 and 2006, whereas the  
403 winter values in the same area ranged from 32 days in 2008 to 51 days in 2003 and 2009.  
404 The flushing times in the western and eastern part of the validation area were smaller due to  
405 the smaller box sizes. Due to the position, flushing times in the western part were  
406 consistently shorter than in the eastern part. These differences ranged from 5 days in winter  
407 2002 to 14 days in summer 2006 and 2008. The interannual variabilities of all areas were  
408 higher in summer than in winter.

409 The North Sea is mainly characterised by an anti-clockwise circulation pattern (Otto et al.,  
410 1990; Pätsch et al., 2017). This can be observed for the summer months in 2008 (Fig. 7).  
411 More disturbed circulation patterns in the south-eastern part of the model domain occurred  
412 in June 2003: In the German Bight and in the adjacent western area two gyres with reversed  
413 rotating direction are dominant. In August 2003 the complete eastern part shows a  
414 clockwise rotation which is due to the effect of easterly winds as opposed to prevalent  
415 westerlies. In this context such a situation is called meteorological blocking situation.

### 416 **3.4. Seasonal and interannual variability of TA and DIC**

417 The period from 2001 to 2009 was simulated for the scenarios A and B. For both scenarios  
418 monthly mean surface TA was calculated in the validation area and are shown in Fig. 8a and  
419 8b. The highest TA in scenario A was  $2329 \mu\text{mol TA kg}^{-1}$  and occurred in July 2003. The  
420 lowest TA in each year was about 2313 to  $2318 \mu\text{mol TA kg}^{-1}$  and occurred in February and  
421 March. Scenario B showed generally higher values: Summer concentrations were in the  
422 range of 2348 to  $2362 \mu\text{mol TA kg}^{-1}$  and the values peaked in 2003. The lowest values  
423 occurred in the years 2004 – 2008. Also, winter values were higher in scenario B than in  
424 scenario A: They range from 2322 to  $2335 \mu\text{mol TA kg}^{-1}$ .

425

426 Corresponding to TA, monthly mean surface DIC in the validation area is shown in Fig. 8c and  
427 8d. In scenario A the concentrations increased from October to February and decreased  
428 from March to August (Fig. 8c). In scenario B the time interval with increasing concentrations  
429 was extended into March. Maximum values of 2152 to  $2172 \mu\text{mol DIC kg}^{-1}$  in scenario A  
430 occur in February and March of each model year, and minimum values of 2060 to  
431  $2080 \mu\text{mol DIC kg}^{-1}$  in August. Scenario B shows generally higher values: Highest values in  
432 February and March are 2161 to  $2191 \mu\text{mol DIC kg}^{-1}$ . Lowest values in August range from  
433 2095 to  $2112 \mu\text{mol DIC kg}^{-1}$ . The amplitude of the annual cycle is smaller in scenario B,  
434 because the Wadden Sea export shows highest values in summer (Fig. 2).

435 The pattern of monthly TA and DIC of the reference scenario A differ drastically in that TA  
436 does not show a strong seasonal variability, whereas DIC does vary significantly. In case of  
437 DIC this is due to the biological drawdown during summer. Contrariwise, the additional input  
438 (scenario B) from the Wadden Sea in summer creates a strong seasonality for TA and instead  
439 flattens the variations in DIC.

## 440 **4. Discussion**

441

442 Thomas et al. (2009) estimated the contribution of shallow intertidal and subtidal areas to  
443 the alkalinity budget of the SE North Sea. That estimate (by closure of mass fluxes) was  
444 about  $73 \text{ Gmol TA yr}^{-1}$  originating from the Wadden Sea fringing the southern and eastern  
445 coast. These calculations were based on observations from the CANOBA dataset in 2001 and

446 2002. The observed high TA levels in the south-eastern North Sea were also encountered in  
447 August 2008 (Salt et al., 2013) and these measurements were used for the main model  
448 validation in this study. Our simulations result in 39 Gmol TA yr<sup>-1</sup> as export from the Wadden  
449 Sea into the North Sea. Former modelling studies of the carbonate system of the North Sea  
450 (Artioli et al., 2012; Lorkowski et al., 2012) did not consider the Wadden Sea as a source of  
451 TA and DIC, and good to reasonable agreement to observations from the CANOBA dataset  
452 was only achieved in the open North Sea in 2001 / 2002 (Thomas et al., 2009). Subsequent  
453 simulations that included TA export from aerobic and anaerobic processes in the sediment  
454 improved the agreement between data and models (Pätsch et al., 2018). When focusing on  
455 the German Bight, however, the observed high TA levels in summer measurements east of  
456 7° E could not be simulated satisfactorily.

457 The present study confirms the Wadden Sea as an important TA source for the German Bight  
458 and quantifies the annual Wadden Sea TA export rate to 39 Gmol TA yr<sup>-1</sup>. Additionally, the  
459 contributions by most important rivers have been more precisely quantified and narrow  
460 down uncertainties in the budgets of TA and DIC in the German Bight. All steps that were  
461 required to calculate the budget including uncertainties are discussed in the following.

462

#### 463 ***4.1. Uncertainties of Wadden Sea – German Bight exchange rates of TA and DIC***

464 The Wadden Sea is an area of effective benthic decomposition of organic material (Böttcher  
465 et al., 2004; Billerbeck et al., 2006; Al-Rai et al., 2009; van Beusekom et al., 2012) originating  
466 both from land and from the North Sea (Thomas et al., 2009). In general, anaerobic  
467 decomposition of the organic matter generates TA and increases the CO<sub>2</sub> buffer capacity of  
468 seawater. On longer time scales TA can only be generated by processes that involve  
469 permanent loss of anaerobic remineralisation products (Hu and Cai, 2011). A second  
470 precondition is the nutrient availability to produce organic matter, which in turn serves as  
471 necessary component of anaerobic decomposition (Gustafsson et al., 2019). The Wadden  
472 Sea export rates of TA and DIC modelled in the present study are based on concentration  
473 measurements during tidal cycles in the years 2002 and 2009 to 2011 (Table 1), and on  
474 calculated tidal prisms of two day-periods that are considered to be representative of annual  
475 mean values. This approach introduces uncertainties with respect to the true amplitudes of

476 concentrations differences in the tidal cycle and in seasonality due to the fact that  
477 differences in concentrations during falling and rising water levels were linearly interpolated.  
478 These interpolated values are based on four to five measurements in the three export areas  
479 and were conducted in different years. Consequently, the approach does not reproduce the  
480 exact TA and DIC levels in the years 2001 to 2009, because only meteorological forcing, river  
481 loads and nitrogen deposition were specified for these particular years. The simulation of  
482 scenario B thus only approximates Wadden Sea export rates. More measurements  
483 distributed with higher resolution over the annual cycle would clearly improve our  
484 estimates. Nevertheless, the implementation of Wadden Sea export rates here results in  
485 improved reproduction of observed high TA levels in the German Bight in summer in  
486 comparison to the reference run A (Fig. 3).

487 We calculated the sensitivity of our modelled annual TA export rates on uncertainties of the  
488  $\Delta$ -values of Table 1. As the different areas North- and East Frisian Wadden Sea and Jade Bay  
489 has different exchange rates of water, for each region the uncertainty of  $1 \mu\text{mol kg}^{-1}$  in  $\Delta\text{TA}$   
490 at all times has been calculated. The East Frisian Wadden Sea export would differ by  
491  $0.84 \text{ Gmol TA yr}^{-1}$ , the Jade Bay export by  $0.09 \text{ Gmol TA yr}^{-1}$  and the North Frisian export by  
492  $3 \text{ Gmol TA yr}^{-1}$ .

493 Primary processes that contribute to the TA generation in the Wadden Sea are  
494 denitrification, sulphate reduction, or processes that are coupled to sulphate reduction and  
495 other processes (Thomas et al., 2009). In our model, the implemented benthic denitrification  
496 does not generate TA (Seitzinger & Giblin, 1996), because modelled benthic denitrification  
497 does not consume nitrate (Pätsch & Kühn, 2008). Benthic denitrification is coupled to  
498 nitrification in the upper layer of the sediment (Raaphorst et al., 1990), giving reason for  
499 neglecting TA generation by this process in the model. The modelled production of  $\text{N}_2$  by  
500 benthic denitrification falls in the range of  $20 - 25 \text{ Gmol N yr}^{-1}$  in the validation area, which  
501 would result in a TA production of about  $19 - 23 \text{ Gmol TA yr}^{-1}$  (Brenner et al., 2016). In the  
502 model nitrate uptake by phytoplankton produces about  $40 \text{ Gmol TA yr}^{-1}$ . Assuming large  
503 parts of organic matter exported out of the validation area this production compensates the  
504 missing TA generation by benthic denitrification. This amount of nitrate would not fully be  
505 available for primary production if parts of it would be consumed by denitrification. Different

506 from this, the TA budget of Thomas et al. (2009) included estimates for the entire benthic  
507 denitrification as a TA generating process.

508 Sulphate reduction (not modelled here) also contributes to alkalinity generation. On longer  
509 time scales the net effect is vanishing as the major part of the reduced components are  
510 immediately re-oxidised in contact with oxygen. Iron- and sulphate- reduction generates TA  
511 but only their reaction product iron sulphide (essentially pyrite) conserves the reduced  
512 components from re-oxidation. As the formation of pyrite consumes TA, the TA contribution  
513 of iron reduction in the North Sea is assumed to be small and to balance that of pyrite  
514 formation (Brenner et al., 2016).

515 Atmospheric nitrogen deposition is taken into account in the simulations. Oxidised N-species  
516 ( $\text{NO}_x$ ) dominate reduced species ( $\text{NH}_y$ ) slightly in the validation area during 6 out of 9  
517 simulation years. This implies that the deposition of dissolved inorganic nitrogen decreases  
518 TA in 6 of 9 years. The average decrease within 6 years is about  $0.4 \text{ Gmol TA yr}^{-1}$ , whereas  
519 the average increase within 3 years is only  $0.1 \text{ Gmol TA yr}^{-1}$ . Thomas et al. (2009) also  
520 assumed a dominance of oxidised species and consequently defined a negative contribution  
521 to the TA budget.

522 Dissolution of biogenic carbonates may be an efficient additional enhancement of the  $\text{CO}_2$   
523 buffer capacity (that is: source of TA), since most of the tidal flat surface sediments contain  
524 carbonate shell debris (Hild, 1997). Shallow oxidation of biogenic methane formed in deep or  
525 shallow tidal flat sediments (not modelled) (Höpner & Michaelis, 1994; Neira & Rackemann,  
526 1996; Böttcher et al., 2007) has the potential both to lower or enhance the buffer capacity,  
527 thus counteracting or promoting the respective effect of carbonate dissolution. The impact  
528 of methane oxidation on the developing TA / DIC ratio in surface sediments, however, is  
529 complex and controlled by a number of superimposing biogeochemical processes (e.g.,  
530 Akam et al., 2020).

531 The net effect of evaporation and precipitation in the Wadden Sea also has to be considered  
532 in budgeting TA. Although these processes are balanced in the North Sea (Schott, 1966),  
533 enhanced evaporation can occur in the Wadden Sea due to increased heating during low  
534 tide around noon. Onken & Riethmüller (2010) estimated an annual negative freshwater  
535 budget in the Hörnum Basin based on long-term hydrographic time series from observations

536 in a tidal channel. From this data a mean salinity difference between flood and ebb currents  
537 of approximately -0.02 is calculated. This would result in an increase of TA by  $1 \mu\text{mol TA kg}^{-1}$ ,  
538 which is within the range of the uncertainty of measurements. Furthermore, the enhanced  
539 evaporation estimated from subtle salinity changes interferes with potential input of  
540 submarine groundwater into the tidal basins, that been identified by Moore et al. (2011),  
541 Winde et al. (2014), and Santos et al. (2015). The magnitude of this input is difficult to  
542 estimate at present, for example from salinity differences between flood and ebb tides,  
543 because the composition of SGD passing the sediment-water interfacial mixing zone has to  
544 be known. Although first characteristics have been reported (Moore et al., 2011; Winde et  
545 al., 2014; Santos et al., 2015), the quantitative effect of additional DIC, TA, and nutrient input  
546 via both fresh and recirculated SGD into the Wadden Sea remains unclear.

547 An input of potential significance are small inlets that provide fresh water as well as DIC and  
548 TA (Table 3). The current data base for seasonal dynamics of this source, however, is limited  
549 and, therefore, this source cannot yet be considered quantitatively in budgeting approaches.

550

#### 551 **4.2 TA / DIC ratios over the course of the year**

552

553

554 Ratios of TA and DIC generated in the tidal basins (Table 1) give some indication of the  
555 dominant biogeochemical mineralisation and re-oxidation processes occurring in the  
556 sediments of individual Wadden Sea sectors, although these processes have not been  
557 explicitly modelled here (Chen & Wang, 1999; Zeebe & Wolf-Gladrow, 2001; Thomas et al.  
558 2009; Sippo et al., 2016; Wurgaft et al., 2019; Akam et al., 2020). Candidate processes are  
559 numerous and the export ratios certainly express various combinations, but the most  
560 quantitatively relevant likely are aerobic degradation of organic material (resulting in a  
561 reduction of TA due to nitrification of ammonia to nitrate with a TA / DIC ratio of -0.16),  
562 denitrification (TA / DIC ratio of 0.8, see Rassmann et al., 2020), and anaerobic processes  
563 related to sulphate reduction of organoclastic material (TA / DIC ratio of 1, see Sippo et al.,  
564 2016). Other processes are aerobic (adding only DIC) and anaerobic (TA / DIC ratio of 2)  
565 oxidation of upward diffusing methane, oxidation of sedimentary sulphides upon  
566 resuspension into an aerated water column (no effect on TA / DIC) followed by oxidation of

567 iron (consuming TA), and nitrification of ammonium (consuming TA, TA / DIC ratio is -2, see  
568 Pätsch et al., 2018 and Zhai et al. 2017).

569 The TA / DIC export ratios of DIC and TA for the individual tidal basins in three Wadden Sea  
570 sectors (East Frisian, Jade Bay and North Frisian) as calculated from observed  $\Delta$ TA and  $\Delta$ DIC  
571 over tidal cycles in different seasons are depicted in Fig. 9. They may give an indication of  
572 regionally and seasonally varying processes occurring in the sediments of the three study  
573 regions. The ratios vary between 0.2 and 0.5 in the North Frisian Wadden Sea with slightly  
574 more TA than DIC generated in spring, summer and autumn, and winter having a negative  
575 ratio of -0.5. The winter ratio coincides with very small measured differences of DIC in  
576 imported and exported waters ( $\Delta$ DIC = -2  $\mu\text{mol kg}^{-1}$ ) and the negative TA / DIC ratio may thus  
577 be spurious. The range of ratios in the other seasons is consistent with sulphate reduction  
578 and denitrification as the dominant processes in the North Frisian tidal basins.

579 The TA / DIC ratios in the Jade Bay samples were consistently higher than those in the North  
580 Frisian tidal basin and vary between 1 and 2 in spring and summer, suggesting a significant  
581 contribution by organoclastic sulphate reduction and anaerobic oxidation of methane  
582 (Al-Raei et al., 2009). The negative ratio of -0.4 in autumn is difficult to explain with  
583 remineralisation or re-oxidation processes, but as with the fall ratio in Frisian tidal basin, it  
584 coincides with a small change in  $\Delta$ DIC (-3  $\mu\text{mol kg}^{-1}$ ) at positive  $\Delta$ TA (8  $\mu\text{mol kg}^{-1}$ ). Taken at  
585 face value, the resulting negative ratio of -0.4 implicates a re-oxidation of pyrite, normally at  
586 timescales of early diagenesis thermodynamically stable (Hu and Cai, 2011), possibly  
587 promoted by increasing wind forces and associated aeration and sulphide oxidation of  
588 anoxic sediment layers (Kowalski et al., 2013). The DIC export rate from Jade Bay had its  
589 minimum in autumn, consistent with a limited supply and mineralisation of organic matter,  
590 possibly modified by seasonally changing impacts from small tidal inlets (Table 3).

591 The TA / DIC ratio of the East Frisian Wadden Sea is in the approximate range of those in  
592 Jade Bay, but has one unusually high ratio in November caused by a significant increase in TA  
593 of 14  $\mu\text{mol kg}^{-1}$  at a low increase of 5  $\mu\text{mol kg}^{-1}$  in DIC. Barring an analytical artefact, the  
594 maximum ratio of 3 may reflect a short-term effect of iron reduction.

595 Based on these results, processes in the North Frisian Wadden Sea export area differ from  
596 the East Frisian Wadden Sea and the Jade Bay areas. The DIC export rates suggest that  
597 significant amounts of organic matter were degraded in North Frisian tidal basins, possibly

598 controlled by higher daily exchanged water masses in the North Frisian ( $8.1 \text{ km}^3 \text{ d}^{-1}$ ) than in  
599 the East Frisian Wadden Sea ( $2.3 \text{ km}^3 \text{ d}^{-1}$ ) and in the Jade Bay ( $0.8 \text{ km}^3 \text{ d}^{-1}$ ) (compare  
600 Table 2). However, TA export rates of the North Frisian and the East Frisian Wadden Sea  
601 were in the same range.

602 Regional differences in organic matter mineralisation in the Wadden Sea have been  
603 discussed by van Beusekom et al. (2012) and Kowalski et al. (2013) in the context of  
604 connectivity with the open North Sea and influences of eutrophication and sedimentology.  
605 They suggested that the organic matter turnover in the entire Wadden Sea is governed by  
606 organic matter import from the North Sea, but that regionally different eutrophication  
607 effects as well as sediment compositions modulate this general pattern. The reason for  
608 regional differences may be related to the shape and size of the individual tidal basins. van  
609 Beusekom et al. (2012) found that wider tidal basins with a large distance between barrier  
610 islands and mainland, as is the case in the North Frisian Wadden Sea, generally have a lower  
611 eutrophication status than narrower basins predominating in the East Frisian Wadden Sea.  
612 Together with the high-water exchange rate the accumulation of organic matter is reduced  
613 in the North Frisian Wadden Sea and the oxygen demand per volume is lower than in the  
614 more narrow eutrophicated basins. Therefore, aerobic degradation of organic matter  
615 dominated in the North Frisian Wadden Sea, where the distance between barrier islands and  
616 mainland is large. This leads to less TA production (in relation to DIC production) than in the  
617 East Frisian Wadden Sea, where anaerobic degradation of organic matter dominated in more  
618 restricted tidal basins.

619

#### 620 ***4.3. TA budgets and variability of TA inventory in the German Bight***

621 Modelled TA and DIC in the German Bight have a high interannual and seasonal variability  
622 (Fig. 8). The interannual variability of the model results are mainly driven by the physical  
623 prescribed environment. Overall, the TA variability is more sensitive to Wadden Sea export  
624 rates than DIC variability, because the latter is dominated by biological processes. However,  
625 the inclusion of Wadden Sea DIC export rates improved correspondence with observed DIC  
626 concentrations in the near-coastal North Sea.



627 It is a logical step to attribute the TA variability to variabilities of the different sources. In  
628 order to calculate a realistic budget, scenario B was considered. Annual and seasonal  
629 budgets of TA sources and sinks in this scenario are shown in Table 6. Note that  $Riv_{eff}$  is not  
630 taken into account for the budget calculations. This is explained in the Method Section 2.2.2  
631 “River Input”.

632 Comparing the absolute values of all sources and sinks of the mean year results in a relative  
633 ranking of the processes. 41 % of all TA inventory changes in the validation area were due to  
634 river loads, 37 % were due to net transport, 16 % were due to Wadden Sea export rates, 6 %  
635 were due to internal processes. River input ranged from 78 to 152 Gmol TA yr<sup>-1</sup> and had the  
636 highest absolute variability of all TA sources in the validation area. This is mostly due to the  
637 high variability of annual freshwater discharge, which is indicated by low (negative) values of  
638  $Riv_{eff}$ . The latter values show that the riverine TA loads together with the freshwater flux  
639 induce a small dilution of TA in the validation area for each year. Certainly, this ranking  
640 depends mainly on the characteristics of the Elbe estuary. Due to high TA in rivers Rhine and  
641 Meuse (Netherlands) they had an effective river input of +24 Gmol TA yr<sup>-1</sup> in 2008, which  
642 constitutes a much greater impact on TA changes than the Elbe river. In a sensitivity test, we  
643 switched off the TA loads of rivers Rhine and Meuse for the year 2008 and found that the  
644 net flow of -71 Gmol TA yr<sup>-1</sup> decreased to -80 Gmol TA yr<sup>-1</sup>, which indicates that water  
645 entering the validation box from the western boundary is less TA-rich in the test case than in  
646 the reference run.

647 At seasonal time scales (Table 6 lower part) the net transport dominated the variations from  
648 October to March, while internal processes play a more important role from April to June  
649 (28 %). The impact of effective river input was less than 5 % in every quarter. The Wadden  
650 Sea TA export rates had an impact of 36 % on TA mass changes in the validation area from  
651 July to September. Note that these percentages are related to the sum of the absolute  
652 values of the budgeting terms.

653 Summing up the sources and sinks, Wadden Sea exchange rates, internal processes and  
654 effective river loads resulted in highest sums in 2002 and 2003 (51 and 52 Gmol TA yr<sup>-1</sup>) and  
655 lowest in 2009 (44 Gmol TA yr<sup>-1</sup>). For the consideration of TA variation we excluded net  
656 transport and actual river loads, because these fluxes are diluted and do not necessarily  
657 change the TA concentrations. In agreement with this, the highest TA was simulated in

658 summer 2003 (Fig. 8). The high interannual variability of summer concentrations was driven  
659 essentially by hydrodynamic differences between the years. Flushing times and their  
660 interannual variability were higher in summer than in winter (Fig. 6) of every year. High  
661 flushing times or less strong circulation do have an accumulating effect on exported TA in  
662 the validation area. To understand the reasons of the different flushing times monthly  
663 stream patterns were analysed (Fig. 7). Distinct anticlockwise stream patterns defined the  
664 hydrodynamic conditions in every winter. Summer stream patterns were in most years  
665 weaker, especially in the German Bight (compare Fig. 7, June 2003). In August 2003 the  
666 eastern part of the German Bight shows a clockwise rotation, which transports TA-enriched  
667 water from July back to the Wadden-Sea area for further enrichment. This could explain the  
668 highest concentrations in summer 2003.

669 Thomas et al. (2009) estimated that 73 Gmol TA yr<sup>-1</sup> were produced in the Wadden Sea.  
670 Their calculations were based on measurements in 2001 and 2002. The presented model  
671 was validated with data measured in August 2008 (Salt et al., 2013) at the same positions.  
672 High TA in the German Bight was observed in summer 2001 and in summer 2008. Due to the  
673 scarcity of data, the West Frisian Wadden Sea was not considered in the simulations, but, as  
674 the western area is much larger than the eastern area, the amount of exported TA from that  
675 area can be assumed to be in the same range as from the East Frisian Wadden Sea (10 to  
676 14 Gmol TA yr<sup>-1</sup>). With additional export from the West Frisian Wadden Sea, the maximum  
677 overall Wadden Sea export may be as high as 53 Gmol TA yr<sup>-1</sup>. Thus, the TA export from the  
678 Wadden Sea calculated in this study is 20 to 34 Gmol TA yr<sup>-1</sup> lower than that assumed in the  
679 study of Thomas et al. (2009). This is mainly due to the flushing time that was assumed by  
680 Thomas et al. (2009). They considered the water masses to be flushed within six weeks  
681 (Lenhart et al., 1995). Flushing times calculated in the present study were significantly longer  
682 and more variable in summer. Since the Wadden Sea export calculated by Thomas et al.  
683 (2009) was defined as a closing term for the TA budget, underestimated summerly flushing  
684 times led to an overestimation of the exchange with the adjacent North Sea.

685 Table 4 shows that our scenario B underestimates observed TA by about 5.1 µmol kg<sup>-1</sup> in  
686 2008. Scenario A has lower TA than scenario B in the validation area. The difference is about  
687 11 µmol kg<sup>-1</sup>. This means that the Wadden Sea export of 39 Gmol TA yr<sup>-1</sup> results in a  
688 concentration difference of 11 µmol kg<sup>-1</sup>. Assuming linearity, the deviation between

689 scenario B and the observations ( $5.1 \mu\text{mol kg}^{-1}$ ) would be compensated by an additional  
690 Wadden Sea export of about  $18 \text{ Gmol TA yr}^{-1}$ . If we assume that the deviation between  
691 observation and scenario B is entirely due to uncertainties or errors in the Wadden Sea  
692 export estimate, then the uncertainty of this export is  $18 \text{ Gmol TA yr}^{-1}$ .

693 Another problematic aspect in the TA export estimate by Thomas et al. (2009) is the fact that  
694 their TA budget merges the sources of anaerobic TA generation from sediment and from the  
695 Wadden Sea into a single source “anaerobic processes in the Wadden Sea”. Burt et al. (2014)  
696 found a sediment TA generation of  $12 \text{ mmol TA m}^{-2} \text{ d}^{-1}$  at one station in the German Bight  
697 based on Ra-measurements. This fits into the range of microbial gross sulphate reduction  
698 rates reported by Al-Raei et al. (2009) in the back-barrier tidal areas of Spiekeroog island,  
699 and by Brenner et al. (2016) at the Dutch coast. Within the latter paper, the different  
700 sources of TA from the sediment were quantified. The largest term was benthic calcite  
701 dissolution, which would be cancelled out in terms of TA generation assuming a steady-state  
702 compensation by biogenic calcite production. Extrapolating the southern North Sea TA  
703 generation (without calcite dissolution) from the data for one station of Brenner et al. (2016)  
704 results in an annual TA production of  $12.2 \text{ Gmol}$  in the German Bight (Area =  $28.415 \text{ km}^2$ ).  
705 This is likely an upper limit of sediment TA generation, as the measurements were done in  
706 summer when seasonal fluxes are maximal. This calculation reduces the annual Wadden Sea  
707 TA generation estimated by Thomas et al. (2009) from  $73$  to  $61 \text{ Gmol}$ , which is still higher  
708 than our present estimate. In spite of the unidentified additional TA-fluxes, both the  
709 estimate by Thomas et al. (2009) and our present model-based quantification confirm the  
710 importance of the Wadden-Sea export fluxes of TA on the North Sea carbonate system at  
711 present and in the future.

#### 712 ***4.4 The impact of exported TA and DIC on the North Sea and influences on export*** 713 ***magnitude***

714 Observed high TA and DIC in the SE North Sea are mainly caused by TA and DIC export from  
715 the Wadden Sea (Fig. 3-5). TA could be better reproduced than DIC in the model  
716 experiments, which was mainly due to the higher sensitivity of DIC to modelled biology.  
717 Nevertheless, from a present point of view the Wadden Sea is the main driver of TA in the  
718 German Bight. Future forecast studies of the evolution of the carbonate system in the  
719 German Bight will have to specifically focus on the Wadden Sea and on processes occurring

720 there. In this context the Wadden Sea evolution during future sea level rise is the most  
721 important factor. The balance between sediment supply from the North Sea and sea level  
722 rise is a general precondition for the persistence of the Wadden Sea (Flemming and Davis,  
723 1994; van Koningsveld et al., 2008). An accelerating sea level rise could lead to a deficient  
724 sediment supply from the North Sea and shift the balance at first in the largest tidal basins  
725 and at last in the smallest basins. (CPSL, 2001; van Goor et al., 2003). The share of intertidal  
726 flats as potential sedimentation areas is larger in smaller tidal basins (van Beusekom et al.,  
727 2012), whereas larger basins have a larger share of subtidal areas. Thus, assuming an  
728 accelerating sea level rise, large tidal basins will turn into lagoons, while tidal flats may still  
729 exist in smaller tidal basins. This effect could decrease the overall Wadden Sea export rates  
730 of TA, because sediments would no longer be exposed to the atmosphere and the products  
731 of sulphate reduction would re-oxidise in the water column. Moreover, benthic-pelagic  
732 exchange in the former intertidal flats would be more diffusive and less advective than today  
733 due to a lowering of the hydraulic gradients during ebb tides, when parts of the sediment  
734 become unsaturated with water. This would decrease TA export into the North Sea. Caused  
735 by changes in hydrography and sea level the sedimentological composition may also change.  
736 If sediments become more sandy, aerobic degradation of organic matter is likely to become  
737 more important (de Beer et al., 2005). In fine grained silt diffusive transport plays a key role,  
738 while in the upper layer of coarse (sandy) sediments advection is the dominant process.  
739 Regionally, the North Frisian Wadden Sea will be more affected by rising sea level because  
740 there the tidal basins are larger than the tidal basins in the East Frisian Wadden Sea and  
741 even larger than the inner Jade Bay.

742 The Wadden Sea export of TA and DIC is driven by the turnover of organic material.  
743 Decreasing anthropogenic eutrophication can lead to decreasing phytoplankton biomass and  
744 production (Cadée & Hegeman, 2002; van Beusekom et al., 2009). Thus, the natural  
745 variability of the North Sea primary production becomes more important in determining the  
746 organic matter turnover in the Wadden Sea (McQuatters-Gollop et al., 2007; McQuatters-  
747 Gollop & Vermaat, 2011). pH values in Dutch coastal waters decreased from 1990 to 2006  
748 drastically. Changes in nutrient variability were identified as possible drivers (Provoost et al.,  
749 2010), which is consistent with model simulations by Borges and Gypens (2010). Moreover,  
750 despite the assumption of decreasing overall TA export rates from the Wadden Sea the  
751 impact of the North Frisian Wadden Sea on the carbonate system of the German Bight could

752 potentially adjust to a change of tidal prisms and thus a modulation in imported organic  
753 matter. If less organic matter is remineralised in the North Frisian Wadden Sea, less TA and  
754 DIC will be exported into the North Sea.

755 In the context of climate change, processes that have impact on the freshwater budget of  
756 tidal mud flats will gain in importance. Future climate change will have an impact in coastal  
757 hydrology due to changes in ground water formation rates (Faneca Sánchez et al., 2012;  
758 Sulzbacher et al., 2012), that may change both surface and subterranean run-off into the  
759 North Sea. An increasing discharge of small rivers and groundwater into the Wadden Sea is  
760 likely to increase DIC, TA, and possibly nutrient loads and may enhance the production of  
761 organic matter. Evaporation could also increase due to increased warming and become a  
762 more important process than today (Onken & Riethmüller, 2010), as will methane cycling  
763 change due to nutrient changes, sea level and temperature rise (e.g., Höpner and Michaelis,  
764 1994; Akam et al., 2020).

765 Concluding, in the course of climate change the North Frisian Wadden Sea will be affected  
766 first by sea level rise, which will result in decreased TA and DIC export rates due to less  
767 turnover of organic matter there. This could lead to a decreased buffering capacity in the  
768 German Bight for atmospheric CO<sub>2</sub>. Overall, less organic matter will be remineralised in the  
769 Wadden Sea.

770

771

## 772 **5 Conclusion and Outlook**

773

774 We present a budget calculation of TA sources in the German Bight and relate 16 % of the  
775 annual TA inventory changes to TA exports from the Wadden Sea. The impact of riverine  
776 bulk TA seems to be less important due to the comparatively low TA levels in the Elbe  
777 estuary, a finding that has to be proven by future research.

778 The evolution of the carbonate system in the German Bight under future changes depends  
779 on the development of the Wadden Sea. The amount of TA and DIC that is exported from  
780 the Wadden Sea depends on the amount of organic matter and / or nutrient that are  
781 imported from the North Sea and finally remineralised in the Wadden Sea. Decreasing

782 riverine nutrient loads led to decreasing phytoplankton biomass and production (Cadée &  
783 Hegeman, 2002; van Beusekom et al., 2009), a trend that is expected to continue in the  
784 future (European Water Framework Directive). However, altered natural dynamics of  
785 nutrient cycling and productivity can override the decreasing riverine nutrient loads (van  
786 Beusekom et al., 2012), but these will not generate TA in the magnitude of denitrification of  
787 river-borne nitrate.

788 Sea level rise in the North Frisian Wadden Sea will potentially be more affected by a loss of  
789 intertidal areas than the East Frisian Wadden Sea (van Beusekom et al., 2012). This effect will  
790 likely reduce the turnover of organic material in this region of the Wadden Sea, which may  
791 decrease TA production and transfer into the southern North Sea.

792 Thomas et al. (2009) estimated that the Wadden Sea facilitates approximately 7 – 10% of the  
793 annual CO<sub>2</sub> uptake of the North Sea. This is motivation for model studies on the future role  
794 of the Wadden Sea in the CO<sub>2</sub> balance of the North Sea under regional climate change.

795 Future research will also have to address the composition and amount of submarine ground  
796 water discharge, as well as the magnitude and seasonal dynamics in discharge and  
797 composition of small water inlets at the coast, which are in this study only implicitly included  
798 and in other studies mostly ignored due to a lacking data base.

#### 799 **Data availability**

800 The river data are available at [https://wiki.cen.uni-hamburg.de/ifm/ECOHAM/DATA\\_RIVER](https://wiki.cen.uni-hamburg.de/ifm/ECOHAM/DATA_RIVER)  
801 and [www.waterbase.nl](http://www.waterbase.nl). Meteorological data are stored at <https://psl.noaa.gov/>. The North  
802 Sea TA and DIC data are stored at <https://doi.org/10.1594/PANGAEA.438791> (2001),  
803 <https://doi.org/10.1594/PANGAEA.441686> (2005). The data of the North Sea cruise 2008  
804 have not been published, yet, but can be requested via the CODIS data portal  
805 (<http://www.nioz.nl/portals-en>; registration required). Additional Wadden Sea TA and DIC  
806 data are deposited under [doi:10.1594/PANGAEA.841976](https://doi.org/10.1594/PANGAEA.841976).

807

#### 808 **Author contributions**

809 The scientific concept for this study was originally developed by JP and MEB. FS wrote the  
810 basic manuscript as part of his PhD thesis. VW provided field analytical data, as part of her  
811 PhD thesis. JP developed the original text further with contributions from all co-authors.

#### 812 **Competing interests**

813 The authors declare that they have no conflict of interest.

814

#### 815 **Acknowledgements**

816 The authors appreciate the two constructive reviews, which greatly helped to improve the  
817 manuscript, and the editorial handling by Jack Middelburg. I. Lorkowski, W. Kühn, and F.  
818 Große are acknowledged for stimulating discussions, S. Grashorn for providing tidal prisms  
819 and P. Escher for laboratory support. This work was financially supported by BMBF during  
820 the Joint Research Project BIOACID (TP 5.1, 03F0608L and TP 3.4.1, 03F0608F), with further  
821 support from Leibniz Institute for Baltic Sea Research. We also acknowledge the support by  
822 the Cluster of Excellence 'CliSAP' (EXC177), University of Hamburg, funded by the German  
823 Science Foundation (DFG) and the support by the German Academic Exchange service  
824 (DAAD, MOPGA-GRI, #57429828) with funds of the German Federal Ministry of Education  
825 and Research (BMBF). We used NCEP Reanalysis data provided by the NOAA/OAR/ESRL  
826 PSL, Boulder, Colorado, USA, from their Web site at <https://psl.noaa.gov/>.

827

828

829

830 **Tables**

831 **Table 1: Mean TA and DIC concentrations [ $\mu\text{mol l}^{-1}$ ] during rising and falling water levels**  
832 **and the respective differences ( $\Delta$ -values) that were used as wad\_sta in (1). Areas are the**  
833 **North Frisian (N), the East Frisian (E) Wadden Sea and the Jade Bay (J).**

Area	Date	TA (rising)	TA (falling)	$\Delta$ TA	DIC (rising)	DIC (falling)	$\Delta$ DIC
N	29.04.2009	2343	2355	12	2082*	2106	24
	17.06.2009	2328	2332	4	2170	2190	20
	26.08.2009	2238	2252	14	2077	2105	28
	05.11.2009	2335	2333	-2	2205	2209	4
J	20.01.2010	2429	2443	14	2380	2392	12
	21.04.2010	2415	2448	33	2099	2132	33
	26.07.2010	2424	2485	61	2159	2187	28
	09.11.2010	2402	2399	-3	2302	2310	8
E	03.03.2010	2379	2393	14	2313	2328	15
	07.04.2010	2346	2342	-4	2068	2082	14
	17./18.05.2011	2445	2451	6	2209	2221	12
	20.08.2002	2377	2414	37	2010	2030	20
	01.11.2010	2423	2439	16	2293	2298	5

834 \*: This value was estimated.

835

836 **Table 2: Daily Wadden Sea runoff to the North Sea at different export areas.**

Position	wad_exc [ $10^6 \text{ m}^3 \text{ d}^{-1}$ ]
N1	273
N2	1225
N3	1416
N4	1128
N5	4038
N6	18
J1 - J3	251
E1	380
E2	634
E3	437
E4	857

837

838



839

840 **Table 3: Examples for the carbonate system composition of small fresh water inlets**  
 841 **draining into the Jade Bay and the backbarrier tidal area of Spiekeroog Island, given in**  
 842 **( $\mu\text{mol kg}^{-1}$ ). Autumn results (A) (October 31<sup>st</sup>, 2010) are taken from Winde et al. (2014);**  
 843 **spring sampling (S) took place on May 20<sup>th</sup>, 2011.**

Site	Position	DIC(A)	TA(A)	DIC(S)	TA(S)
Neuharlingersiel	53°41.944 N 7°42.170 E	2319	1773	1915	1878
Harlesiel	53°42.376 N 7°48.538 E	3651	3183	1939	1983
Wanger- /Horumersiel	53°41.015 N 8°1.170 E	5405	4880	6270	6602
Hooksiel	53°38.421 N 8°4.805 E	2875	3105	3035	3302
Maade	53°33.534 N 8°7.082 E	5047	4448	5960	6228
Mariensiel	53°30.895 N 8°2.873 E	6455	5904	3665	3536
Dangaster Siel	53°26.737N 8°6.577 E	1868	1246	1647	1498
Wappellersiel	53°23.414 N 8°12.437 E	1373	630	1358	1152
Schweiburger Siel	53°24.725 N 8°16.968 E	4397	3579	4656	4493
Eckenwarder Siel	53°31.249 N 8°16.527 E	6542	6050	2119	4005

844

845

846

847

848

849 **Table 4: Averages ( $\mu\text{mol kg}^{-1}$ ), standard deviations ( $\mu\text{mol kg}^{-1}$ ), RMSE ( $\mu\text{mol kg}^{-1}$ ), and**  
850 **correlation coefficients  $r$  for the observed TA concentrations and the corresponding**  
851 **scenarios A and B within the validation area.**

TA	Average	Stdv	RMSE	$r$
Obs 2008	2333.52	32.51		
Obs 2005	2332.09	21.69		
Obs 2001	2333.83	33.19		
Sim A 2008	2327.64	6.84	27.97	0.77
Sim A 2005	2322.16	5.21	22.05	0.45
Sim A 2001	2329.79	5.32	31.89	0.24
Sim B 2008	2338.60	22.09	18.34	0.86
Sim B 2005	2339.48	26.81	31.81	0.18
Sim B 2001	2342.96	17.28	30.07	0.47

852

853

854

855

856

857

858

859

860

861

862

863

864

865 **Table 5: Averages ( $\mu\text{mol kg}^{-1}$ ), standard deviations ( $\mu\text{mol kg}^{-1}$ ), RMSE ( $\mu\text{mol kg}^{-1}$ ), and**  
866 **correlation coefficients  $r$  for the observed DIC concentrations and the corresponding**  
867 **scenarios A and B within the validation area.**

868

DIC	Average	Stdv	RMSE	$r$
Obs 2008	2107.05	24.23		
Obs 2005	2098.20	33.42		
Obs 2001	2105.49	25.21		
Sim A 2008	2080.93	14.24	43.48	-0.64
Sim A 2005	2083.53	21.94	26.97	0.73
Sim A 2001	2077.53	17.61	38.89	0.22
Sim B 2008	2091.15	9.25	25.87	0.55
Sim B 2005	2101.26	10.97	33.96	0.10
Sim B 2001	2092.69	11.71	25.33	0.48

869

870

871

872

873

874

875

876

877

878

879 **Table 6: Annual TA budgets in the validation area of the years 2001 to 2009, annual**  
880 **averages and seasonal budgets of January to March, April to June, July to September and**  
881 **October to December [Gmol]. Net Flow is the annual net TA transport across the**  
882 **boundaries of the validation area. Negative values indicate a net export from the**  
883 **validation area to the adjacent North Sea.  $\Delta$ content indicates the difference of the TA**  
884 **contents between the last and the first time steps of the simulated year or quarter.**

	Wadden Sea export Gmol/yr	internal processes Gmol/yr	river loads Gmol/yr	Riv <sub>eff</sub> Gmol/yr	net flow Gmol/yr	$\Delta$ content Gmol
2001	39	13	87	-5	38	177
2002	39	19	152	-7	-223	-13
2003	39	16	91	-3	-98	48
2004	39	13	78	-5	-8	122
2005	39	12	89	-5	-98	42
2006	39	12	88	-4	-56	83
2007	39	12	110	-5	-132	29
2008	39	14	93	-5	-71	75
2009	39	10	83	-5	-151	-19
Average	Gmol/yr 39	Gmol/yr 14	Gmol/yr 101	Gmol/yr -5	Gmol/yr -89	Gmol 65
t = 3 mon	Gmol/t	Gmol/t	Gmol/t	Gmol/t	Gmol/t	Gmol
Jan - Mar	7	-1	38	-1	-49	-5
Apr - Jun	10	15	23	-2	6	54
Jul - Sep	17	-2	15	-2	13	43
Oct - Dec	4	1	25	0	-56	-26

885 **6. Figure Captions**

886

887 Figure 1: Upper panel: Map of the south-eastern North Sea and the bordering land. Lower  
888 panel: Model domains of ECOHAM (red) and FVCOM (blue), positions of rivers 1 – 16 (left,  
889 see Table 2) and the Wadden Sea export areas grid cells (right). The magenta edges identify  
890 the validation area, western and eastern part separated by the magenta dashed line.

891 Figure 2: Monthly Wadden Sea export of DIC and TA [ $\text{Gmol mon}^{-1}$ ] at the North Frisian  
892 coast (N), East Frisian coast (E) and the Jade Bay in scenario B. The export rates were  
893 calculated for DIC and TA based on measured concentrations and simulated water fluxes.

894 Figure 3: Surface TA [ $\mu\text{mol TA kg}^{-1}$ ] in August 2008 observed (a) and simulated with  
895 scenario A (b) and B (c). The black lines indicate the validation box.

896 Figure 4: Differences between TA surface summer observations and results from  
897 scenario A (a) and B (b) and the differences between DIC surface observations and results  
898 from scenario A (c) and B (d), all in  $\mu\text{mol kg}^{-1}$ . The black lines indicate the validation box.

899 Figure 5: Surface DIC concentrations [ $\mu\text{mol DIC kg}^{-1}$ ] in August 2008 observed (a) and  
900 simulated with scenario A (b) and B (c). The black lines indicate the validation box.

901 Figure 6: Flushing times in the validation area in summer (June to August) and winter  
902 (January to March). The whole validation area is represented in blue, green is the western  
903 part of the validation area ( $4.5^\circ \text{ E}$  to  $7^\circ \text{ E}$ ) and red is the eastern part (east of  $7^\circ \text{ E}$ ).

904 Figure 7: Monthly mean simulated streamlines for summer months 2003 and 2008.

905 Figure 8: Simulated monthly mean TA (scenario A (a), scenario B (b)) [ $\mu\text{mol TA kg}^{-1}$ ] and DIC  
906 (scenario A (c), scenario B (d)) [ $\mu\text{mol DIC kg}^{-1}$ ] in the validation area for the years 2001-2009.

907 Figure 9: Temporally interpolated TA/DIC ratio of the export rates in the North Frisian, East  
908 Frisian, and Jade Bay. These ratios are calculated using the  $\Delta$ -values of Table 1.

909

910

911 **7. References**

912

913 Akam, S.A., Coffin, R.B., Abdulla, H.A.N., and Lyons T.W.: Dissolved inorganic carbon pump in  
914 methane-charged shallow marine sediments: State of the art and new model perspectives.  
915 *Frontiers in Marine Sciences* 7, 206, DOI: 10.3389/FMARS.2020.00206, 2020.

916 Al-Raei, A.M., Bosselmann, K., Böttcher, M.E., Hespeneide, B., and Tauber, F.: Seasonal  
917 dynamics of microbial sulfate reduction in temperate intertidal surface sediments: Controls  
918 by temperature and organic matter. *Ocean Dynamics* 59, 351-370, 2009.

919 Amann, T., Weiss, A., and Hartmann, J.: Inorganic Carbon Fluxes in the Inner Elbe Estuary,  
920 Germany, *Estuaries and Coasts* 38(1), 192-210, doi:10.1007/s12237-014-9785-6, 2015.

921

922 Artioli, Y., Blackford, J. C., Butenschön, M., Holt, J. T., Wakelin, S. L., Thomas, H., Borges, A.  
923 V., and Allen, J. I.: The carbonate system in the North Sea: Sensitivity and model validation,  
924 *Journal of Marine Systems*, 102-104, 1-13, doi:10.1016/j.jmarsys.2012.04.006, 2012.

925

926 Backhaus, J.O.: A three-dimensional model for the simulation of shelf sea dynamics, *Ocean*  
927 *Dynamics*, 38(4), 165–187, doi:10.1016/0278-4343(84)90044-X, 1985.

928

929 Backhaus, J.O., and Hainbucher, D.: A finite difference general circulation model for shelf  
930 seas and its application to low frequency variability on the North European Shelf, Elsevier  
931 *Oceanography Series*, 45, 221–244, doi:10.1016/S0422-9894(08)70450-1, 1987.

932

933 Ben-Yaakov, S.: pH BUFFERING OF PORE WATER OF RECENT ANOXIC MARINE SEDIMENTS,  
934 *Limnology and Oceanography*, 18, doi: 10.4319/lo.1973.18.1.0086, 1973.

935

936 Berner, R. A., Scott, M. R., and Thomlinson, C.: Carbonate alkalinity in the pore waters of  
937 anoxic marine sediments. *Limnology & Oceanography*, 15, 544–549,  
938 doi:10.4319/lo.1970.15.4.0544, 1970.

939

940 Billerbeck, M., Werner, U., Polerecky, L., Walpersdorf, E., de Beer, D., and Hüttel, M.:  
941 Surficial and deep pore water circulation governs spatial and temporal scales of nutrient  
942 recycling in intertidal sand flat sediment. *Mar Ecol Prog Ser* 326, 61-76, 2006.  
943

944 Böttcher, M.E., Al-Raei, A.M., Hilker, Y., Heuer, V., Hinrichs, K.-U., and Segl, M.: Methane and  
945 organic matter as sources for excess carbon dioxide in intertidal surface sands:  
946 Biogeochemical and stable isotope evidence. *Geochimica et Cosmochim Acta* 71, A111,  
947 2007.  
948

949 Böttcher, M.E., Hespeneide, B., Brumsack, H.-J., and Bosselmann, K.: Stable isotope  
950 biogeochemistry of the sulfur cycle in modern marine sediments: I. Seasonal dynamics in a  
951 temperate intertidal sandy surface sediment. *Isotopes Environ. Health Stud.* 40, 267-283,  
952 2004.  
953

954 Borges, A. V.: Present day carbon dioxide fluxes in the coastal ocean and possible feedbacks  
955 under global change, In *Oceans and the atmospheric carbon content* (P.M. da Silva Duarte &  
956 J.M. Santana Casiano Eds), Chapter 3, 47-77, doi:10.1007/978-90-481-9821-4, 2011.  
957

958 Borges, A. V. and Gypens, N.: Carbonate chemistry in the coastal zone responds more  
959 strongly to eutrophication than to ocean acidification. *Limn. Oceanogr.* 55(1): 346-353, 2010.  
960

961 Brasse, J., Reimer, A., Seifert, R., and Michaelis, W.: The influence of intertidal mudflats on  
962 the dissolved inorganic carbon and total alkalinity distribution in the German Bight,  
963 southeastern North Sea, *J. Sea Res.* 42, 93-103, doi: 10.1016/S1385-1101(99)00020-9, 1999.  
964

965 Brenner, H., Braeckman, U., Le Guitton, M., and Meysman, F. J. R.: The impact of  
966 sedimentary alkalinity release on the water column CO<sub>2</sub> system in the North Sea,  
967 *Biogeosciences*, 13(3), 841-863, doi:10.5194/bg-13-841-2016, 2016.  
968

969 Burt, W. J., Thomas, H., Pätsch, J., Omar, A. M., Schrum, C., Daewel, U., Brenner, H., and de  
970 Baar, H. J. W.: Radium isotopes as a tracer of sediment-water column exchange in the North  
971 Sea, *Global Biogeochemical Cycles* 28, pp 19, doi:10.1002/2014GB004825, 2014.

972

973 Burt, W. J., Thomas, H., Hagens, M., Pätsch, J., Clargo, N. M., Salt, L. A., Winde, V., and  
974 Böttcher, M. E.: Carbon sources in the North Sea evaluated by means of radium and stable  
975 carbon isotope tracers, *Limnology and Oceanography*, 61(2), 666-683,  
976 doi:10.1002/lno.10243, 2016.

977

978 Cadée, G. C., and Hegeman, J.: Phytoplankton in the Marsdiep at the end of the 20<sup>th</sup> century;  
979 30 years monitoring biomass, primary production, and Phaeocystis blooms, *J. Sea Res.* 48,  
980 97-110, doi:10.1016/S1385-1101(02)00161-2, 2002.

981

982 Cai, W.-J., Hu, X., Huang, W.-J., Jiang, L.-Q., Wang, Y., Peng, T.-H., and Zhang, X.: Surface  
983 ocean alkalinity distribution in the western North Atlantic Ocean margins, *Journal of*  
984 *Geophysical Research*, 115, C08014, doi:10.1029/2009JC005482, 2010.

985

986 Carvalho, A. C. O., Marins, R. V., Dias, F. J. S., Rezende, C. E., Lefèvre, N., Cavalcante, M. S.,  
987 and Eschrique, S. A.: Air-sea CO<sub>2</sub> fluxes for the Brazilian northeast continental shelf in a  
988 climatic transition region, *Journal of Marine Systems*, 173, 70-80,  
989 doi:10.1016/j.jmarsys.2017.04.009, 2017.

990

991 Chambers, R. M., Hollibaugh, J. T., and Vink, S. M.: Sulfate reduction and sediment  
992 metabolism in Tomales Bay, California, *Biogeochemistry*, 25, 1–18, doi:10.1007/BF00000509,  
993 1994.

994

995 Chen, C.-T. A., and Wang, S.-L.: Carbon, alkalinity and nutrient budgets on the East China Sea  
996 continental shelf. *Journal of Geophysical Research*, 104, 20,675–20,686,  
997 doi:10.1029/1999JC900055, 1999.

998

999 Chen, C., Liu, H., and Beardsley, R. C.: An Unstructured Grid, Finite-Volume, Three-  
1000 Dimensional, Primitive Equations Ocean Model: Application to Coastal Ocean and Estuaries, *J*  
1001 *Atmos Oceanic Technol*, 20 (1), 159-186,  
1002 doi:10.1175/1520-0426(2003)020<0159:AUGFVT>2.0.CO;2, 2003.

1003



1004 CPSL. Final Report of the Trilateral Working Group on Coastal Protection and Sea Level Rise.  
1005 Wadden Sea Ecosystem No. 13. Common Wadden Sea Secretariat, Wilhelmshaven,  
1006 Germany. 2001.  
1007  
1008 de Beer, D., Wenzhöfer, F., Ferdelman, T.G., Boehme, S., Huettel, M., van Beusekom, J.,  
1009 Böttcher, M.E., Musat, N., Dubilier, N.: Transport and mineralization rates in North Sea sandy  
1010 intertidal sediments (Sylt-Rømø Basin, Waddensea). *Limnol. Oceanogr.* 50, 113-127, 2005.  
1011  
1012 Dickson, A.G., Afghan, J.D., Anderson, G.C.: Reference materials for oceanic CO<sub>2</sub> analysis: a  
1013 method for the certification of total alkalinity. *Marine Chemistry* 80, 185-197, 2003.  
1014  
1015 Dollar, S. J., Smith, S. V., Vink, S. M., Obrebski, S., and Hollibaugh, J.T.: Annual cycle of  
1016 benthic nutrient fluxes in Tomales Bay, California, and contribution of the benthos to total  
1017 ecosystem metabolism, *Marine Ecology Progress Series*, 79, 115–125,  
1018 doi:10.3354/meps079115, 1991.  
1019  
1020 Duarte, C. M., Hendriks, I. E., Moore, T. S., Olsen, Y. S., Steckbauer, A., Ramajo, L.,  
1021 Carstensen, J., Trotter, J. A., and McCulloch, M. Is Ocean Acidification an Open-Ocean  
1022 Syndrome? Understanding Anthropogenic Impacts on Seawater pH. *Estuaries and Coasts*  
1023 36(2): 221-236. 2013.  
1024  
1025 Ehlers, J.: Geomorphologie und Hydrologie des Wattenmeeres. In: Lozan, J.L., Rachor, E., Von  
1026 Westernhagen, H., Lenz, W. (Eds.), *Warnsignale aus dem Wattenmeer*. Blackwell  
1027 Wissenschaftsverlag, Berlin, pp. 1–11. 1994.  
1028  
1029 Faneca Sánchez, M., Gunnink, J. L., van Baaren, E. S., Oude Essink, G. H. P., Siemon, B.,  
1030 Auken, E., Elderhorst, W., de Louw, P. G. B.: Modelling climate change effects on a Dutch  
1031 coastal groundwater system using airborne electromagnetic measurements. *Hydrol. Earth*  
1032 *Syst. Sci.* 16(12), 4499-4516, 2012.  
1033  
1034 Flemming, B. W., and Davis, R. A. J.: Holocene evolution, morphodynamics and

1035 sedimentology of the Spiekeroog barrier island system (southern North Sea). *Senckenb.*  
1036 *Marit.* 25, 117-155, 1994.

1037

1038 Große, F., Kreuz, M., Lenhart, H.-J., Pätsch, J., and Pohlmann, T.: A Novel Modeling Approach  
1039 to Quantify the Influence of Nitrogen Inputs on the Oxygen Dynamics of the North Sea,  
1040 *Frontiers in Marine Science* 4(383), pp 21, doi:10.3389/fmars.2017.00383, 2017.

1041

1042 Grashorn, S., Lettmann, K. A., Wolff, J.-O., Badewien, T. H., and Stanev, E. V.: East Frisian  
1043 Wadden Sea hydrodynamics and wave effects in an unstructured-grid model, *Ocean*  
1044 *Dynamics* 65(3), 419-434, doi:10.1007/s10236-014-0807-5, 2015.

1045

1046 Gustafsson, E., Hagens, M., Sun, X., Reed, D. C., Humborg, C., Slomp, C. P., Gustafsson, B. G.:  
1047 Sedimentary alkalinity generation and long-term alkalinity development in the Baltic Sea.  
1048 *Biogeosciences* 16(2): 437-456, 2019.

1049 HASEC: OSPAR Convention for the Protection of the Marine Environment of the North-East  
1050 Atlantic. Meeting of the Hazardous Substances and Eutrophication Committee (HASEC), Oslo  
1051 27 February – 2 March 2012.

1052

1053 Hild, A.: Geochemie der Sedimente und Schwebstoffe im Rückseitenwatt von Spiekeroog  
1054 und ihre Beeinflussung durch biologische Aktivität. *Forschungszentrum Terramare Berichte*  
1055 5, 71 pp., 1997.

1056 Höpner, T., and Michaelis, H.: Sogenannte ‚Schwarze Flecken‘ – ein Eutrophierungssymptom  
1057 des Wattenmeeres. In: L. Lozán, E. Rachor, K. Reise, H. von Westernhagen und W. Lenz.  
1058 *Warnsignale aus dem Wattenmeer*. Berlin: Blackwell, 153-159, 1997.

1059

1060 Hoppema, J. M. J.; The distribution and seasonal variation of alkalinity in the southern bight  
1061 of the North Sea and in the western Wadden Sea, *Netherlands Journal of Sea Research*, 26  
1062 (1), 11-23, doi: 10.1016/0077-7579(90)90053-J, 1990.

1063

1064 Hu, X. and Cai, W.-J.: An assessment of ocean margin anaerobic processes on oceanic  
1065 alkalinity budget. *Global Biogeochemical Cycles* 25: 1-11, 2011.

1066  
1067 Johannsen, A., Dähnke, K., and Emeis, K.-C.: Isotopic composition of nitrate in five German  
1068 rivers discharging into the North Sea, *Organic Geochemistry*, 39, 1678-1689  
1069 doi:10.1016/j.orggeochem.2008.03.004, 2008.  
1070  
1071 Johnson, K.M., Wills, K.D., Buttler, D.B., Johnson, W.K., and Wong, C.S.: Coulometric total  
1072 carbon dioxide analysis for marine studies: maximizing the performance of an automated  
1073 gas extraction system and coulometric detector. *Marine Chemistry* 44, 167-187, 1993.  
1074  
1075 Kalnay, E., Kanamitsu, M., Kistler, R., Collins, W., Deaven, D., Gandin, L., Iredell, M., Saha S.,  
1076 White, G., Woollen, J., Zhu, Y., Chelliah, M., Ebisuzaki, W., Higgins, W., Janowiak, J., Mo, K.C.,  
1077 Ropelewski, C., Wang, J., Leetmaa, A., Reynolds, R., Jenne, R., and Joseph, D.: The  
1078 NCEP/NCAR 40-year reanalysis project, *Bulletin of The American Meteorological Society*,  
1079 77(3), 437–471, doi: 10.1175/1520-0477(1996)077<0437:TNYRP>2.0.CO;2, 1996.  
1080  
1081 Kempe, S. and Pegler, K.: Sinks and sources of CO<sub>2</sub> in coastal seas: the North Sea, *Tellus* 43 B,  
1082 224-235, doi: 10.3402/tellusb.v43i2.15268, 1991.  
1083  
1084 Kerimoglu, O., Große, F., Kreuz, M., Lenhart, H.-J., and van Beusekom, J. E. E.: A model-based  
1085 projection of historical state of a coastal ecosystem: Relevance of phytoplankton  
1086 stoichiometry, *Science of The Total Environment* 639, 1311-1323,  
1087 doi:10.1016/j.scitotenv.2018.05.215, 2018.  
1088  
1089 Kohlmeier, C., and Ebenhöf, W.: Modelling the biogeochemistry of a tidal flat ecosystem  
1090 with EcoTiM, *Ocean Dynamics*, 59(2), 393-415, doi: 10.1007/s10236-009-0188-3, 2009.  
1091  
1092 Kowalski, N., Dellwig, O., Beck, M., Gräwe, U., Pierau, N., Nägler, T., Badewien, T., Brumsack,  
1093 H.-J., van Beusekom, J.E., and Böttcher, M. E. Pelagic molybdenum concentration anomalies  
1094 and the impact of sediment resuspension on the molybdenum budget in two tidal systems of  
1095 the North Sea. *Geochimica et Cosmochimica Acta* 119, 198-211, 2013.  
1096  
1097 Kühn, W., Pätsch, J., Thomas, H., Borges, A. V., Schiettecatte, L.-S., Bozec, Y., and Prowe, A. E.

1098 F.: Nitrogen and carbon cycling in the North Sea and exchange with the North Atlantic-A  
1099 model study, Part II: Carbon budget and fluxes, *Continental Shelf Research*, 30, 1701-1716,  
1100 doi:10.1016/j.csr.2010.07.001, 2010.

1101

1102 Laruelle, G. G., Lauerwald, R., Pfeil, B., and Regnier, P.: Regionalized global budget of the CO<sub>2</sub>  
1103 exchange at the air-water interface in continental shelf seas, *Global Biogeochemical Cycles*,  
1104 28 (11), 1199-1214, doi: 10.1002/2014gb004832, 2014.

1105

1106 Lenhart, H.-J., Radach, G., Backhaus, J. O., and Pohlmann, T.: Simulations of the North Sea  
1107 circulation, its variability, and its implementation as hydrodynamical forcing in ERSEM, *Neth.*  
1108 *J. Sea Res.*, 33, 271–299, doi:10.1016/0077-7579(95)90050-0, 1995.

1109

1110 Lettmann, K. A., Wolff, J.-O., and Badewien, T.H.: Modeling the impact of wind and waves on  
1111 suspended particulate matter fluxes in the East Frisian Wadden Sea (southern North Sea),  
1112 *Ocean Dynamics*, 59(2), 239-262, doi: 10.1007/s10236-009-0194-5, 2009.

1113

1114 Lipinski, M.: Nährstoffelemente und Spurenmetalle in Wasserproben der Hunte und Jade.  
1115 Diploma thesis, C.v.O. University of Oldenburg, 82 pp., 1999.

1116

1117 Lorkowski, I., Pätsch, J., Moll, A., and Kühn, W.: Interannual variability of carbon fluxes in the  
1118 North Sea from 1970 to 2006 – Competing effects of abiotic and biotic drivers on the gas-  
1119 exchange of CO<sub>2</sub>, *Estuarine, Coastal and Shelf Science*, 100, 38-57,  
1120 doi:10.1016/j.ecss.2011.11.037, 2012.

1121

1122 Łukawska-Matuszewska, K. and Graca, B.: Pore water alkalinity below the permanent  
1123 halocline in the Gdańsk Deep (Baltic Sea) - Concentration variability and benthic fluxes.  
1124 *Marine Chemistry* 204: 49-61, 2017.

1125

1126 Mayer, B., Rixen, T., and Pohlmann, T.: The Spatial and Temporal Variability of Air-Sea CO<sub>2</sub>  
1127 Fluxes and the Effect of Net Coral Reef Calcification in the Indonesian Seas: A Numerical  
1128 Sensitivity Study. *Frontiers in Marine Science* 5(116), 2018.

1129

1130 McQuatters-Gollop, A., Raitzos, D. E., Edwards, M., Pradhan, Y., Mee, L. D., Lavender, S. J.,  
1131 and Attrill, M. J.: A long-term chlorophyll data set reveals regime shift in North Sea  
1132 phytoplankton biomass unconnected to nutrient trends, *Limnology & Oceanography*, 52,  
1133 635-648, doi:10.4319/lo.2007.52.2.0635, 2007.

1134

1135 McQuatters-Gollop, A., and Vermaat, J. E.: Covariance among North Sea ecosystem state  
1136 indicators during the past 50 years e contrasts between coastal and open waters, *Journal of*  
1137 *Sea Research*, 65, 284-292, doi:10.1016/j.seares.2010.12.004, 2011.

1138

1139 Moore, W.S., Beck, M., Riedel, T., Rutgers van der Loeff, M., Dellwig, O., Shaw, T.J.,  
1140 Schnetger, B., and Brumsack, H.-J.: Radium-based pore water fluxes of silica, alkalinity,  
1141 manganese, DOC, and uranium: A decade of studies in the German Wadden Sea, *Geochimica*  
1142 *et Cosmochimica Acta*, 75, 6535 – 6555, doi:10.1016/j.gca.2011.08.037, 2011.

1143

1144 Neal, C.: Calcite saturation in eastern UK rivers, *The Science of the Total Environment*, 282-  
1145 283, 311-326, doi:10.1016/S0048-9697(01)00921-4, 2002.

1146

1147 Neira, C., and Rackemann, M.: Black spots produced by buried macroalgae in intertidal sandy  
1148 sediments of the Wadden Sea: Effects on the meiobenthos. *J. Sea Res.*, 36, 153 - 170, 1996.

1149

1150 Onken, R., and Riethmüller, R.: Determination of the freshwater budget of tidal flats from  
1151 measurements near a tidal inlet, *Continental Shelf Research*, 30, 924-933,  
1152 doi:10.1016/j.csr.2010.02.004, 2010.

1153

1154 Otto, L., Zimmerman, J.T.F., Furnes, G.K., Mork, M., Saetre, R., and Becker, G.: Review of the  
1155 physical oceanography of the North Sea, *Netherlands Journal of Sea Research*, 26 (2-4), 161–  
1156 238, doi:10.1016/0077-7579(90)90091-T, 1990.

1157

1158 Pätsch, J., and Kühn, W.: Nitrogen and carbon cycling in the North Sea and exchange with  
1159 the North Atlantic – a model study Part I: Nitrogen budget and fluxes, *Continental Shelf*  
1160 *Research*, 28, 767–787, doi: 10.1016/j.csr.2007.12.013, 2008.

1161

1162 Pätsch, J., and Lenhart, H.-J.: Daily Loads of Nutrients, Total Alkalinity, Dissolved Inorganic  
1163 Carbon and Dissolved Organic Carbon of the European Continental Rivers for the Years  
1164 1977–2006, Berichte aus dem Zentrum für Meeres- und Klimaforschung  
1165 ([https://wiki.cen.uni-hamburg.de/ifm/ECOHAM/DATA\\_RIVER](https://wiki.cen.uni-hamburg.de/ifm/ECOHAM/DATA_RIVER)), 2008.  
1166

1167 Pätsch, J., Serna, A., Dähnke, K., Schlarbaum, T., Johannsen, A., and Emeis, K.-C.: Nitrogen  
1168 cycling in the German Bight (SE North Sea) - Clues from modelling stable nitrogen isotopes.  
1169 *Continental Shelf Research*, 30, 203-213, doi:10.1016/j.csr.2009.11.003, 2010.  
1170

1171 Pätsch, J., Kühn, W., and Six, K. D.: Interannual sedimentary effluxes of alkalinity in the  
1172 southern North Sea: model results compared with summer observations, *Biogeosciences*  
1173 15(11), 3293-3309, doi: 10.5194/bg-15-3293-2018, 2018.  
1174

1175 Pätsch, J., Burchard, H., Dieterich, C., Gräwe, U., Gröger, M., Mathis, M., Kapitza, H.,  
1176 Bersch, M., Moll, A., Pohlmann, T., Su, J., Ho-Hagemann, H.T.M., Schulz, A., Elizalde, A., and  
1177 Eden, C.: An evaluation of the North Sea circulation in global and regional models relevant  
1178 for ecosystem simulations, *Ocean Modelling*, 116, 70-95,  
1179 doi:10.1016/j.ocemod.2017.06.005, 2017.  
1180

1181 Pohlmann, T.: Predicting the thermocline in a circulation model of the North Sea – Part I:  
1182 model description, calibration and verification, *Continental Shelf Research*, 16(2), 131–146,  
1183 doi:10.1016/0278-4343(95)90885-S, 1996.  
1184

1185 Provoost, P., van Heuven, S., Soetaert, K., Laane, R. W. P. M., and Middelburg, J. J.: Seasonal  
1186 and long-term changes in pH in the Dutch coastal zone, *Biogeoscience*, 7, 3869-3878,  
1187 doi:10.5194/bg-7-3869-2010, 2010.  
1188

1189 Raaphorst, W., Kloosterhuis H. T., Cramer, A., and Bakker, K. J. M.: Nutrient early diagenesis  
1190 in the sandy sediments of the Dogger Bank area, North Sea: pore water results, *Neth. J. Sea.*  
1191 *Res.*, 26(1), 25-52, doi: 10.1016/0077-7579(90)90054-K, 1990.  
1192

1193 Radach, G. and Pätsch, J.: Variability of Continental Riverine Freshwater and Nutrient Inputs  
1194 into the North Sea for the Years 1977-2000 and Its Consequences for the Assessment of  
1195 Eutrophication, *Estuaries and Coasts* 30(1), 66-81, doi: 10.1007/BF02782968, 2007.  
1196

1197 Rassmann, J., Eitel, E. M., Lansard, B., Cathalot, C., Brandily, C., Taillefert, M., and Rabouille,  
1198 C.: Benthic alkalinity and dissolved inorganic carbon fluxes in the Rhône River prodelta  
1199 generated by decoupled aerobic and anaerobic processes. *Biogeosciences*, 17, 13-33,  
1200 doi:10.5194/bg-17-13-2020, 2020.

1201

1202 Reimer, S., Brasse, S., Doerffer, R., Dürselen, C. D., Kempe, S., Michaelis, W., and Seifert, R.:  
1203 Carbon cycling in the German Bight: An estimate of transformation processes and transport,  
1204 *Deutsche Hydr. Zeitschr.* 51, 313-329, doi: /10.1007/BF02764179, 1999.

1205

1206 Riedel, T., Lettmann, K., Beck, M., and Brumsack, H.-J.: Tidal variations in groundwater  
1207 storage and associated discharge from an intertidal coastal aquifer. *Journal of Geophysical*  
1208 *Research* 115, 1-10, 2010.

1209

1210 Rullkötter, J.: The back-barrier tidal flats in the southern North Sea—a multidisciplinary  
1211 approach to reveal the main driving forces shaping the system, *Ocean Dynamics*, 59(2), 157-  
1212 165, doi: 10.1007/s10236-009-0197-2, 2009.

1213

1214 Salt, L. A., Thomas, H., Prowe, A. E. F., Borges, A. V., Bozec, Y., and de Baar, H. J. W.:  
1215 Variability of North Sea pH and CO<sub>2</sub> in response to North Atlantic Oscillation forcing, *Journal*  
1216 *of Geophysical Research*, *Biogeosciences*, 118, pp 9, doi:10.1002/2013JG002306, 2013.

1217

1218 Santos, I. R., Eyre, B. D., and Huettel, M.: The driving forces of porewater and groundwater  
1219 flow in permeable coastal sediments: A review, *Estuarine, Coastal and Shelf Science*, 98, 1-  
1220 15, doi:10.1016/j.ecss.2011.10.024, 2012.

1221

1222 Santos, I. R., Beck, M., Brumsack, H.-J., Maher, D.T., Dittmar, T., Waska, H., and Schnetger,  
1223 B.: Porewater exchange as a driver of carbon dynamics across a terrestrial-marine transect:

1224 Insights from coupled  $^{222}\text{Rn}$  and  $\text{pCO}_2$  observations in the German Wadden Sea, *Marine*  
1225 *Chemistry*, 171, 10-20, doi:10.1016/j.marchem.2015.02.005, 2015.  
1226

1227 Schott, F.: Der Oberflächensalzgehalt in der Nordsee, *Deutsche Hydr. Zeitschr.*, Reihe A Nr. 9,  
1228 SUPPL. A9, pp 1-29, 1966.  
1229

1230 Schwichtenberg, F.: Drivers of the carbonate system variability in the southern North Sea:  
1231 River input, anaerobic alkalinity generation in the Wadden Sea and internal processes,  
1232 (Doktorarbeit/PhS), Universität Hamburg, Hamburg, Germany, 161 pp, 2013.  
1233

1234 Seibert, S.L., Greskowiak J., Prommer H., Böttcher M.E., Waska H., and Massmann G.:  
1235 Modeling biogeochemical processes in a barrier island freshwater lens (Spiekeroog,  
1236 Germany). *J. Hydrol.*, 575, 1133-1144, 2019.  
1237

1238 Seitzinger, S., and Giblin, A.E.: Estimating denitrification in North Atlantic continental shelf  
1239 sediments, *Biogeochemistry*, 35, 235–260, doi: 10.1007/BF02179829, 1996.  
1240

1241 Shadwick, E. H., Thomas, H., Azetsu-Scott, K., Greenan, B. J. W., Head, E., and Horne, E.:  
1242 Seasonal variability of dissolved inorganic carbon and surface water  $\text{pCO}_2$  in the Scotian Shelf  
1243 region of the Northwestern Atlantic, *Marine Chemistry*, 124 (1–4), 23-37,  
1244 doi:10.1016/j.marchem.2010.11.004, 2011.  
1245

1246 Sippo, J.Z., Maher, D.T., Tait, D.R., Holloway, C., Santos, I.R.: Are mangroves drivers or  
1247 buffers of coastal acidification? Insights from alkalinity and dissolved inorganic carbon export  
1248 estimates across a latitudinal transect. *Global Biogeochemical Cycles*, 30, 753-766, 2016.  
1249

1250 Smith, S. V., and Hollibaugh, J. T.: Coastal metabolism and the oceanic organic carbon  
1251 balance, *Reviews of Geophysics*, 31, 75–89, doi:10.1029/92RG02584, 1993.  
1252

1253 Streif, H.: Das ostfriesische Wattenmeer. Nordsee, Inseln, Watten und Marschen. Gebrüder  
1254 Borntraeger, Berlin, 1990.  
1255



1256 Su, J. and Pohlmann, T.: Wind and topography influence on an upwelling system at the  
1257 eastern Hainan coast. *Journal of Geophysical Research: Oceans* 114(C6), 2009.  
1258

1259 Sulzbacher, H., Wiederhold, H., Siemon, B., Grinat, M., Igel, J., Burschil, T., Günther, T.,  
1260 Hinsby, K.: Numerical modelling of climate change impacts on freshwater lenses on the  
1261 North Sea Island of Borkum using hydrological and geophysical methods." *Hydrol. Earth Syst.*  
1262 *Sci.* 16(10): 3621-3643, 2012.

1263  
1264 Thomas, H., Bozec, Y., Elkalay, K., and de Baar, H. J. W.: Enhanced open ocean storage of CO<sub>2</sub>  
1265 from shelf sea pumping, *Science*, 304, 1005-1008, doi:10.1126/science.1095491, 2004.  
1266

1267 Thomas, H., Schiettecatte, L.-S., Suykens, K., Kone, Y. J. M., Shadwick, E. H., Prowe, A. E. F.,  
1268 Bozec, Y., De Baar, H. J. W., and Borges, A. V.: Enhanced ocean carbon storage from  
1269 anaerobic alkalinity generation in coastal sediments, *Biogeosciences*, 6, 267-274,  
1270 doi:10.5194/bg-6-267-2009, 2009.  
1271

1272 van Beusekom, J. E. E., Carstensen, J., Dolch, T., Grage, A., Hofmeister, R., Lenhart, H.-J.,  
1273 Kerimoglu, O., Kolbe, K., Pätsch, J., Rick, J., Rönn, L., and Ruitter, H.: Wadden Sea  
1274 Eutrophication: Long-Term Trends and Regional Differences. *Frontiers in Marine Science*  
1275 6(370), 2019

1276  
1277 van Beusekom, J. E. E., Loebel, M., and Martens, P.: Distant riverine nutrient supply and local  
1278 temperature drive the long-term phytoplankton development in a temperate coastal basin,  
1279 *J. Sea Res.* 61, 26-33, doi:10.1016/j.seares.2008.06.005, 2009.  
1280

1281 van Beusekom, J. E. E., Buschbaum, C., and Reise, K.: Wadden Sea tidal basins and the  
1282 mediating role of the North Sea in ecological processes: scaling up of management? *Ocean &*  
1283 *Coastal Management*, 68, 69-78, doi:10.1016/j.ocecoaman.2012.05.002, 2012.  
1284

1285 van Goor, M. A., Zitman, T. J., Wang, Z. B., and Stive, M. J. F.: Impact of sea-level rise on the  
1286 equilibrium state of tidal inlets, *Mar. Geol.* 202, 211-227, doi:10.1016/S0025-3227(03)00262-  
1287 7, 2003.

1288

1289 van Koningsveld, M., Mulder, J. P. M., Stive, M. J. F., Van der Valk, L., and Van der Weck,  
1290 A.W.: Living with sea-level rise and climate change: a case study of the Netherlands, *J. Coast.*  
1291 *Res.* 24, 367-379, doi:10.2112/07A-0010.1, 2008.

1292

1293 Wang, Z. A., and Cai, W.-J.: Carbon dioxide degassing and inorganic carbon export from a  
1294 marsh-dominated estuary (the Duplin River): A marsh CO<sub>2</sub> pump, *Limnology &*  
1295 *Oceanography*, 49, 341–354, doi:10.4319/lo.2004.49.2.0341, 2004.

1296

1297 Winde, V.: Zum Einfluss von benthischen und pelagischen Prozessen auf das Karbonatsystem  
1298 des Wattenmeeres der Nordsee. Dr.rer.nat. thesis, EMA University of Greifswald, 2012.

1299

1300 Winde, V., Böttcher, M. E., Escher, P., Böning, P., Beck, M., Liebezeit, G., and Schneider, B.:  
1301 Tidal and spatial variations of  $\delta^{13}\text{C}$  and aquatic chemistry in a temperate tidal basin during  
1302 winter time, *Journal of Marine Systems*, 129, 396-404, doi:10.1016/j.jmarsys.2013.08.005,  
1303 2014.

1304

1305 Wolf-Gladrow, D. A., Zeebe, R. E., Klaas, C., Kortzinger, A., and Dickson, A. G.: Total alkalinity:  
1306 The explicit conservative expression and its application to biogeochemical processes, *Marine*  
1307 *Chemistry*, 106, 287–300, doi:10.1016/j.marchem.2007.01.006, 2007.

1308

1309 Wurgaft E., Findlay A.J., Vigderovich H., Herut B., and Sivan O.: Sulfate reduction rates in the  
1310 sediments of the Mediterranean continental shelf inferred from combined dissolved  
1311 inorganic carbon and total alkalinity profiles. *Marine Chemistry*, 211,64-74, 2019.

1312

1313 Zhai, W.-D., Yan, X.-L., and Qi, D.: Biogeochemical generation of dissolved inorganic carbon  
1314 and nitrogen in the North Branch of inner Changjiang Estuary in a dry season. *Estuarine,*  
1315 *Coastal and Shelf Science* 197: 136-149, 2017.

1316

1317 Zeebe, R.E., and Wolf-Gladrow, D. 2001. CO<sub>2</sub> in seawater: Equilibrium, Kinetics, Isotopes.  
1318 Elsevier Science Ltd., 2001.

1319

1320

1321

1322

1323

1324

1325

1326

1327

1328

1329

1330 **8. Appendix**

1331

1332 **Table A1: Annual riverine freshwater discharge [ $\text{km}^3 \text{ yr}^{-1}$ ]. The numbering refers to Fig. 1.**

	2001	2002	2003	2004	2005	2006	2007	2008	2009
1) Elbe	23.05	43.38	23.95	19.56	25.56	26.98	26.61	24.62	24.28
2) Ems	3.47	4.48	3.15	3.52	2.99	2.54	4.32	3.32	2.58
3) Noordzeekanaal	3.21	2.98	2.49	3.05	3.03	2.96	1.55	3.05	2.46
4) IJsselmeer (east)	9.55	9.94	6.27	7.97	7.35	7.30	9.10	8.23	6.59
5) IJsselmeer (west)	9.55	9.94	6.27	7.97	7.35	7.30	9.10	8.23	6.59
6) Nieuwe Waterweg	50.37	51.33	34.72	42.91	41.61	44.21	49.59	49.76	44.69
7) Haringvliet	33.10	35.18	17.92	10.77	12.36	16.02	24.00	15.70	11.06
8) Scheldt	7.28	2.74	4.31	3.64	3.59	3.74	4.63	4.57	3.63
9) Weser	11.43	18.97	11.80	10.52	10.37	9.72	16.21	12.59	9.58
10) Firth of Forth	2.72	3.76	2.06	3.01	3.00	2.84	2.85	3.59	3.66
11) Tyne	1.81	2.25	1.18	2.04	1.92	1.78	2.09	2.70	2.05
12) Tees	1.33	1.78	0.94	1.59	1.27	1.45	1.49	1.99	1.55
13) Humber	10.76	12.10	7.16	10.51	7.68	11.11	12.03	13.87	9.60
14) Wash	5.46	4.39	3.08	3.91	1.96	2.72	5.24	4.77	3.21
15) Thames	4.47	3.23	2.41	2.13	0.96	1.57	3.52	3.20	2.38
16) Eider	0.67	0.97	0.47	0.70	0.68	0.67	0.63	0.58	0.57
Sum	178.2	207.4	128.1	133.7	131.6	142.9	172.9	160.7	134.4

1333

1334

1335

1336

1337

1338

1339

1340

1341

1342 **Table A2: River numbers in Fig. 1, their positions and source of data**

Number in Fig. 1	Name	River mouth position	Data source
1	Elbe	53°53'20"N 08°55'00"E	Pätsch & Lenhart (2008); TA-, DIC- and nitrate- concentrations by Amann (2015)
2	Ems	53°29'20"N 06°55'00"E	Pätsch & Lenhart (2008)
3	Noordzeekanaal	52°17'20"N 04°15'00"E	Pätsch & Lenhart (2008); TA-, DIC- and nitrate-

			concentrations from waterbase.nl
4	Ijsselmeer (east)	53°17'20"N 05°15'00"E	As above
5	Ijsselmeer (west)	53°05'20"N 04°55'00"E	As above
6	Nieuwe Waterweg	52°05'20"N 03°55'00"E	As above
7	Haringvliet	51°53'20"N 03°55'00"E	As above
8	Scheldt	51°29'20"N 03°15'00"E	As above
9	Weser	53°53'20"N 08°15'00"E	Pätsch & Lenhart (2008)
10	Firth of Forth	56°05'20"N 02°45'00"W	HASEC (2012)
11	Tyne	55°05'20"N 01°25'00"W	HASEC (2012)
12	Tees	54°41'20"N 01°05'00"W	HASEC (2012)
13	Humber	53°41'20"N 00°25'00"W	HASEC (2012)
14	Wash	52°53'20"N 00°15'00"E	HASEC (2012): sum of 4 rivers: Nene, Ouse, Welland and Witham
15	Thames	51°29'20"N 00°55'00"E	HASEC (2012)
16	Eider	54°05'20"N 08°55'00"E	Johannsen et al, 2008

1343

1344 **Table A3: Monthly values of TA, DIC and NO<sub>3</sub> concentrations [ $\mu\text{mol kg}^{-1}$ ] of rivers, the annual**  
1345 **mean and the standard deviation**

River parameter	Jan	Feb	Mar	Apr	May	Jun	Jul	Aug	Sep	Oct	Nov	Dec	Mean	SD
Elbe TA	2380	2272	2293	2083	2017	1967	1916	1768	1988	2156	2342	2488	2139	218
Noordzeekanaal TA	3762	3550	3524	3441	4748	3278	3419	3183	3027	3299	3210	3413	3488	441
Nieuwe Waterweg TA	2778	2708	2765	3006	2883	2658	2876	2695	2834	2761	2834	2927	2810	102
Haringvliet TA	2588	2635	2532	3666	2826	2829	2659	2660	2496	2816	2758	2585	2754	309
Scheldt TA	3781	3863	3708	3725	3758	3626	3722	3514	3367	3666	3825	3801	3696	140
Ijsselmeer TA	2829	3005	2472	2259	2611	1864	1672	1419	1445	2172	2286	2551	2215	521
Elbe DIC	2415	2319	2362	2179	2093	2025	1956	1853	2018	2200	2428	2512	2197	211
Noordzeekanaal DIC	3748	3579	3470	3334	3901	3252	3331	3136	2977	3214	3183	3405	3378	264
Nieuwe Waterweg DIC	2861	2794	2823	2991	2879	2657	2886	2706	2828	2773	2907	3036	2845	108
Haringvliet DIC	2673	2735	2600	3661	2850	2846	2687	2681	2512	2859	2803	2670	2798	292
Scheldt DIC	3798	3909	3829	3737	3704	3592	3705	3490	3316	3648	3733	3868	3694	167
Ijsselmeer DIC	2824	3008	2458	2234	2576	1826	1636	1369	1399	2134	2285	2565	2193	538
Elbe NO <sub>3</sub>	247	330	277	225	193	161	129	103	112	157	267	164	197	72
Noordzeekanaal NO <sub>3</sub>	150	168	190	118	79	71	64	73	78	92	107	137	111	42
Nieuwe Waterweg NO <sub>3</sub>	232	243	231	195	150	140	132	135	113	145	201	220	178	47
Haringvliet NO <sub>3</sub>	233	252	218	200	143	144	133	117	128	127	143	228	172	50
Scheldt NO <sub>3</sub>	320	341	347	345	243	221	219	215	189	202	190	274	259	63
Ijsselmeer NO <sub>3</sub>	136	159	190	192	135	46	20	14	7	18	20	79	85	73

1346

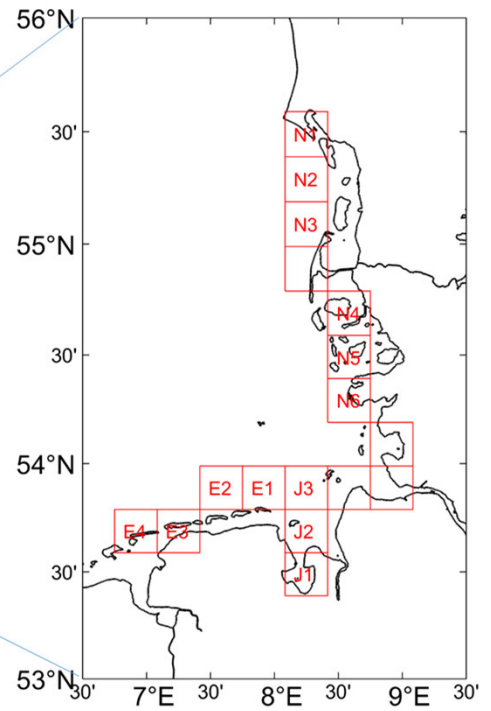
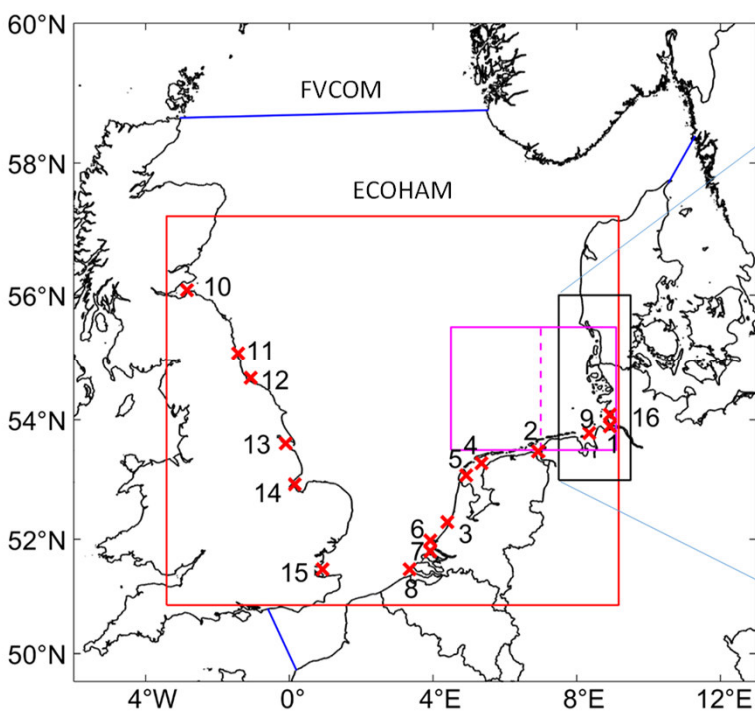
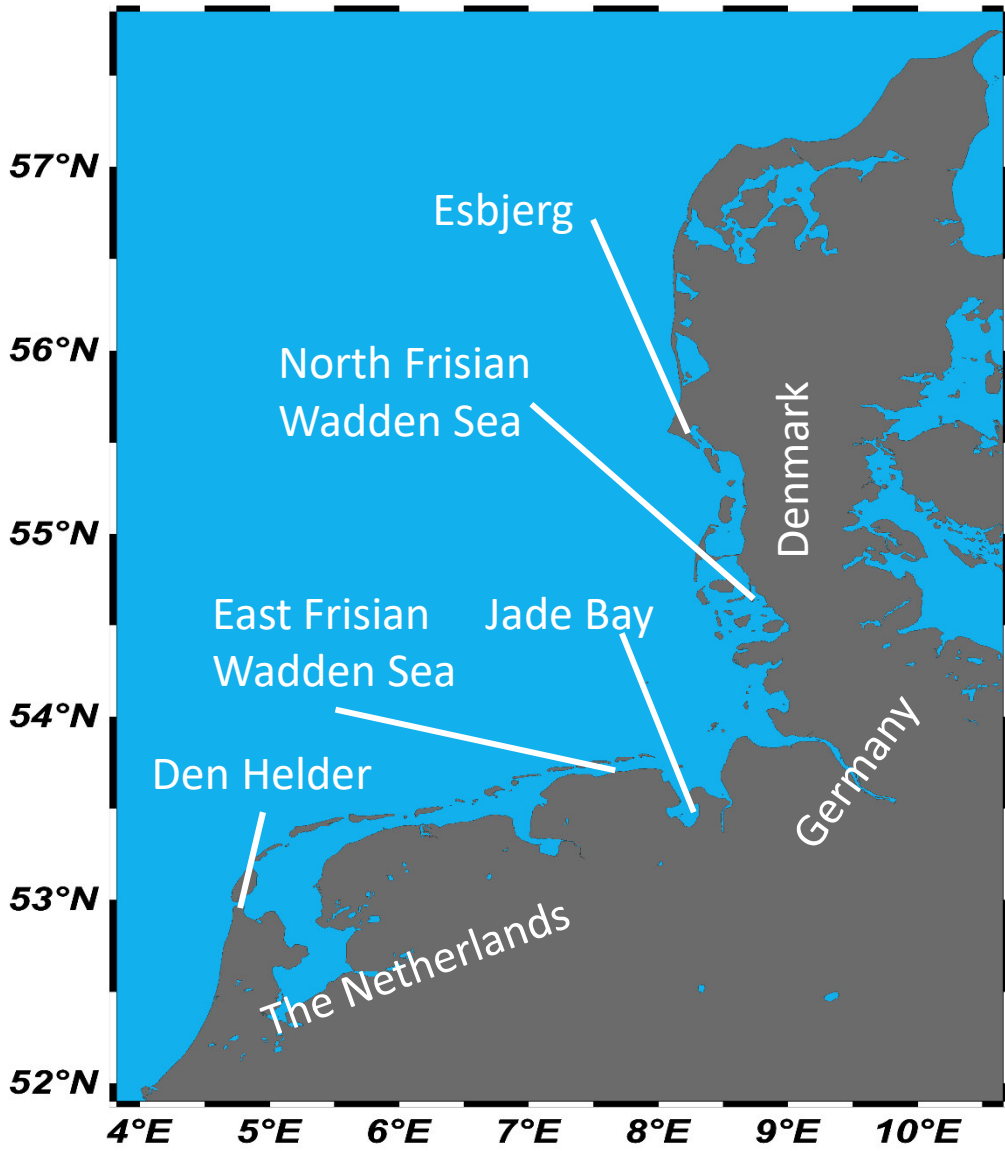


Fig. 1

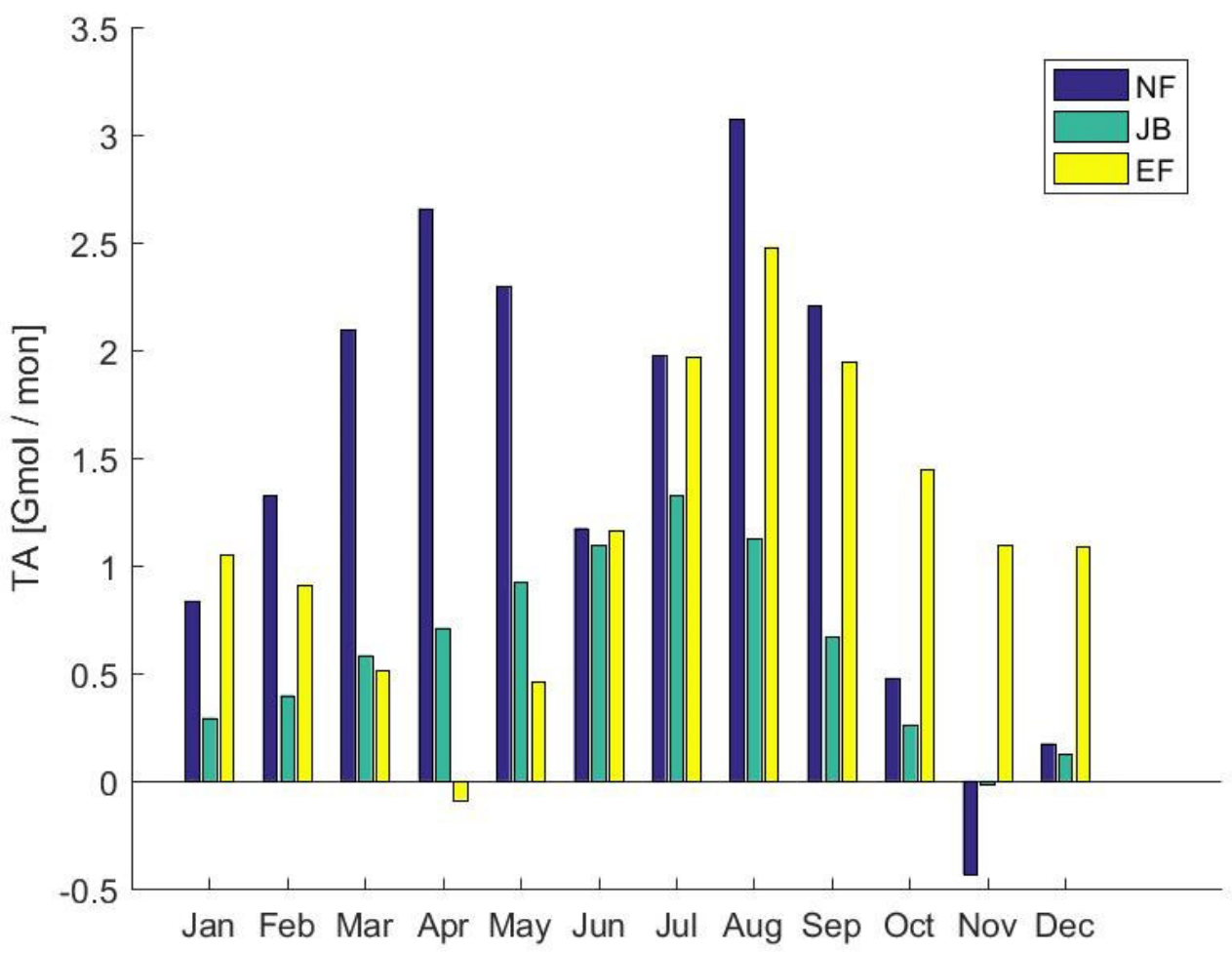
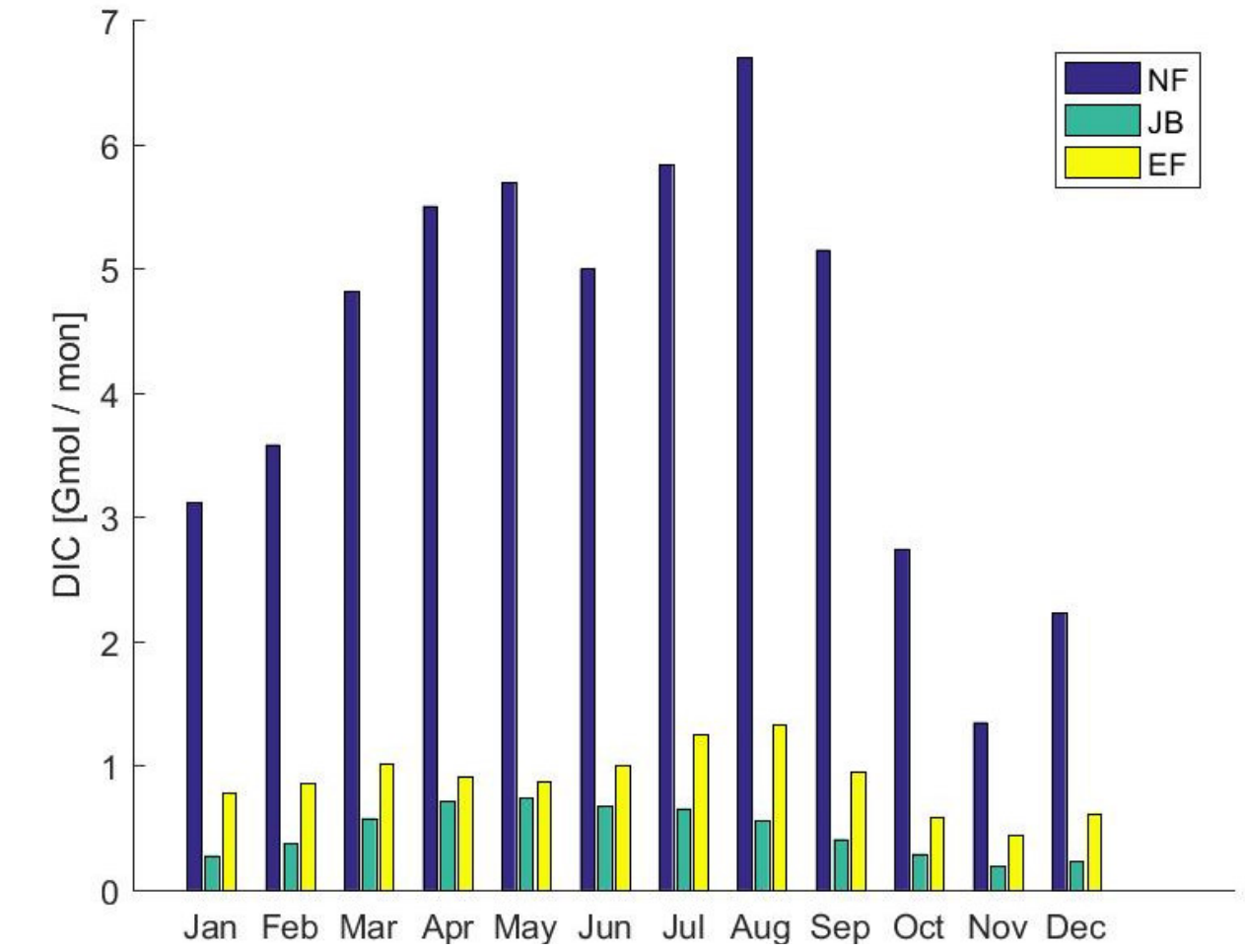


Fig. 2

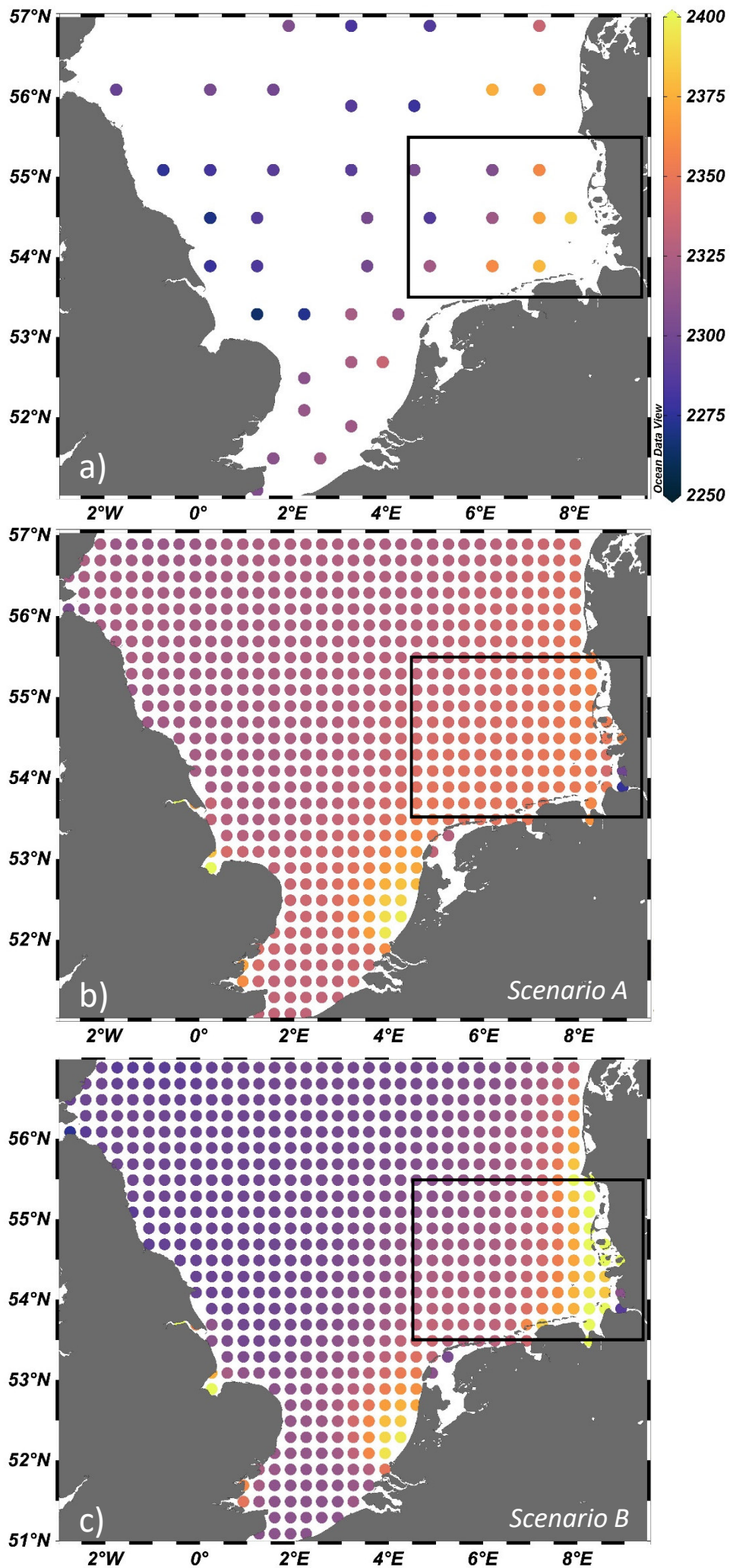


Fig. 3



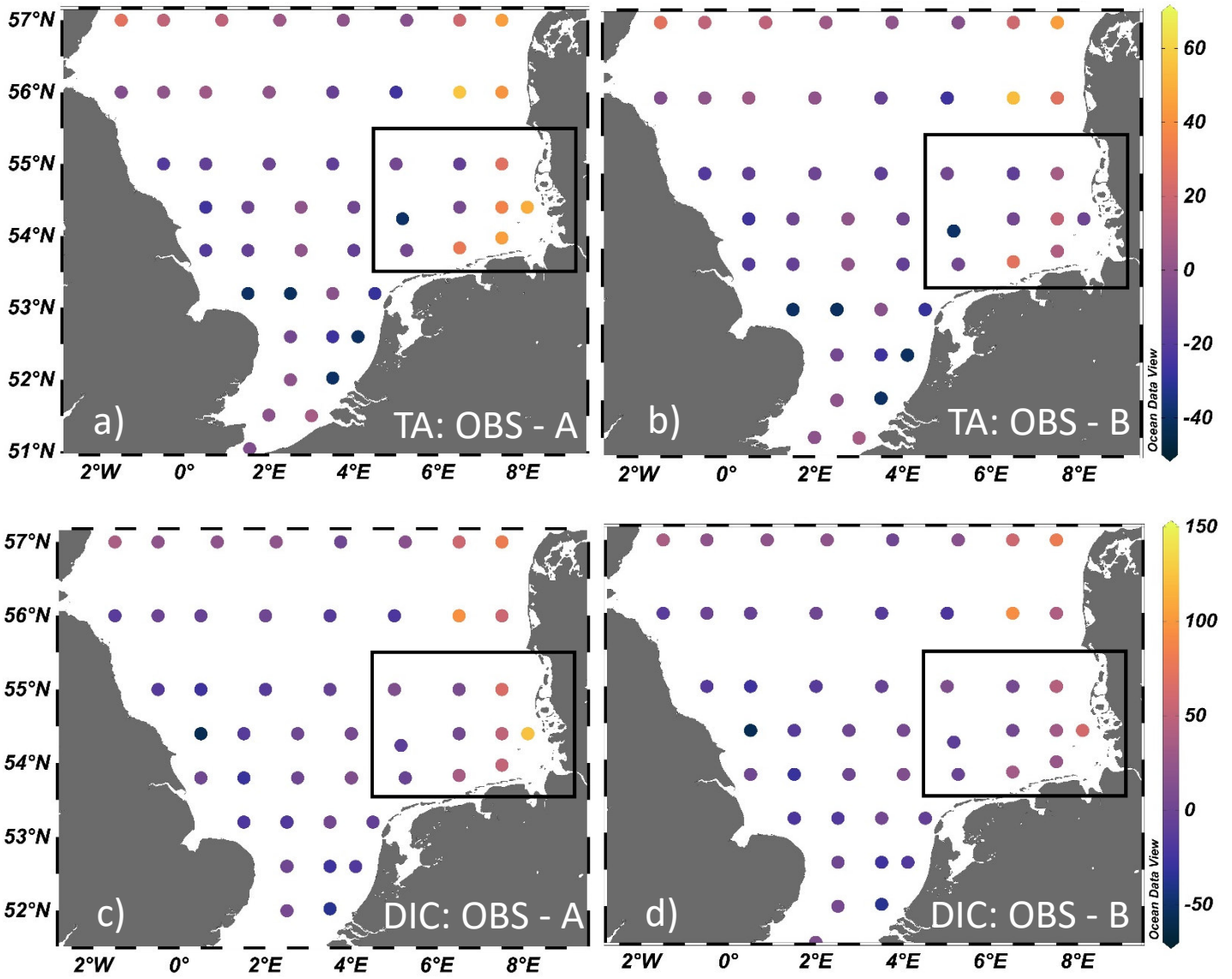


Fig. 4

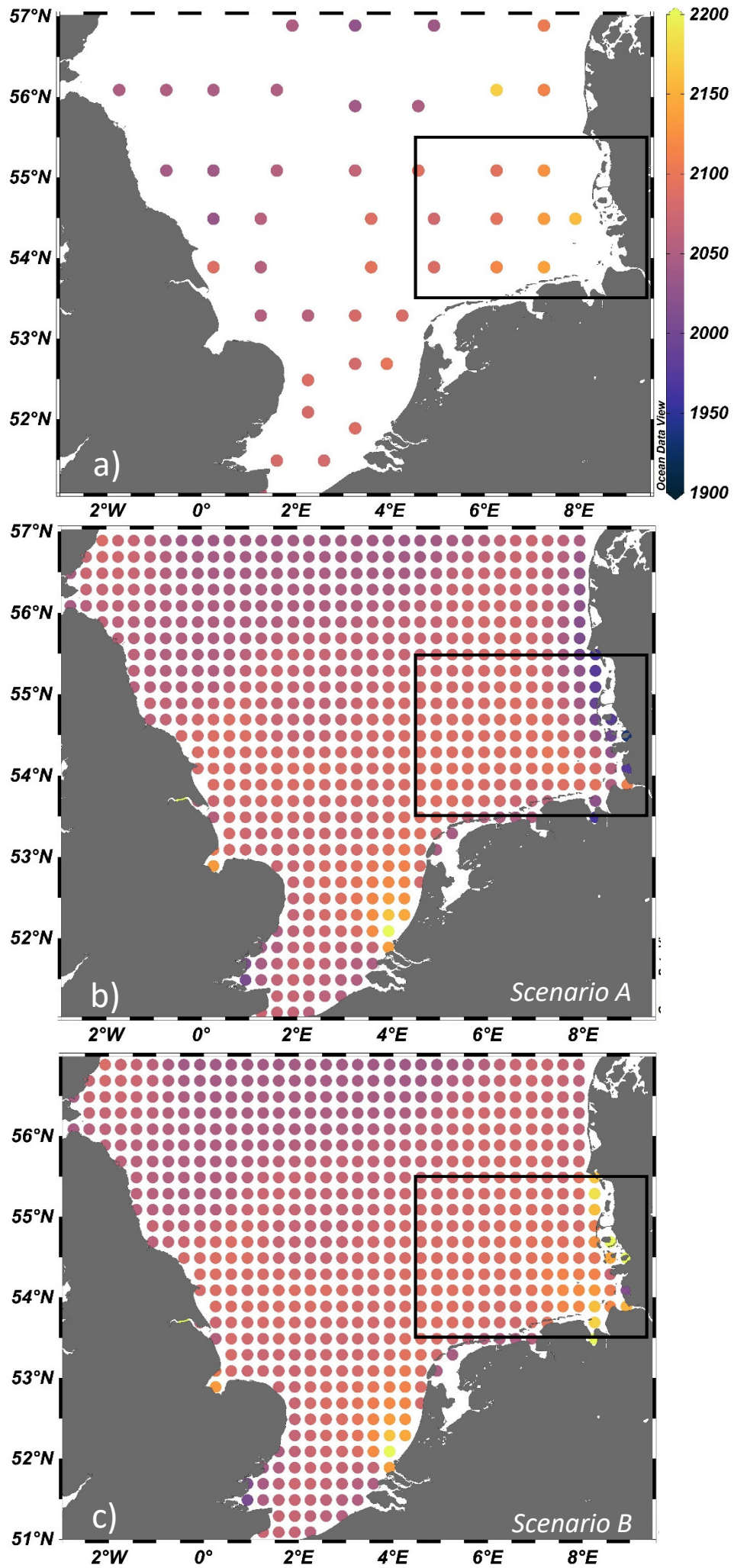


Fig. 5

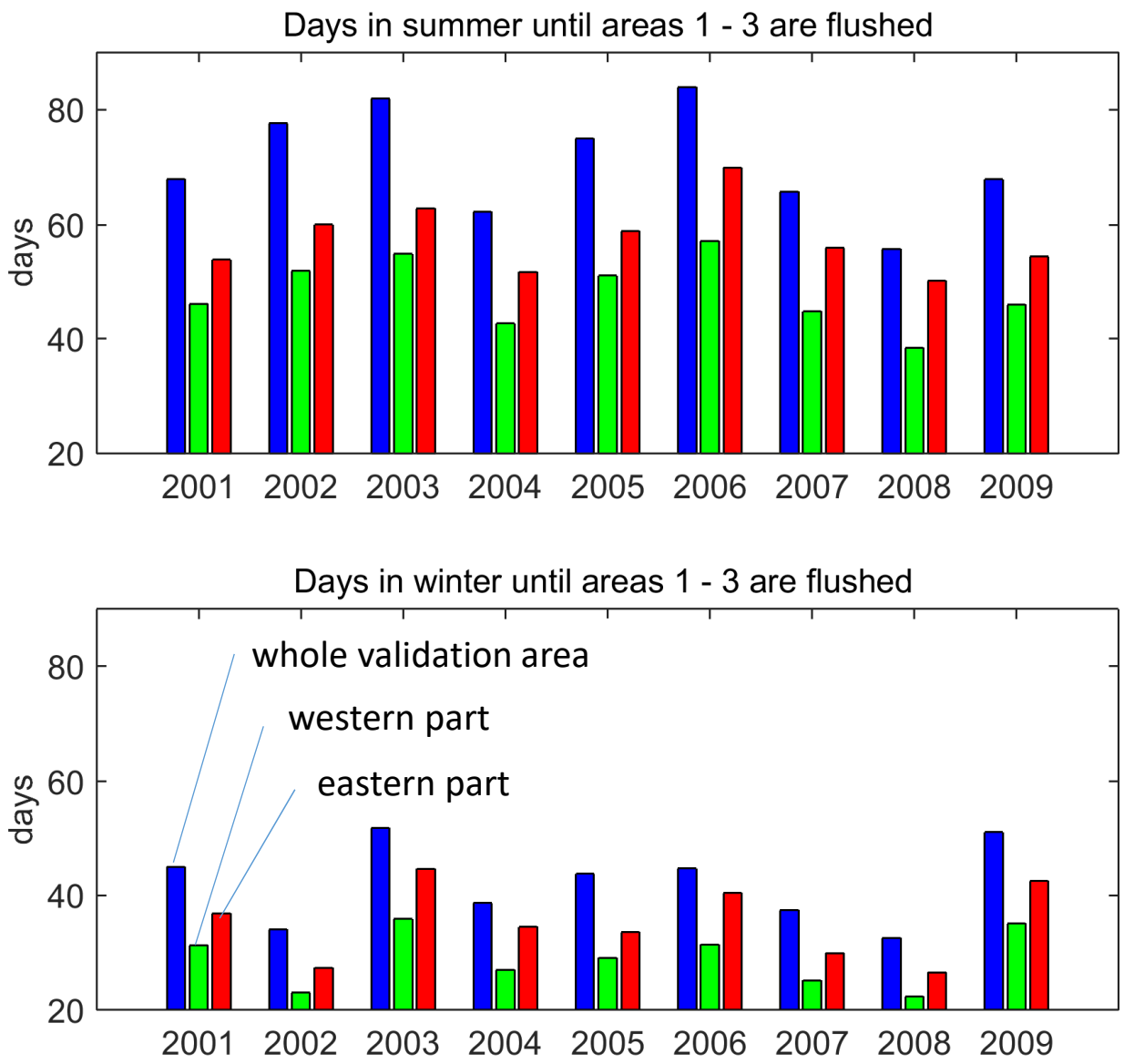


Fig. 6

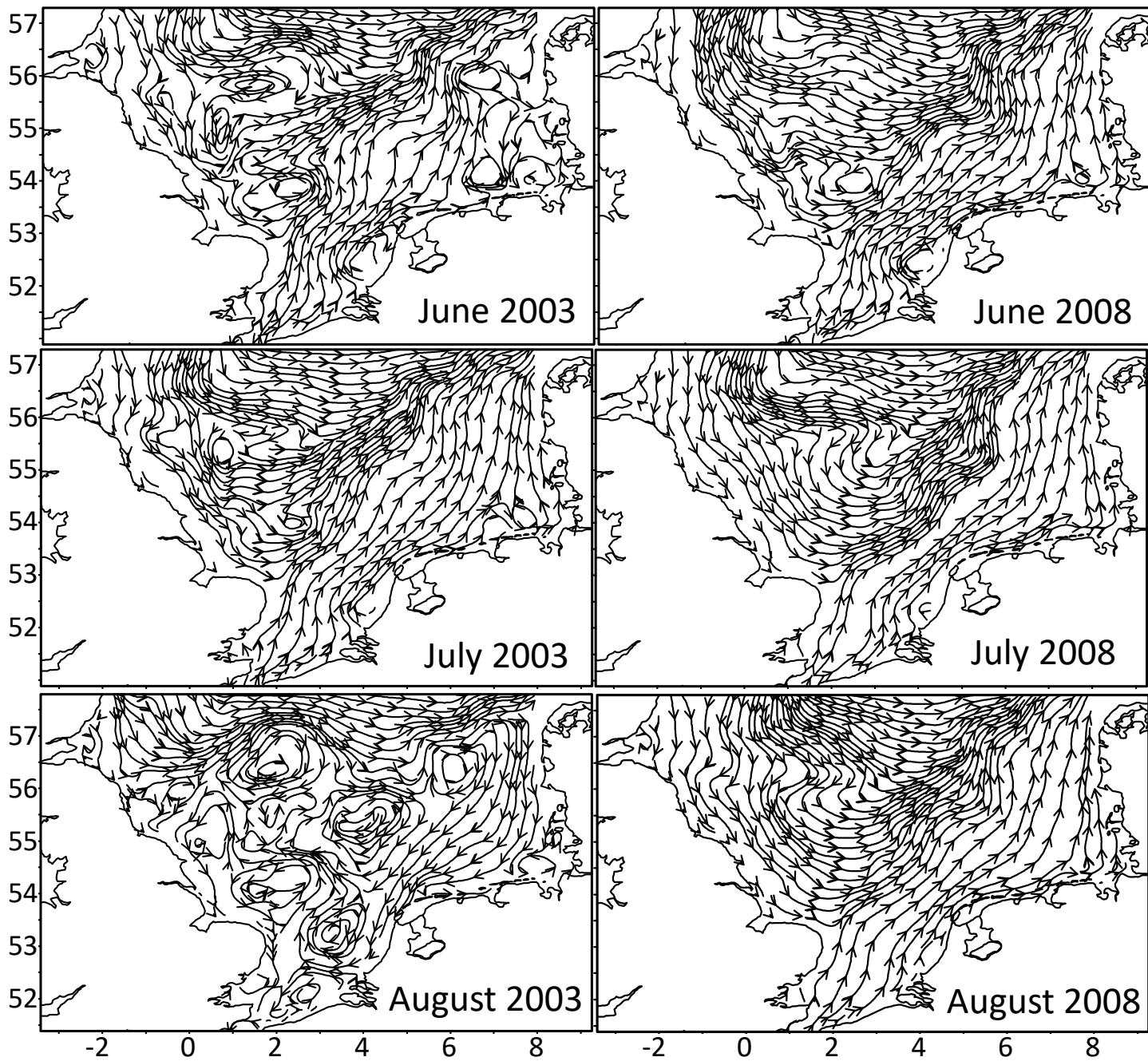


Fig. 7

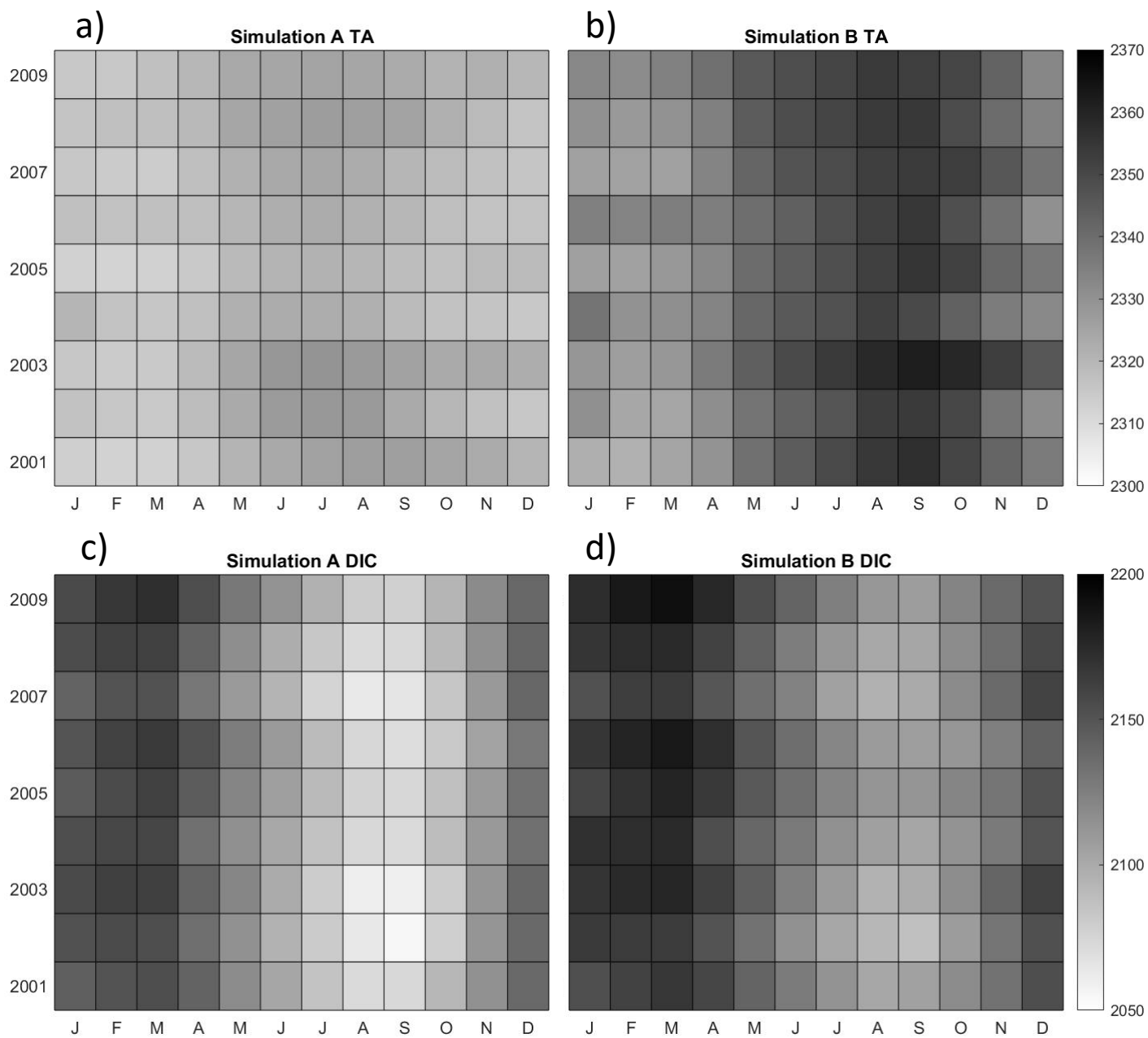


Fig. 8

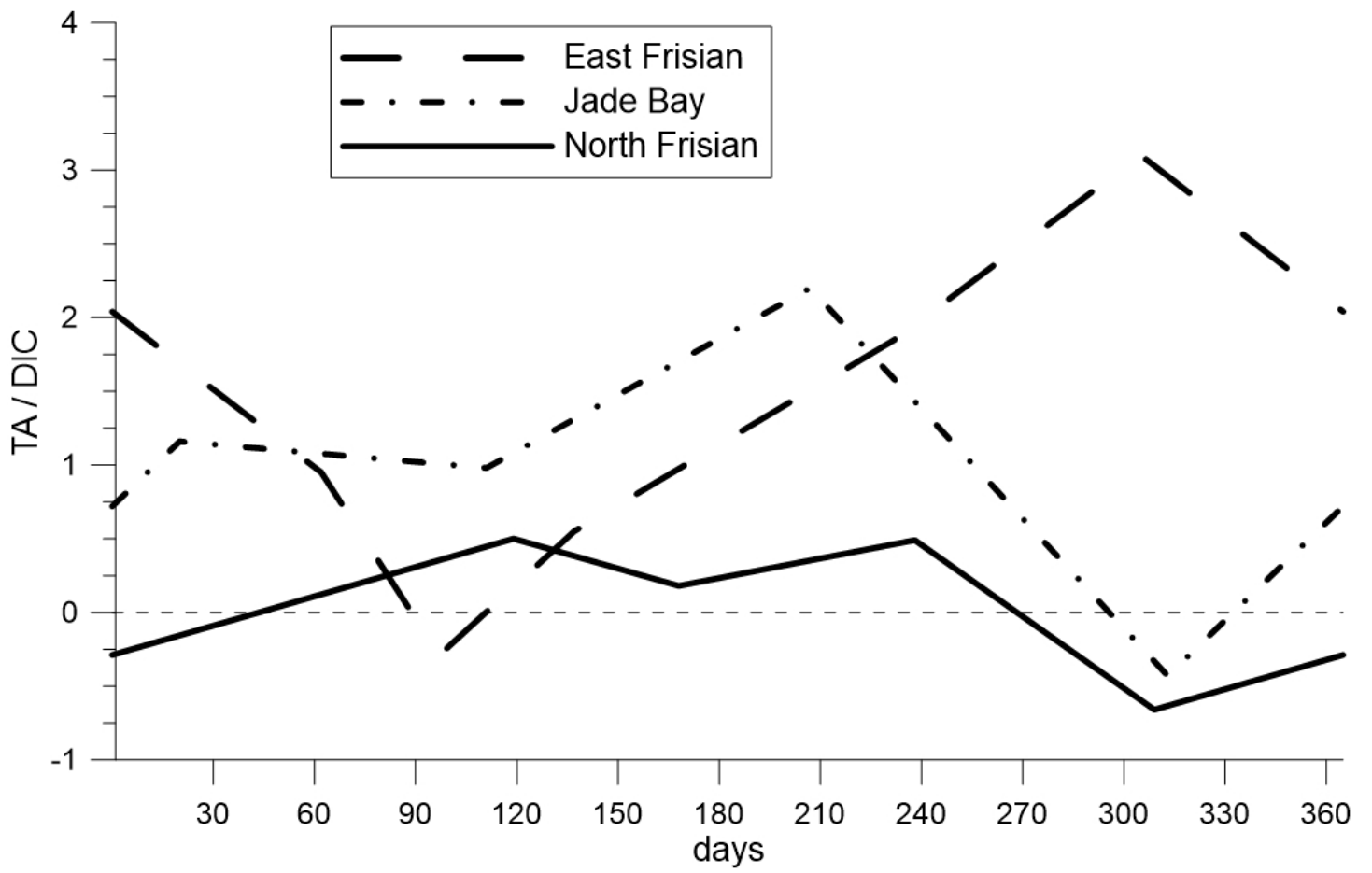


Fig. 9

# The impact of intertidal areas on the carbonate system of the southern North Sea

Fabian Schwichtenberg<sup>1,6</sup>, Johannes Pätsch<sup>1,5</sup>, Michael Ernst Böttcher<sup>2,3,4</sup>, Helmuth Thomas<sup>5</sup>,  
Vera Winde<sup>2</sup>, Kay-Christian Emeis<sup>5</sup>

<sup>1</sup> Theoretical Oceanography, Universität Hamburg, Bundesstr. 53, D-20146 Hamburg, Germany

<sup>2</sup> Geochemistry & Isotope Biogeochemistry Group, Department of Marine Geology, Leibniz Institute of Baltic Sea Research (IOW), Seestr. 15, D-18119 Warnemünde, Germany

<sup>3</sup> Marine Geochemistry, University of Greifswald, Friedrich-Ludwig-Jahn Str. 17a, D-17489 Greifswald, Germany

<sup>4</sup> Department of Maritime Systems, Interdisciplinary Faculty, University of Rostock, Albert-Einstein-Str. 21, D-18059 Rostock, Germany

<sup>5</sup> Institute of Coastal Research, Helmholtz Zentrum Geesthacht (HZG), Max-Planck-Str. 1, D-21502 Geesthacht, Germany

<sup>6</sup> Present Address: German Federal Maritime and Hydrographic Agency, Bernhard-Nocht-Str. 78, D-20359 Hamburg, Germany

Correspondence to Johannes Pätsch ([johannes.paetsch@uni-hamburg.de](mailto:johannes.paetsch@uni-hamburg.de))

## Abstract

The coastal ocean is strongly affected by ocean acidification because of its shallow water depths, low volume, and the closeness to terrestrial dynamics. Earlier observations of dissolved inorganic carbon (DIC) and total alkalinity (TA) in the southern part of the North Sea, a Northwest-European shelf sea, revealed lower acidification effects than expected. It has been assumed that anaerobic degradation and subsequent TA release in the adjacent back-barrier tidal areas ('Wadden Sea') in summer time is responsible for this phenomenon. In this study the exchange rates of TA and DIC between the Wadden Sea tidal basins and the North Sea and the consequences for the carbonate system in the German Bight are estimated using a 3-D ecosystem model. The aim of this study is to differentiate the various sources contributing to observed high summer TA ~~concentrations~~ in the southern North Sea.

30 Measured TA and DIC ~~concentrations~~ in the Wadden Sea are considered as model boundary  
31 conditions. This procedure acknowledges the dynamic behaviour of the Wadden Sea as an  
32 area of effective production and decomposition of organic material. According to the  
33 modelling results, 39 Gmol TA yr<sup>-1</sup> were exported from the Wadden Sea into the North Sea,  
34 which is less than a previous estimate, but within a comparable range. The interannual  
35 variabilities of TA and DIC ~~concentrations~~, mainly driven by hydrodynamic conditions, were  
36 examined for the years 2001 – 2009. Dynamics in the carbonate system is found to be related  
37 to specific weather conditions. The results suggest that the Wadden Sea is an important driver  
38 for the carbonate system in the southern North Sea. On average 41 % of TA inventory changes  
39 in the German Bight were caused by riverine input, 37 % by net transport from adjacent North  
40 Sea sectors, 16 % by Wadden Sea export, and 6 % are caused by internal net production of  
41 TA. The dominant role of river input for the TA inventory disappears when focussing on TA  
42 concentration changes due to the corresponding freshwater fluxes diluting the marine TA  
43 concentrations. The ratio of exported TA versus DIC reflects the dominant underlying  
44 biogeochemical processes in the Wadden Sea. Whereas, aerobic degradation of organic  
45 matter plays a key role in the North Frisian Wadden Sea during all seasons of the year,  
46 anaerobic degradation of organic matter dominated in the East Frisian Wadden Sea. Despite  
47 of the scarcity of high-resolution field data it is shown that anaerobic degradation in the  
48 Wadden Sea is one of the main contributors of elevated summer TA values in the southern  
49 North Sea.

50

## 51 **1. Introduction**

52 Shelf seas are highly productive areas constituting the interface between the inhabited coastal  
53 areas and the global ocean. Although they represent only 7.6 % of the world ocean's area,  
54 current estimates assume that they contribute approximately 21 % to total global ocean CO<sub>2</sub>  
55 sequestration (Borges, 2011). At the global scale the uncertainties of these estimates are  
56 significant due to the lack of spatially and temporally resolved field data. Some studies  
57 investigated regional carbon cycles in detail (e.g., Kempe & Pegler, 1991; Brasse et al., 1999;  
58 Reimer et al., 1999; Thomas et al., 2004; 2009; Artioli et al., 2012; Lorkowski et al., 2012; Burt  
59 et al., 2016; Shadwick et al., 2011; Laruelle et al., 2014; Carvalho et al., 2017) and pointed out  
60 sources of uncertainties specifically for coastal settings.



61 However, natural pH dynamics in coastal- and shelf- regions, for example, have been shown  
62 to be up to an order of magnitude higher than in the open ocean (Provoost et al, 2010).

63 Also, the nearshore effects of CO<sub>2</sub> uptake and acidification are difficult to determine, because  
64 of the shallow water depth and a possible superposition by benthic-pelagic coupling, and  
65 strong variations in fluxes of TA are associated with inflow of nutrients from rivers, pelagic  
66 nutrient driven production and respiration (Provoost et al., 2010), submarine groundwater  
67 discharge (SGD; Winde et al., 2014), and from benthic-pelagic pore water exchange (e.g.,  
68 Billerbeck et al., 2006; Riedel et al., 2010; Moore et al., 2011; Winde et al., 2014; Santos et al.,  
69 2012; 2015; Brenner et al., 2016; Burt et al., 2014; 2016; Seibert et al., 2019). Finally, shifts  
70 within the carbonate system are driven by impacts from watershed processes and modulated  
71 by changes in ecosystem structure and metabolism (Duarte et al., 2013).

72 Berner et al. (1970) and Ben-Yakoov (1973) were among the first who investigated elevated  
73 TA and pH variations caused by microbial dissimilatory sulphate reduction in the anoxic pore  
74 water of sediments. At the Californian coast, the observed enhanced TA export from  
75 sediments was related to the burial of reduced sulphur compounds (pyrite) (Dollar et al., 1991;  
76 Smith & Hollibaugh, 1993; Chambers et al., 1994). Other studies conducted in the Satilla and  
77 Altamaha estuaries and the adjacent continental shelf found non-conservative mixing lines of  
78 TA versus salinity, which was attributed to anaerobic TA production in nearshore sediments  
79 (Wang & Cai, 2004; Cai et al., 2010). Iron dynamics and pyrite formation in the Baltic Sea were  
80 found to impact benthic TA generation from the sediments (Gustafsson et al., 2019; Łukawska-  
81 Matuszewska and Graca, 2017).

82 The focus of the present study is the southern part of the North Sea, located on the Northwest-  
83 European Shelf. This shallow part of the North Sea is connected with the tidal basins of the  
84 Wadden Sea via channels between barrier islands enabling an exchange of water, and  
85 dissolved and suspended material (Rullkötter, 2009; Lettmann et al., 2009; Kohlmeier and  
86 Ebenhöf, 2009). The Wadden Sea extends from Den Helder (The Netherlands) in the west to  
87 Esbjerg (Denmark) in the north and covers an area of about 9500 km<sup>2</sup> (Ehlers, 1994). The  
88 entire system is characterised by semidiurnal tides with a tidal range between 1.5 m in the  
89 westernmost part and 4 m in the estuaries of the rivers Weser and Elbe (Streif, 1990). During  
90 low tide about 50 % of the area are falling dry (van Beusekom et al., 2019). Large rivers  
91 discharge nutrients into the Wadden Sea, which in turn shows a high degree of eutrophication,

92 aggravated by mineralisation of organic material imported into the Wadden Sea from the  
93 open North Sea (van Beusekom et al., 2012).

94 In comparison to the central and northern part of the North Sea, TA concentrationslevels in  
95 the southern part are significantly elevated during summer (Salt et al., 2013; Thomas et al.,  
96 2009; Brenner et al., 2016; Burt et al., 2016). The observed high TA concentrationslevels have  
97 been attributed to an impact from the adjacent tidal areas (Hoppema, 1990; Kempe & Pegler,  
98 1991; Brasse et al., 1999; Reimer et al., 1999; Thomas et al., 2009; Winde et al., 2014), but this  
99 impact has not been rigorously quantified. Using several assumptions, Thomas et al. (2009)  
100 calculated an annual TA export from the Wadden Sea / Southern Bight of 73 Gmol TA yr<sup>-1</sup> to  
101 close the TA budget for the southern North Sea.

102 The aim of this study is to reproduce the elevated summer concentrationslevels of TA in the  
103 southern North Sea with a 3D biogeochemical model that has TA as prognostic variable. With  
104 this tool at hand, we balance the budget TA in the relevant area on an annual basis.  
105 Quantifying the different budget terms, like river input, Wadden Sea export, internal pelagic  
106 and benthic production, degradation and respiration allows us to determine the most  
107 important contributors to TA variations. In this way we refine the budget terms by Thomas et  
108 al. (2009) and replace the original closing term by data. The new results are discussed on the  
109 background of the budget approach proposed by Thomas et al. (2009).

## 110 **2. Methods**

### 111 **2.1. Model specifications**

#### 112 ***2.1.1. Model domain and validation area***

113 The ECOHAM model domain for this study (Fig. 1) was first applied by Pätsch et al. (2010). For  
114 model validations (magenta: validation area, Fig. 1), an area was chosen that includes the  
115 German Bight as well as parts along the Danish and the Dutch coast. The western boundary of  
116 the validation area is situated at 4.5° E. The southern and northern boundaries are at 53.5°  
117 and 55.5° N, respectively. The validation area is divided by the magenta dashed line at 7° E  
118 into the western and eastern part. For the calculation of box averages of DIC and TA a bias  
119 towards the deeper areas with more volume and more data should be avoided. Therefore,  
120 each water column covered with data within the validation area delivered one mean value,  
121 which is calculated by vertical averaging. These mean water column averages were

122 horizontally interpolated onto the model grid. After this procedure average box values were  
123 calculated. In case of box-averaging model output, the same procedure was applied, but  
124 without horizontal interpolation.

### 125 **2.1.2. The hydrodynamic module**

126 The physical parameters temperature, salinity, horizontal and vertical advection as well as  
127 turbulent mixing were calculated by the submodule HAMSOM (Backhaus, 1985), which was  
128 integrated in the ECOHAM model. It is a baroclinic primitive equation model using the  
129 hydrostatic and Boussinesq approximation. It is applied to several regional sea areas  
130 worldwide (Mayer et al., 2018; Su & Pohlmann, 2009). Details are described by Backhaus &  
131 Hainbucher (1987) and Pohlmann (1996). The hydrodynamic model ran prior to the  
132 biogeochemical part. Daily result fields were stored for driving the biogeochemical model in  
133 offline mode. Surface elevation, temperature and salinity resulting from the Northwest-  
134 European Shelf model application (Lorkowski et al., 2012) were used as boundary conditions  
135 at the southern and northern boundaries. The temperature of the shelf run by Lorkowski et  
136 al. (2012) showed a constant offset compared with observations (their Fig. 3), because  
137 incoming solar radiation was calculated too high. For the present simulations the shelf run has  
138 been repeated with adequate solar radiation forcing.

139 River-induced horizontal transport due to the hydraulic gradient is incorporated (Große et al.,  
140 2017; Kerimoglu et al., 2018). This component of the hydrodynamic horizontal transport  
141 corresponds to the amount of freshwater discharge.

142 Within this study we use the term flushing time. It is the average time when a basin is filled  
143 with laterally advected water. The flushing time depends on the specific basin: large basins  
144 have usually higher flushing times than smaller basins. High flushing times correspond with  
145 low water renewal times.

### 146 **2.1.3. The biogeochemical module**

147 The relevant biogeochemical processes and their parameterisations have been detailed in  
148 Lorkowski et al. (2012). In former model setups TA was restored to prescribed values derived  
149 from observations (Thomas et al., 2009) with a relaxation time of two weeks (Kühn et al., 2010;  
150 Lorkowski et al., 2012). The changes in TA treatment for the study at hand is described below.  
151 Results from the Northwest-European Shelf model application (Lorkowski et al., 2012) were

152 used as boundary conditions for the recent biogeochemical simulations at the southern and  
153 northern boundaries (Fig. 1).

154 The main model extension was the introduction of a prognostic treatment of TA in order to  
155 study the impact of biogeochemical and physical driven changes of TA onto the carbonate  
156 system and especially on acidification (Pätsch et al., 2018). The physical part contains  
157 advective and mixing processes as well as dilution by riverine freshwater input. The pelagic  
158 biogeochemical part is driven by planktonic production and respiration, formation and  
159 dissolution of calcite, pelagic and benthic degradation and remineralisation, and also by  
160 atmospheric deposition of reduced and oxidised nitrogen. All these processes impact TA. In  
161 this model version benthic denitrification has no impact on pelagic TA ~~concentrations~~. Other  
162 benthic anaerobic processes are not considered. Only the carbonate ions from benthic calcite  
163 dilution increase pelagic TA ~~concentrations~~. Aerobic remineralisation releases ammonium  
164 and phosphate, which enter the pelagic system across the benthic-pelagic interface and alter  
165 the pelagic TA ~~concentration~~. The theoretical background to this has been outlined by Wolf-  
166 Gladrow et al. (2007).

167 The years 2001 to 2009 were simulated with 3 spin up years in 2000. Two different scenarios  
168 (A and B) were conducted. Scenario A is the reference scenario without implementation of  
169 any Wadden Sea processes. For scenario B we used the same model configuration as for  
170 scenario A and additionally implemented Wadden Sea export rates of TA and DIC as described  
171 in section 2.3.1. The respective Wadden Sea export rates (Fig. 2) are calculated by the  
172 temporal integration of the product of wad\_sta and wad\_exc over one month (see section  
173 2.3.1, equation 2).

## 174 **2.2. External sources and boundary conditions**

### 175 **2.2.1. Freshwater discharge**

176 Daily data of freshwater fluxes from 16 rivers were used (Fig. 1). For the German Bight and the  
177 other continental rivers daily observations of runoff provided by Pätsch & Lenhart (2008) were  
178 incorporated. The discharges of the rivers Elbe, Weser and Ems were increased by 21 %, 19 %  
179 and 30 % in order to take additional drainage into account that originated from the area  
180 downstream of the respective points of observation (Radach and Pätsch, 2007). The respective  
181 tracer loads were increased accordingly. The data of Neal (2002) were implemented for the

182 British rivers for all years with daily values for freshwater. The annual amounts of freshwater  
183 of the different rivers are shown in the appendix (Table A1). Riverine freshwater discharge  
184 was also considered for the calculation of the concentrations of all biogeochemical tracers in  
185 the model.

## 186 **2.2.2. River input**

### 187 **Data sources**

188 River load data for the main continental rivers were taken from the report by Pätsch & Lenhart  
189 (2008) that was kept up to date continuously so that data for the years 2007 – 2009 were also  
190 available ([https://wiki.cen.uni-hamburg.de/ifm/ECOHAM/DATA\\_RIVER](https://wiki.cen.uni-hamburg.de/ifm/ECOHAM/DATA_RIVER)). They calculated  
191 daily loads of nutrients and organic matter based on data provided by the different river  
192 authorities. Additionally, loads of the River Eider were calculated according to Johannsen et  
193 al. (2008).

194 Up to now, all ECOHAM applications used constant riverine DIC concentrations. TA was not  
195 used. For the study at hand we introduced time varying riverine TA and DIC  
196 ~~concentrations-values~~. New data of freshwater discharge were introduced, as well as TA and  
197 DIC loads for the British rivers (Neal, 2002). Monthly mean concentrations of nitrate, TA and  
198 DIC were added for the Dutch rivers ([www.waterbase.nl](http://www.waterbase.nl)) and for the German river Elbe  
199 (Amann et al., 2015). The Dutch river data were observed in the years 2007 – 2009. The river  
200 Elbe data were taken in the years 2009 – 2011. These concentration data were prescribed for  
201 all simulation years as mean annual cycle.

202 The data sources and positions of the river mouths of all 16 rivers are shown in Table A2 and  
203 in Fig. 1. The respective riverine concentrations of TA and DIC are given in Table A3.  
204 Schwichtenberg (2013) describes the river data in detail.

205 A few small flood gates (“Siel”) and rivers transport fresh water from the recharge areas into  
206 the intertidal areas (Streif, 1990). The recharge areas for these inlets differ considerably from  
207 each other, leading to different relative contributions for the fresh water input. Whereas the  
208 catchments of Schweiburger Siel (22.2 km<sup>2</sup>) and the Hooksiel Binnentief are only of minor  
209 importance, the Vareler Siel, the Eckenwarder Siel, and the Maade Siel are of medium  
210 importance, and the highest contribution may originate from the Wangersiel, the Dangaster  
211 Siel, and the Jade-Wapeler Siel (Lipinski, 1999).

212

### 213 **Effective river input**

214 In order to analyse the net effect on concentrations in the sea due to river input, the effective  
215 river input ( $Riv_{eff}$  [Gmol yr<sup>-1</sup>]) is introduced:

216

$$Riv_{eff} = \frac{\Delta C|_{riv}}{\rho \cdot yr} \cdot V \cdot C \quad (1)$$

217

218 with  $\Delta C|_{riv}$  [μmol kg<sup>-1</sup>]: the concentration change in the river mouth cell due to river load  $riv$   
219 and the freshwater flux from the river.  $V$  [l] is the volume of the river mouth cell,  $\rho$  [kg l<sup>-1</sup>]  
220 density of water,  $yr$  is one year,  $C$  [10<sup>-15</sup> l<sup>-1</sup>] is a constant.

221 Bulk alkalinity discharged by rivers is quite large but most of the rivers entering the North Sea  
222 (here the German Bight) have lower TA concentrations than the sea water. In case of identical  
223 concentrations, the effective river load  $Riv_{eff}$  is zero. The TA related molecules enter the sea,  
224 and in most cases, they are leaving it via transport. In case of tracing or budgeting both the  
225 real TA river discharge and the transport must be recognized. In order to understand TA  
226 concentration changes in the sea  $Riv_{eff}$  is appropriate.

227

### 228 **2.2.3. Meteorological forcing**

229 The meteorological forcing was provided by NCEP Reanalysis (Kalnay et al., 1996) and  
230 interpolated on the model grid field. It consisted of six-hourly fields of air temperature,  
231 relative humidity, cloud coverage, wind speed, atmospheric pressure, and wind stress for  
232 every year. 2-hourly and daily mean short wave radiation were calculated from astronomic  
233 insolation and cloudiness with an improved formula (Lorkowski et al., 2012).

## 234 **2.3. The Wadden Sea**

### 235 **2.3.1. Implementation of Wadden Sea dynamics**

236 For the present study the exchange of TA and DIC between North Sea and Wadden Sea was  
237 implemented into the model by defining sinks and sources of TA and DIC for some of the  
238 south-eastern cells of the North Sea grid (Fig. 1). The cells with adjacent Wadden Sea were

239 separated into three exchange areas: The East Frisian, the North Frisian Wadden Sea and the  
240 Jade Bay, marked by “E”, “N” and “J” (Fig. 1, right side).

241 Two parameters were determined in order to quantify the TA and DIC exchange between the  
242 Wadden Sea and the North Sea.

- 243 1. Concentration changes of pelagic TA and DIC in the Wadden Sea during one tide, and
- 244 2. Water mass exchange between the back-barrier islands and the open sea during one  
245 tide

246 Measured concentrations of TA and DIC (Winde, 2013; Winde et al., 2014) as well as modelled  
247 water mass exchange rates of the export areas by Grashorn (2015) served as bases for the  
248 calculated exchange. Details on flux calculations and measurements are described below. The  
249 daily Wadden Sea exchange of TA and DIC was calculated as:

$$wad\_flu = \frac{wad\_sta * wad\_exc}{vol} \quad (2)$$

250 Differences in measured concentrations in the Wadden Sea during rising and falling water  
251 levels, as described in section 2.3.2, were temporally interpolated and summarized as *wad\_sta*  
252 [mmol m<sup>-3</sup>]. Modelled daily Wadden Sea exchange rates of water masses (tidal prisms during  
253 falling water level) were defined as *wad\_exc* [m<sup>3</sup> d<sup>-1</sup>], and the volume of the corresponding  
254 North Sea grid cell was *vol* [m<sup>3</sup>]. *wad\_flu* [mmol m<sup>-3</sup> d<sup>-1</sup>] were the daily concentration changes  
255 of TA and DIC in the respective North Sea grid cells.

256 In fact, some amounts of the tidal prisms return without mixing with North Sea water, and  
257 calculations of Wadden Sea – North Sea exchange should therefore consider flushing times in  
258 the respective back-barrier areas. Since differences in measured concentrations between  
259 rising and falling water levels were used, this effect is already assumed to be represented in  
260 the data. This approach enabled the use of tidal prisms without consideration of any flushing  
261 times.

### 262 **2.3.2. Wadden Sea - measurements**

263 The flux calculations for the Wadden Sea – North Sea exchange were carried out in tidal basins  
264 of the East and North Frisian Wadden Sea (Spiekeroog Island, Sylt-Rømø) as well as in the Jade  
265 Bay. For the present study seawater samples representing tidal cycles during different seasons

266 (Winde, 2013). The mean concentrations of TA and DIC during rising and falling water levels  
267 and the respective differences ( $\Delta$ TA and  $\Delta$ DIC) are given in Table 1. Measurements in August  
268 2002 were taken from Moore et al. (2011). The  $\Delta$ -values were used as *wad\_sta* and were  
269 linearly interpolated between the times of observations for the simulations. In this procedure,  
270 the linear progress of the  $\Delta$ -values does not represent the natural behaviour perfectly,  
271 especially if only few data are available. As a consequence, possible short events of high TA  
272 and DIC export rates that occurred in periods outside the observation periods may have been  
273 missed.

274 Due to the low number of concentration measurements a statistical analysis of uncertainties  
275 of  $\Delta$ TA and  $\Delta$ DIC was not possible. They were measured with a lag of 2 hours after low tide  
276 and high tide. This was done in order to obtain representative concentrations of rising and  
277 falling water levels. As a consequence, only 2 - 3 measurements for each location and season  
278 were considered for calculations of  $\Delta$ TA and  $\Delta$ DIC.

### 279 **2.3.3. Wadden Sea – modelling the exchange rates**

280 Grashorn (2015) performed the hydrodynamic computations of exchanged water masses  
281 (*wad\_exc*) with the model FVCOM (Chen et al., 2003) by adding up the cumulative seaward  
282 transport during falling water level (tidal prisms) between the back-barrier islands that were  
283 located near the respective ECOHAM cells with adjacent Wadden Sea area. These values are  
284 given in Table 2 for each ECOHAM cell in the respective export areas. The definition of the first  
285 cell N1 and the last cell E4 is in accordance to the clockwise order in Fig. 1 (right side). The  
286 mean daily runoff of all N-, J- and E-positions was  $8.1 \text{ km}^3 \text{ d}^{-1}$ ,  $0.8 \text{ km}^3 \text{ d}^{-1}$  and  $2.3 \text{ km}^3 \text{ d}^{-1}$   
287 respectively.

### 288 **2.3.4. Additional Sampling of DIC and TA**

289 DIC and TA ~~concentrations~~ for selected freshwater inlets sampled in October 2010 and May  
290 2011 are presented in Table 3. Sampling and analyses took place as described by Winde et al.  
291 (2014) and are here reported for completeness and input for discussion only. The autumn data  
292 are deposited under doi:10.1594/PANGEA.841976. The samples for TA measurements were  
293 filled without headspace into pre-cleaned 12 ccm Exetainer<sup>®</sup>, filled with 0.1 ml saturated  $\text{HgCl}_2$   
294 solution. The samples for DIC analysis were completely filled into 250 ccm ground-glass-  
295 stoppered bottles, and then poisoned with 100  $\mu\text{l}$  of a saturated  $\text{HgCl}_2$  solution. The DIC  
296 concentrations were determined at IOW by coulometric titration according to Johnson et al.



297 (1993), using reference material provided by A. Dickson (University of California, San Diego;  
298 Dickson et al., 2003) for the calibration (batch 102). TA was measured by potentiometric  
299 titration using HCl using a Schott titri plus equipped with an IOline electrode A157. Standard  
300 deviations for DIC and TA measurements were better than +/-2 and +/-10  $\mu\text{mol kg}^{-1}$ ,  
301 respectively.

302

#### 303 **2.4. Statistical analysis**

304 A statistical overview of the simulation results in comparison to the observations (Salt et al.,  
305 2013) is given in Table 4 and 5. In the validation area (magenta box in Fig. 1) observations of  
306 10 different stations were available, each with four to six measurements at different depths  
307 (51 measured points). Measured TA and DIC ~~concentrations~~ of each point were compared with  
308 modelled TA and DIC ~~concentrations~~ in the respective grid cells, respectively. The standard  
309 deviations (Stdv), the root means square errors (RMSE), and correlation coefficients (r) were  
310 calculated for each simulation. In addition to the year 2008, which we focus on in this study,  
311 observations were performed at the same positions in summer 2005 and 2001. These data are  
312 also statistically compared with the model results.

### 313 **3. Results**

#### 314 **3.1. Model validation - TA ~~concentrations~~ in summer 2008**

315 The results of scenarios A and B were compared with observations of TA in August 2008 (Salt  
316 et al., 2013) for surface water. The observations revealed high TA ~~concentrations~~levels in the  
317 German Bight (east of 7° E and south of 55° N) and around the Danish coast (around 56° N) as  
318 shown in Fig. 3a. The observed concentrations in these areas ranged between 2350 and  
319 2387  $\mu\text{mol TA kg}^{-1}$ . These findings were in accordance with observed TA ~~concentrations~~ in  
320 August / September 2001 (Thomas et al., 2009). TA ~~concentrations~~ in other parts of the  
321 observation domain ranged between 2270  $\mu\text{mol TA kg}^{-1}$  near the British coast (53° N – 56° N)  
322 and 2330  $\mu\text{mol TA kg}^{-1}$  near the Dutch coast and the Channel. In the validation box the overall  
323 average and the standard deviation of all observed TA concentrations (Stdv) was 2334 and  
324 33  $\mu\text{mol TA kg}^{-1}$ , respectively.

325 In scenario A the simulated surface TA ~~concentrations~~ showed a more homogeneous pattern  
326 than observations with maximum values of 2396  $\mu\text{mol TA kg}^{-1}$  at the western part of the Dutch

327 coast and even higher ( $2450 \mu\text{mol TA kg}^{-1}$ ) in the river mouth of the Wash estuary at the British  
328 coast. Minimum values of  $2235$  and  $2274 \mu\text{mol TA kg}^{-1}$  were simulated at the mouths of the  
329 rivers Elbe and Firth of Forth. The modelled TA ~~concentration~~ ranged from  $2332$  to  
330  $2351 \mu\text{mol TA kg}^{-1}$  in the German Bight and in the Jade Bay. Strongest underestimations in  
331 relation to observations are located in a band close to the coast stretching from the East  
332 Frisian Islands to  $57^\circ \text{N}$  at the Danish coast (Fig. 4a). The deviation of simulation results of  
333 scenario A from observations in the validation box was represented by a RMSE of  
334  $28 \mu\text{mol TA kg}^{-1}$ . The standard deviation was  $7 \mu\text{mol TA kg}^{-1}$  and the correlation amounted to  
335  $r = 0.77$  (Table 4). In the years 2005 and 2001 similar statistical values are found, but the  
336 correlation coefficient was smaller.

337 The scenario B was based on a Wadden Sea export of TA and DIC as described above. The  
338 major difference in TA ~~concentrations~~ of this scenario compared to A occurred east of  $6.5^\circ \text{E}$ .  
339 Surface TA ~~concentrations~~ there peaked in the Jade Bay ( $2769 \mu\text{mol TA kg}^{-1}$ ) and were  
340 elevated off the North Frisian and Danish coasts from  $54.2^\circ$  to  $56^\circ \text{N}$  ( $> 2400 \mu\text{mol TA kg}^{-1}$ ).  
341 Strongest underestimations in relation to observations are noted off the Danish coast  
342 between  $56^\circ$  and  $57^\circ \text{N}$  (Fig. 4b). In the German Bight the model overestimated the  
343 observations slightly, while at the East Frisian Islands the model underestimates TA. When  
344 approaching the Dutch Frisian Islands the simulation overestimates TA compared to  
345 observations and strongest overestimations can be seen near the river mouth of River Rhine.  
346 Compared to scenario A the simulation of scenario B was closer to the observations in terms  
347 of RMSE ( $18 \mu\text{mol TA kg}^{-1}$ ) and the standard deviation (Stdv =  $22 \mu\text{mol TA kg}^{-1}$ ). Also, the  
348 correlation ( $r = 0.86$ ) improved (Table 4). In the years 2001 and 2005 the observed mean  
349 values are slightly overestimated by the model. The statistical values for 2001 are better than  
350 for 2005, where scenario A better compares with the observations.

351

### 352 **3.2. Model validation - DIC concentrations in summer 2008**

353 Analogously to TA the simulation results were compared with surface observations of DIC  
354 ~~concentrations~~ in summer 2008 (Salt et al., 2013). They also revealed high values in the  
355 German Bight (east of  $7^\circ \text{E}$  and south of  $55^\circ \text{N}$ ) and around the Danish coast (near  $56^\circ \text{N}$ ) which  
356 is shown in Fig. 5. The observed DIC concentrations in these areas ranged between  $2110$  and  
357  $2173 \mu\text{mol DIC kg}^{-1}$ . Observed DIC concentrations in other parts of the model domain ranged

358 between 2030 and 2070  $\mu\text{mol DIC kg}^{-1}$  in the north western part and 2080 - 2117  $\mu\text{mol DIC kg}^{-1}$   
359  $^{-1}$  at the Dutch coast. In the validation box the overall average and the standard deviation of  
360 all observed DIC concentrations were 2108 and 25.09  $\mu\text{mol DIC kg}^{-1}$ , respectively.

361 The DIC concentrations in scenario A ranged between 1935 and 1977  $\mu\text{mol DIC kg}^{-1}$  at the  
362 North Frisian and Danish coast (54.5° N - 55.5° N) and 1965  $\mu\text{mol DIC kg}^{-1}$  in the Jade Bay.  
363 Maxima of up to 2164  $\mu\text{mol DIC kg}^{-1}$  were modelled at the western part of the Dutch coast  
364 north of the mouth of River Rhine (Fig. 5). The DIC concentrations in the German Bight showed  
365 a heterogeneous pattern in the model, and sometimes values decreased from west to east,  
366 which contrasts the observations (Fig. 5a). This may be the reason for the negative correlation  
367 coefficient  $r = -0.64$  between model and observations (Table 5). The significant deviation from  
368 observation of results from scenario A is also indicated by the RMSE of 43  $\mu\text{mol DIC kg}^{-1}$ , and  
369 a standard deviation of 14  $\mu\text{mol DIC kg}^{-1}$ . In 2001 and 2005 the simulation results of this  
370 scenario A are better, which is expressed in positive correlation coefficients and small RMSE  
371 values.

372 In scenario B the surface DIC concentrations at the Wadden Sea coasts increased: The North  
373 Frisian coast shows concentrations of up to 2200  $\mu\text{mol DIC kg}^{-1}$  while the German Bight has  
374 values of 2100 – 2160  $\mu\text{mol DIC kg}^{-1}$ , and Jade Bay concentrations were higher than  
375 2250  $\mu\text{mol DIC kg}^{-1}$ . The other areas are comparable to scenario A. In scenario B the RMSE in  
376 the validation box decreased to 26  $\mu\text{mol DIC kg}^{-1}$  in comparison to scenario A. The standard  
377 deviation decreased to 9.1  $\mu\text{mol DIC kg}^{-1}$ , and the correlation improved to  $r = 0.55$  (Table 5).  
378 The average values are close to the observed ones for all years, even though in 2005 a large  
379 RMSE was found.

380 The comparison between observations and simulation results of scenario A (Fig. 4c) clearly  
381 show model underestimations in the south-eastern area and are strongest in the inner  
382 German Bight towards the North Frisian coast ( $> 120 \mu\text{mol DIC kg}^{-1}$ ). Scenario B also models  
383 values lower than observations in the south-eastern area (Fig. 4d), but the agreement  
384 between observation and model results is reasonable. Only off the Danish coast near 6.5° E,  
385 56° N the model underestimates DIC by 93  $\mu\text{mol DIC kg}^{-1}$ .

### 386 **3.3. Hydrodynamic conditions and flushing times**

387 The calculations of Wadden Sea TA export in Thomas et al. (2009) were based on several  
388 assumptions concerning riverine input of bulk TA and nitrate, atmospheric deposition of NO<sub>x</sub>,  
389 water column inventories of nitrate and the exchange between the Southern Bight and the  
390 adjacent North Sea (Lenhart et al., 1995). The latter was computed by considering that the  
391 water in the Southern Bight is flushed with water of the adjacent open North Sea at time scales  
392 of six weeks. For the study at hand, flushing times in the validation area in summer and winter  
393 are presented for the years 2001 to 2009 in Fig. 6. Additionally, monthly mean flow patterns  
394 of the model area are presented for June, July and August for the years 2003 and 2008,  
395 respectively (Fig. 7). They were chosen to highlight the pattern in summer 2003 with one of  
396 the highest flushing times (lowest water renewal times), and that in 2008 corresponding to  
397 one of the lowest flushing times (highest water renewal times).

398 The flushing times were determined for the three areas 1 – validation area, 2 – western part  
399 of the validation area, 3 – eastern part of the validation area. They were calculated by dividing  
400 the total volume of the respective areas 1 – 3 by the total inflow into the areas  $\text{m}^3 (\text{m}^3 \text{s}^{-1})^{-1}$ .  
401 Flushing times (rounded to integer values) were consistently higher in summer than in winter,  
402 meaning that highest inflow occurred in winter. Summer flushing times in the whole validation  
403 area ranged from 54 days in 2008 to 81 days in 2003 and 2006, whereas the winter values in  
404 the same area ranged from 32 days in 2008 to 51 days in 2003 and 2009. The flushing times in  
405 the western and eastern part of the validation area were smaller due to the smaller box sizes.  
406 Due to the position, flushing times in the western part were consistently shorter than in the  
407 eastern part. These differences ranged from 5 days in winter 2002 to 14 days in summer 2006  
408 and 2008. The interannual variabilities of all areas were higher in summer than in winter.

409 The North Sea is mainly characterised by an anti-clockwise circulation pattern (Otto et al.,  
410 1990; Pätsch et al., 2017). This can be observed for the summer months in 2008 (Fig. 7). More  
411 disturbed circulation patterns in the south-eastern part of the model domain occurred in June  
412 2003: In the German Bight and in the adjacent western area two gyres with reversed rotating  
413 direction are dominant. In August 2003 the complete eastern part shows a clockwise rotation  
414 which is due to the effect of easterly winds as opposed to prevalent westerlies. In this context  
415 such a situation is called meteorological blocking situation.

### 3.4. Seasonal and interannual variability of TA and DIC concentrations

The period from 2001 to 2009 was simulated for the scenarios A and B. For both scenarios monthly mean surface concentrations of TA were calculated in the validation area and are shown in Fig. 8a and 8b. The highest TA concentration in scenario A was 2329  $\mu\text{mol TA kg}^{-1}$  and occurred in July 2003. The lowest TA concentrations in each year were about 2313 to 2318  $\mu\text{mol TA kg}^{-1}$  and occurred in February and March. Scenario B showed generally higher values: Summer concentrations were in the range of 2348 to 2362  $\mu\text{mol TA kg}^{-1}$  and the values peaked in 2003. The lowest values occurred in the years 2004 – 2008. Also, winter values were higher in scenario B than in scenario A: They range from 2322 to 2335  $\mu\text{mol TA kg}^{-1}$ .

425

Corresponding to TA, monthly mean surface DIC concentrations in the validation area are shown in Fig. 8c and 8d. In scenario A the concentrations increased from October to February and decreased from March to August (Fig. 8c). In scenario B the time interval with increasing concentrations was extended into March. Maximum values of 2152 to 2172  $\mu\text{mol DIC kg}^{-1}$  in scenario A occur in February and March of each model year, and minimum values of 2060 to 2080  $\mu\text{mol DIC kg}^{-1}$  in August. Scenario B shows generally higher values: Highest values in February and March are 2161 to 2191  $\mu\text{mol DIC kg}^{-1}$ . Lowest values in August range from 2095 to 2112  $\mu\text{mol DIC kg}^{-1}$ . The amplitude of the annual cycle is smaller in scenario B, because the Wadden Sea export shows highest values in summer (Fig. 2).

The pattern of the monthly TA and DIC concentrations of the reference scenario A differ drastically in that TA does not show a strong seasonal variability, whereas DIC does vary significantly. In case of DIC this is due to the biological drawdown during summer. On the other hand, contrariwise, the additional input (scenario B) from the Wadden Sea in summer creates a strong seasonality for TA and instead flattens the variations in DIC.

## 4. Discussion

441

Thomas et al. (2009) estimated the contribution of shallow intertidal and subtidal areas to the alkalinity budget of the SE North Sea. That estimate (by closure of mass fluxes) was about 73  $\text{Gmol TA yr}^{-1}$  originating from the Wadden Sea fringing the southern and eastern coast. These calculations were based on observations from the CANOBA dataset in 2001 and 2002.

446 The observed high TA ~~concentrations~~levels in the south-eastern North Sea were also  
447 encountered in August 2008 (Salt et al., 2013) and these measurements were used for the  
448 main model validation in this study. Our simulations result in 39 Gmol TA yr<sup>-1</sup> as export from  
449 the Wadden Sea into the North Sea. Former modelling studies of the carbonate system of the  
450 North Sea (Artioli et al., 2012; Lorkowski et al., 2012) did not consider the Wadden Sea as a  
451 source of TA and DIC, and good to reasonable agreement to observations from the CANOBA  
452 dataset was only achieved in the open North Sea in 2001 / 2002 (Thomas et al., 2009).  
453 Subsequent simulations that included TA export from aerobic and anaerobic processes in the  
454 sediment improved the agreement between data and models (Pätsch et al., 2018). When  
455 focusing on the German Bight, however, the observed high TA ~~concentrations~~levels in summer  
456 measurements east of 7° E could not be simulated satisfactorily.

457 The present study confirms the Wadden Sea as an important TA source for the German Bight  
458 and quantifies the annual Wadden Sea TA export rate to 39 Gmol TA yr<sup>-1</sup>. Additionally, the  
459 contributions by most important rivers have been more precisely quantified and narrow down  
460 uncertainties in the budgets of TA and DIC in the German Bight. All steps that were required  
461 to calculate the budget including uncertainties are discussed in the following.

462

#### 463 ***4.1. Uncertainties of Wadden Sea – German Bight exchange rates of TA and DIC***

464 The Wadden Sea is an area of effective benthic decomposition of organic material (Böttcher  
465 et al., 2004; Billerbeck et al., 2006; Al-Rai et al., 2009; van Beusekom et al., 2012) originating  
466 both from land and from the North Sea (Thomas et al., 2009). In general, anaerobic  
467 decomposition of the organic matter generates TA and increases the CO<sub>2</sub> buffer capacity of  
468 seawater. On longer time scales TA can only be generated by processes that involve  
469 permanent loss of anaerobic remineralisation products (Hu and Cai, 2011). A second  
470 precondition is the nutrient availability to produce organic matter, which in turn serves as  
471 necessary component of anaerobic decomposition (Gustafsson et al., 2019). The Wadden Sea  
472 export rates of TA and DIC modelled in the present study are based on concentration  
473 measurements during tidal cycles in the years 2002 and 2009 to 2011 (Table 1), and on  
474 calculated tidal prisms of two day-periods that are considered to be representative of annual  
475 mean values. This approach introduces uncertainties with respect to the true amplitudes of

476 concentrations differences in the tidal cycle and in seasonality due to the fact that differences  
477 in concentrations during falling and rising water levels were linearly interpolated. These  
478 interpolated values are based on four to five measurements in the three export areas and  
479 were conducted in different years. Consequently, the approach does not reproduce the exact  
480 TA and DIC concentrations|levels in the years 2001 to 2009, because only meteorological  
481 forcing, river loads and nitrogen deposition were specified for these particular years. The  
482 simulation of scenario B thus only approximates Wadden Sea export rates. More  
483 measurements distributed with higher resolution over the annual cycle would clearly improve  
484 our estimates. Nevertheless, the implementation of Wadden Sea export rates here results in  
485 improved reproduction of observed high TA concentrations|levels in the German Bight in  
486 summer in comparison to the reference run A (Fig. 3).

487 We calculated the sensitivity of our modelled annual TA export rates on uncertainties of the  
488  $\Delta$ -values of Table 1. As the different areas North- and East Frisian Wadden Sea and Jade Bay  
489 has different exchange rates of water, for each region the uncertainty of  $1 \mu\text{mol kg}^{-1}$  in  $\Delta\text{TA}$  at  
490 all times has been calculated. The East Frisian Wadden Sea export would differ by  
491  $0.84 \text{ Gmol TA yr}^{-1}$ , the Jade Bay export by  $0.09 \text{ Gmol TA yr}^{-1}$  and the North Frisian export by  
492  $3 \text{ Gmol TA yr}^{-1}$ .

493 Primary processes that contribute to the TA generation in the Wadden Sea are denitrification,  
494 sulphate reduction, or processes that are coupled to sulphate reduction and other processes  
495 (Thomas et al., 2009). In our model, the implemented benthic denitrification does not  
496 generate TA (Seitzinger & Giblin, 1996), because modelled benthic denitrification does not  
497 consume nitrate (Pätsch & Kühn, 2008). Benthic denitrification is coupled to nitrification in the  
498 upper layer of the sediment (Raaphorst et al., 1990), giving reason for neglecting TA  
499 generation by this process in the model. The modelled production of  $\text{N}_2$  by benthic  
500 denitrification falls in the range of  $20 - 25 \text{ Gmol N yr}^{-1}$  in the validation area, which would  
501 result in a TA production of about  $19 - 23 \text{ Gmol TA yr}^{-1}$  (Brenner et al., 2016). In the model  
502 nitrate uptake by phytoplankton produces about  $40 \text{ Gmol TA yr}^{-1}$ , ~~which partly.~~ Assuming  
503 large parts of organic matter exported out of the validation area this production compensates  
504 the missing TA generation by benthic denitrification. This amount of nitrate would not fully be  
505 available for primary production if parts of it would be consumed by denitrification. Different

506 from this, the TA budget of Thomas et al. (2009) included estimates for the entire benthic  
507 denitrification as a TA generating process.

508 Sulphate reduction (not modelled here) also contributes to alkalinity generation. On longer  
509 time scales the net effect is vanishing as the major part of the reduced components are  
510 immediately re-oxidised in contact with oxygen. Iron- and sulphate- reduction generates TA  
511 but only their reaction product iron sulphide (essentially pyrite) conserves the reduced  
512 components from re-oxidation. As the formation of pyrite consumes TA, the TA contribution  
513 of iron reduction in the North Sea is assumed to be small and to balance that of pyrite  
514 formation (Brenner et al., 2016).

515 Atmospheric nitrogen deposition is taken into account in the simulations. Oxidised N-species  
516 ( $\text{NO}_x$ ) dominate reduced species ( $\text{NH}_y$ ) slightly in the validation area during 6 out of 9  
517 simulation years. This implies that the deposition of dissolved inorganic nitrogen decreases TA  
518 in 6 of 9 years. The average decrease within 6 years is about  $0.4 \text{ Gmol TA yr}^{-1}$ , whereas the  
519 average increase within 3 years is only  $0.1 \text{ Gmol TA yr}^{-1}$ . Thomas et al. (2009) also assumed a  
520 dominance of oxidised species and consequently defined a negative contribution to the TA  
521 budget.

522 Dissolution of biogenic carbonates may be an efficient additional enhancement of the  $\text{CO}_2$   
523 buffer capacity (that is: source of TA), since most of the tidal flat surface sediments contain  
524 carbonate shell debris (Hild, 1997). ~~On the other hand, shallow~~Shallow oxidation of biogenic  
525 methane formed in deep ~~and/or~~ shallow tidal flat sediments (not modelled) (Höpner &  
526 Michaelis, 1994; Neira & Rackemann, 1996; Böttcher et al., 2007) has the potential both to  
527 lower or enhance the buffer capacity, thus counteracting or ~~balancing~~promoting the  
528 respective effect of carbonate dissolution. The impact of methane oxidation on the developing  
529 TA / DIC ratio in surface sediments, however, is complex and controlled by a number of  
530 superimposing biogeochemical processes (e.g., Akam et al., 2020).

531 The net effect of evaporation and precipitation in the Wadden Sea also has to be considered  
532 in budgeting TA. Although these processes are balanced in the North Sea (Schott, 1966),  
533 enhanced evaporation can occur in the Wadden Sea due to increased heating during low tide  
534 around noon. Onken & Riethmüller (2010) estimated an annual negative freshwater budget  
535 in the Hörnum Basin based on long-term hydrographic time series from observations in a tidal



536 channel. From this data a mean salinity difference between flood and ebb currents of  
537 approximately -0.02 is calculated. This would result in an ~~increased~~increase of TA  
538 ~~concentration of~~by  $1 \mu\text{mol TA kg}^{-1}$ , which is within the range of the uncertainty of  
539 measurements. Furthermore, the enhanced evaporation estimated from subtle salinity  
540 changes interferes with potential input of submarine groundwater into the tidal basins, that  
541 been identified by Moore et al. (2011), Winde et al. (2014), and Santos et al. (2015). The  
542 magnitude of this input is difficult to estimate at present, for example from salinity differences  
543 between flood and ebb tides, because the composition of SGD passing the sediment-water  
544 interfacial mixing zone has to be known. Although first characteristics have been reported  
545 (Moore et al., 2011; Winde et al., 2014; Santos et al., 2015), the quantitative effect of  
546 additional DIC, TA, and nutrient input via both fresh and recirculated SGD into the Wadden  
547 Sea remains unclear.

548 An input of potential significance are small inlets that provide fresh water as well as DIC and  
549 TA (Table 3). The current data base for seasonal dynamics of this source, however, is limited  
550 and, therefore, this source cannot yet be considered quantitatively in budgeting approaches.

551

#### 552 **4.2 TA / DIC ratios over the course of the year**

553

554

555 Ratios of TA and DIC generated in the tidal basins (Table 1) give some indication of the  
556 dominant biogeochemical mineralisation and re-oxidation processes occurring in the  
557 sediments of individual Wadden Sea sectors, although these processes have not been  
558 explicitly modelled here (Chen & Wang, 1999; Zeebe & Wolf-Gladrow, 2001; Thomas et al.  
559 2009; Sippo et al., 2016; Wurgaft et al., 2019; Akam et al., 2020). Candidate processes are  
560 numerous and the export ratios certainly express various combinations, but the most  
561 quantitatively relevant likely are aerobic degradation of organic material (resulting in a  
562 reduction of TA due to nitrification of ammonia to nitrate with a TA / DIC ratio of -0.16),  
563 denitrification (TA / DIC ratio of 0.8, see Rassmann et al., 2020), and anaerobic processes  
564 related to sulphate reduction of organoclastic material (TA / DIC ratio of 1, see Sippo et al.,  
565 2016). Other processes are aerobic (adding only DIC) and anaerobic (TA / DIC ratio of 2)  
566 oxidation of upward diffusing methane, oxidation of sedimentary sulphides upon

567 resuspension into an aerated water column (no effect on TA / DIC) followed by oxidation of  
568 iron (consuming TA), and nitrification of ammonium (consuming TA, TA / DIC ratio is -2, see  
569 Pätsch et al., 2018 and Zhai et al. 2017).

570 The TA / DIC export ratios of DIC and TA for the individual tidal basins in three Wadden Sea  
571 sectors (East Frisian, Jade Bay and North Frisian) as calculated from observed  $\Delta$ TA and  $\Delta$ DIC  
572 over tidal cycles in different seasons are depicted in Fig. 9. They may give an indication of  
573 regionally and seasonally varying processes occurring in the sediments of the three study  
574 regions. The ratios vary between 0.2 and 0.5 in the North Frisian Wadden Sea with slightly  
575 more TA than DIC generated in spring, summer and autumn, and winter having a negative  
576 ratio of -0.5. The winter ratio coincides with very small measured differences of DIC in  
577 imported and exported waters ( $\Delta$ DIC = -2  $\mu$ mol kg<sup>-1</sup>) and the negative TA / DIC ratio may thus  
578 be spurious. The range of ratios in the other seasons is consistent with sulphate reduction and  
579 denitrification as the dominant processes in the North Frisian tidal basins.

580 The TA / DIC ratios in the Jade Bay samples were consistently higher than those in the North  
581 Frisian tidal basin and vary between 1 and 2 in spring and summer, suggesting a significant  
582 contribution by organoclastic sulphate reduction and anaerobic oxidation of methane (Al-Raei  
583 et al., 2009). The negative ratio of -0.4 in autumn is difficult to explain with remineralisation  
584 or re-oxidation processes, but as with the fall ratio in Frisian tidal basin, it coincides with a  
585 small change in  $\Delta$ DIC (-3  $\mu$ mol kg<sup>-1</sup>) at positive  $\Delta$ TA (8  $\mu$ mol kg<sup>-1</sup>). Taken at face value, the  
586 resulting negative ratio of -0.4 implicates a re-oxidation of pyrite, normally at timescales of  
587 early diagenesis thermodynamically stable (Hu and Cai, 2011), possibly promoted by  
588 increasing wind forces and associated aeration and sulphide oxidation of anoxic sediment  
589 layers (Kowalski et al., 2013). The DIC export rate from Jade Bay had its minimum in autumn,  
590 consistent with a limited supply and mineralisation of organic matter, possibly modified by  
591 seasonally changing impacts from small tidal inlets (Table 3).

592 The TA / DIC ratio of the East Frisian Wadden Sea is in the approximate range of those in Jade  
593 Bay, but has one unusually high ratio in November caused by a significant increase in TA of  
594 14  $\mu$ mol kg<sup>-1</sup> at a low increase of 5  $\mu$ mol kg<sup>-1</sup> in DIC. Barring an analytical artefact, the  
595 maximum ratio of 3 may reflect a short-term effect of iron reduction.

596 Based on these results, processes in the North Frisian Wadden Sea export area differ from the  
597 East Frisian Wadden Sea and the Jade Bay areas. The DIC export rates suggest that significant

598 amounts of organic matter were degraded in North Frisian tidal basins, possibly controlled by  
599 higher daily exchanged water masses in the North Frisian ( $8.1 \text{ km}^3 \text{ d}^{-1}$ ) than in the East Frisian  
600 Wadden Sea ( $2.3 \text{ km}^3 \text{ d}^{-1}$ ) and in the Jade Bay ( $0.8 \text{ km}^3 \text{ d}^{-1}$ ) (compare Table 2). ~~On the other~~  
601 ~~hand~~ However, TA export rates of the North Frisian and the East Frisian Wadden Sea were in  
602 the same range.

603 Regional differences in organic matter mineralisation in the Wadden Sea have been discussed  
604 by van Beusekom et al. (2012) and Kowalski et al. (2013) in the context of connectivity with  
605 the open North Sea and influences of eutrophication and sedimentology. They suggested that  
606 the organic matter turnover in the entire Wadden Sea is governed by organic matter import  
607 from the North Sea, but that regionally different eutrophication effects as well as sediment  
608 compositions modulate this general pattern. The reason for regional differences may be  
609 related to the shape and size of the individual tidal basins. van Beusekom et al. (2012) found  
610 that wider tidal basins with a large distance between barrier islands and mainland, as is the  
611 case in the North Frisian Wadden Sea, generally have a lower eutrophication status than  
612 narrower basins predominating in the East Frisian Wadden Sea. Together with the high-water  
613 exchange rate the accumulation of organic matter is reduced in the North Frisian Wadden Sea  
614 and the oxygen demand per volume is lower than in the more narrow eutrophicated basins.  
615 Therefore, aerobic degradation of organic matter dominated in the North Frisian Wadden Sea,  
616 where the distance between barrier islands and mainland is large. This leads to less TA  
617 production (in relation to DIC production) than in the East Frisian Wadden Sea, where  
618 anaerobic degradation of organic matter dominated in more restricted tidal basins.

619

#### 620 **4.3. TA budgets and variability of TA inventory in the German Bight**

621 Modelled TA and DIC ~~concentrations~~ in the German Bight have a high interannual and seasonal  
622 variability (Fig. 8). The interannual variability of the model results are mainly driven by the  
623 physical prescribed environment. Overall, the TA variability is more sensitive to Wadden Sea  
624 export rates than DIC variability, because the latter is dominated by biological processes.  
625 However, the inclusion of Wadden Sea DIC export rates improved correspondence with  
626 observed DIC concentrations in the near-coastal North Sea.

627 It is a logical step to attribute the TA variability to variabilities of the different sources. In order  
628 to calculate a realistic budget, scenario B was considered. Annual and seasonal budgets of TA  
629 sources and sinks in this scenario are shown in Table 6. Note that  $Riv_{eff}$  is not taken into  
630 account for the budget calculations. This is explained in the Method Section 2.2.2 “River  
631 Input”.

632 Comparing the absolute values of all sources and sinks of the mean year results in a relative  
633 ranking of the processes. 41 % of all TA inventory changes in the validation area were due to  
634 river loads, 37 % were due to net transport, 16 % were due to Wadden Sea export rates, 6 %  
635 were due to internal processes. River input ranged from 78 to 152 Gmol TA yr<sup>-1</sup> and had the  
636 highest absolute variability of all TA sources in the validation area. This is mostly due to the  
637 high variability of annual freshwater discharge, which is indicated by low (negative) values of  
638  $Riv_{eff}$ . The latter values show that the riverine TA loads together with the freshwater flux  
639 induce a small dilution of TA in the validation area for each year. Certainly, this ranking  
640 depends mainly on the characteristics of the Elbe estuary. Due to ~~the high concentration of~~  
641 TA in rivers Rhine and Meuse (Netherlands) they had an effective river input of  
642 +24 Gmol TA yr<sup>-1</sup> in 2008, which constitutes a much greater impact on TA ~~concentration~~  
643 changes than the Elbe river. In a sensitivity test, we switched off the TA loads of rivers Rhine  
644 and Meuse for the year 2008 and found that the net flow of -71 Gmol TA yr<sup>-1</sup> decreased  
645 to -80 Gmol TA yr<sup>-1</sup>, which indicates that water entering the validation box from the western  
646 boundary is less TA-rich in the test case than in the reference run.

647 At seasonal time scales (Table 6 lower part) the net transport dominated the variations from  
648 October to March, while internal processes play a more important role from April to June  
649 (28 %). The impact of effective river input was less than 5 % in every quarter. The Wadden Sea  
650 TA export rates had an impact of 36 % on TA mass changes in the validation area from July to  
651 September. Note that these percentages are related to the sum of the absolute values of the  
652 budgeting terms.

653 Summing up the sources and sinks, Wadden Sea exchange rates, internal processes and  
654 effective river loads resulted in highest sums in 2002 and 2003 (51 and 52 Gmol TA yr<sup>-1</sup>) and  
655 lowest in 2009 (44 Gmol TA yr<sup>-1</sup>). For the consideration of TA variation we excluded net  
656 transport and actual river loads, because these fluxes are diluted and do not necessarily  
657 change the TA concentrations. In agreement with this, the highest TA ~~concentrations were~~was

658 simulated in summer 2003 (Fig. 8). The high interannual variability of summer concentrations  
659 was driven essentially by hydrodynamic differences between the years. Flushing times and  
660 their interannual variability were higher in summer than in winter (Fig. 6) of every year. High  
661 flushing times or less strong circulation do have an accumulating effect on exported TA in the  
662 validation area. To understand the reasons of the different flushing times monthly stream  
663 patterns were analysed (Fig. 7). Distinct anticlockwise stream patterns defined the  
664 hydrodynamic conditions in every winter. Summer stream patterns were in most years  
665 weaker, especially in the German Bight (compare Fig. 7, June 2003). In August 2003 the  
666 eastern part of the German Bight shows a clockwise rotation, which transports TA-enriched  
667 water from July back to the Wadden-Sea area for further enrichment. This could explain the  
668 highest concentrations in summer 2003.

669 Thomas et al. (2009) estimated that 73 Gmol TA yr<sup>-1</sup> were produced in the Wadden Sea. Their  
670 calculations were based on measurements in 2001 and 2002. The presented model was  
671 validated with data measured in August 2008 (Salt et al., 2013) at the same positions. High TA  
672 ~~concentrations~~ in the German Bight ~~were~~was observed in summer 2001 and in summer 2008.  
673 Due to the scarcity of data, the West Frisian Wadden Sea was not considered in the  
674 simulations, but, as the western area is much larger than the eastern area, the amount of  
675 exported TA from that area can be assumed to be in the same range as from the East Frisian  
676 Wadden Sea (10 to 14 Gmol TA yr<sup>-1</sup>). With additional export from the West Frisian Wadden  
677 Sea, the maximum overall Wadden Sea export may be as high as 53 Gmol TA yr<sup>-1</sup>. Thus, the TA  
678 export from the Wadden Sea calculated in this study is 20 to 34 Gmol TA yr<sup>-1</sup> lower than that  
679 assumed in the study of Thomas et al. (2009). This is mainly due to the flushing time that was  
680 assumed by Thomas et al. (2009). They considered the water masses to be flushed within six  
681 weeks (Lenhart et al., 1995). Flushing times calculated in the present study were significantly  
682 longer and more variable in summer. Since the Wadden Sea export calculated by Thomas et  
683 al. (2009) was defined as a closing term for the TA budget, underestimated summerly flushing  
684 times led to an overestimation of the exchange with the adjacent North Sea.

685 Table 4 shows that our scenario B underestimates ~~the~~ observed TA ~~concentration~~ by about  
686 5.1 µmol kg<sup>-1</sup> in 2008. Scenario A has lower TA ~~concentration~~ than scenario B in the validation  
687 area. The difference is about 11 µmol kg<sup>-1</sup>. This means that the Wadden Sea export of  
688 39 Gmol TA yr<sup>-1</sup> results in a concentration difference of 11 µmol kg<sup>-1</sup>. Assuming linearity, the

689 deviation between scenario B and the observations ( $5.1 \mu\text{mol kg}^{-1}$ ) would be compensated by  
690 an additional Wadden Sea export of about  $18 \text{ Gmol TA yr}^{-1}$ . If we assume that the deviation  
691 between observation and scenario B is entirely due to uncertainties or errors in the Wadden  
692 Sea export estimate, then the uncertainty of this export is  $18 \text{ Gmol TA yr}^{-1}$ .

693 Another problematic aspect in the TA export estimate by Thomas et al. (2009) is the fact that  
694 their TA budget merges the sources of anaerobic TA generation from sediment and from the  
695 Wadden Sea into a single source “anaerobic processes in the Wadden Sea”. Burt et al. (2014)  
696 found a sediment TA generation of  $12 \text{ mmol TA m}^{-2} \text{ d}^{-1}$  at one station in the German Bight  
697 based on Ra-measurements. This fits into the range of microbial gross sulphate reduction rates  
698 reported by Al-Raei et al. (2009) in the back-barrier tidal areas of Spiekeroog island, and by  
699 Brenner et al. (2016) at the Dutch coast. Within the latter paper, the different sources of TA  
700 from the sediment were quantified. The largest term was benthic calcite dissolution, which  
701 would be cancelled out in terms of TA generation assuming a steady-state compensation by  
702 biogenic calcite production. Extrapolating the southern North Sea TA generation (without  
703 calcite dissolution) from the data for one station of Brenner et al. (2016) results in an annual  
704 TA production of  $12.2 \text{ Gmol}$  in the German Bight (Area =  $28.415 \text{ km}^2$ ). This is likely an upper  
705 limit of sediment TA generation, as the measurements were done in summer when seasonal  
706 fluxes are maximal. This calculation reduces the annual Wadden Sea TA generation estimated  
707 by Thomas et al. (2009) from  $73$  to  $61 \text{ Gmol}$ , which is still higher than our present estimate. In  
708 spite of the unidentified additional TA-fluxes, both the estimate by Thomas et al. (2009) and  
709 our present model-based quantification confirm the importance of the Wadden-Sea export  
710 fluxes of TA on the North Sea carbonate system at present and in the future.

#### 711 ***4.4 The impact of exported TA and DIC on the North Sea and influences on export*** 712 ***magnitude***

713 Observed high TA and DIC concentrations in the SE North Sea are mainly caused by TA and DIC  
714 export from the Wadden Sea (Fig. 3-5). TA concentrations could be better reproduced than  
715 DIC concentrations in the model experiments, which was mainly due to the higher sensitivity  
716 of DIC to modelled biology. Nevertheless, from a present point of view the Wadden Sea is the  
717 main driver of TA concentrations in the German Bight. Future forecast studies of the evolution  
718 of the carbonate system in the German Bight will have to specifically focus on the Wadden  
719 Sea and on processes occurring there. In this context the Wadden Sea evolution during future

720 sea level rise is the most important factor. The balance between sediment supply from the  
721 North Sea and sea level rise is a general precondition for the persistence of the Wadden Sea  
722 (Flemming and Davis, 1994; van Koningsveld et al., 2008). An accelerating sea level rise could  
723 lead to a deficient sediment supply from the North Sea and shift the balance at first in the  
724 largest tidal basins and at last in the smallest basins. (CPSL, 2001; van Goor et al., 2003). The  
725 share of intertidal flats as potential sedimentation areas is larger in smaller tidal basins (van  
726 Beusekom et al., 2012), whereas larger basins have a larger share of subtidal areas. Thus,  
727 assuming an accelerating sea level rise, large tidal basins will turn into lagoons, while tidal flats  
728 may still exist in smaller tidal basins. This effect could decrease the overall Wadden Sea export  
729 rates of TA, because sediments would no longer be exposed to the atmosphere and the  
730 products of sulphate reduction would re-oxidise in the water column. Moreover, benthic-  
731 pelagic exchange in the former intertidal flats would be more diffusive and less advective than  
732 today due to a lowering of the hydraulic gradients during ebb tides, when parts of the  
733 sediment become unsaturated with water. This would decrease TA export into the North Sea.  
734 Caused by changes in hydrography and sea level the sedimentological composition may also  
735 change. If sediments become more sandy, aerobic degradation of organic matter is likely to  
736 become more important (de Beer et al., 2005). In fine grained silt diffusive transport plays a  
737 key role, while in the upper layer of coarse (sandy) sediments advection is the dominant  
738 process. Regionally, the North Frisian Wadden Sea will be more affected by rising sea level  
739 because there the tidal basins are larger than the tidal basins in the East Frisian Wadden Sea  
740 and even larger than the inner Jade Bay.

741 The Wadden Sea export of TA and DIC is driven by the turnover of organic material. Decreasing  
742 anthropogenic eutrophication can lead to decreasing phytoplankton biomass and production  
743 (Cadée & Hegeman, 2002; van Beusekom et al., 2009). Thus, the natural variability of the  
744 North Sea primary production becomes more important in determining the organic matter  
745 turnover in the Wadden Sea (McQuatters-Gollop et al., 2007; McQuatters-Gollop & Vermaat,  
746 2011). pH values in Dutch coastal waters decreased from 1990 to 2006 drastically. Changes in  
747 nutrient variability were identified as possible drivers (Provoost et al., 2010), which is  
748 consistent with model simulations by Borges and Gypens (2010). Moreover, despite the  
749 assumption of decreasing overall TA export rates from the Wadden Sea the impact of the  
750 North Frisian Wadden Sea on the carbonate system of the German Bight could potentially  
751 adjust to a change of tidal prisms and thus a modulation in imported organic matter. If less

752 organic matter is remineralised in the North Frisian Wadden Sea, less TA and DIC will be  
753 exported into the North Sea.

754 In the context of climate change, processes that have impact on the freshwater budget of tidal  
755 mud flats will gain in importance. Future climate change will have an impact in coastal  
756 hydrology due to changes in ground water formation rates (Faneca Sánchez et al., 2012;  
757 Sulzbacher et al., 2012), that may change both surface and subterranean run-off into the  
758 North Sea. An increasing discharge of small rivers and groundwater into the Wadden Sea is  
759 likely to increase DIC, TA, and possibly nutrient loads and may enhance the production of  
760 organic matter. Evaporation could also increase due to increased warming and become a more  
761 important process than today (Onken & Riethmüller, 2010), as will methane cycling change  
762 due to nutrient changes, sea level and temperature rise (e.g., Höpner and Michaelis, 1994;  
763 Akam et al., 2020).

764 Concluding, in the course of climate change the North Frisian Wadden Sea will be affected first  
765 by sea level rise, which will result in decreased TA and DIC export rates due to less turnover of  
766 organic matter there. This could lead to a decreased buffering capacity in the German Bight  
767 for atmospheric CO<sub>2</sub>. Overall, less organic matter will be remineralised in the Wadden Sea.

768  
769

## 770 **5 Conclusion and Outlook**

771

772 We present a budget calculation of TA sources in the German Bight and relate 16 % of the  
773 annual TA inventory changes to TA exports from the Wadden Sea. The impact of riverine bulk  
774 TA seems to be less important due to the comparatively low TA concentrationslevels in the  
775 Elbe estuary, a finding that has to be proven by future research.

776 The evolution of the carbonate system in the German Bight under future changes depends on  
777 the development of the Wadden Sea. The amount of TA and DIC that is exported from the  
778 Wadden Sea depends on the amount of organic matter and / or nutrient that are imported  
779 from the North Sea and finally remineralised in the Wadden Sea. Decreasing riverine nutrient  
780 loads led to decreasing phytoplankton biomass and production (Cadée & Hegeman, 2002; van  
781 Beusekom et al., 2009), a trend that is expected to continue in the future (European Water



782 Framework Directive). However, altered natural dynamics of nutrient cycling and productivity  
783 can override the decreasing riverine nutrient loads (van Beusekom et al., 2012), but these will  
784 not generate TA in the magnitude of denitrification of river-borne nitrate.

785 Sea level rise in the North Frisian Wadden Sea will potentially be more affected by a loss of  
786 intertidal areas than the East Frisian Wadden Sea (van Beusekom et al., 2012). This effect will  
787 likely reduce the turnover of organic material in this region of the Wadden Sea, which may  
788 decrease TA production and transfer into the southern North Sea.

789 Thomas et al. (2009) estimated that the Wadden Sea facilitates approximately 7 – 10% of the  
790 annual CO<sub>2</sub> uptake of the North Sea. This is motivation for model studies on the future role of  
791 the Wadden Sea in the CO<sub>2</sub> balance of the North Sea under regional climate change.

792 Future research will also have to address the composition and amount of submarine ground  
793 water discharge, as well as the magnitude and seasonal dynamics in discharge and  
794 composition of small water inlets at the coast, which are in this study only implicitly included  
795 and in other studies mostly ignored due to a lacking data base.

#### 796 **Data availability**

797 The river data are available at [https://wiki.cen.uni-hamburg.de/ifm/ECOHAM/DATA\\_RIVER](https://wiki.cen.uni-hamburg.de/ifm/ECOHAM/DATA_RIVER)  
798 and [www.waterbase.nl](http://www.waterbase.nl). Meteorological data are stored at <https://psl.noaa.gov/>. The North  
799 Sea TA and DIC data are stored at <https://doi.org/10.1594/PANGAEA.438791> (2001),  
800 <https://doi.org/10.1594/PANGAEA.441686> (2005). The data of the North Sea cruise 2008 have  
801 not been published, yet, but can be requested via the CODIS data portal  
802 (<http://www.nioz.nl/portals-en>; registration required). Additional Wadden Sea TA and DIC  
803 data are deposited under doi:10.1594/PANGAEA.841976.

804

#### 805 **Author contributions**

806 The scientific concept for this study was originally developed by JP and MEB. FS wrote the  
807 basic manuscript as part of his PhD thesis. VW provided field analytical data, as part of her  
808 PhD thesis. JP developed the original text further with contributions from all co-authors.

#### 809 **Competing interests**

810 The authors declare that they have no conflict of interest.

811

## 812 **Acknowledgements**

813 The authors appreciate the two constructive reviews, which greatly helped to improve the  
814 manuscript, and the editorial handling by Jack Middelburg, I. Lorkowski, W. Kühn, and F. Große  
815 are acknowledged for stimulating discussions, S. Grashorn for providing tidal prisms and P.  
816 Escher for laboratory support. This work was financially supported by BMBF during the Joint  
817 Research Project BIOACID (TP 5.1, 03F0608L and TP 3.4.1, 03F0608F), with further support  
818 from Leibniz Institute for Baltic Sea Research. We also acknowledge the support by the Cluster  
819 of Excellence 'CliSAP' (EXC177), University of Hamburg, funded by the German Science  
820 Foundation (DFG) and the support by the German Academic Exchange service (DAAD,  
821 MOPGA-GRI, #57429828) with funds of the German Federal Ministry of Education and  
822 Research (BMBF). We used NCEP Reanalysis data provided by the NOAA/OAR/ESRL PSL,  
823 Boulder, Colorado, USA, from their Web site at <https://psl.noaa.gov/>.

824

825

826 **Tables**

827 **Table 1: Mean TA and DIC concentrations [ $\mu\text{mol l}^{-1}$ ] during rising and falling water levels and**  
 828 **the respective differences ( $\Delta$ -values) that were used as wad\_sta in (1). Areas are the North**  
 829 **Frisian (N), the East Frisian (E) Wadden Sea and the Jade Bay (J).**

Area	Date	TA (rising)	TA (falling)	$\Delta$ TA	DIC (rising)	DIC (falling)	$\Delta$ DIC
N	29.04.2009	2343	2355	12	2082*	2106	24
	17.06.2009	2328	2332	4	2170	2190	20
	26.08.2009	2238	2252	14	2077	2105	28
	05.11.2009	2335	2333	-2	2205	2209	4
J	20.01.2010	2429	2443	14	2380	2392	12
	21.04.2010	2415	2448	33	2099	2132	33
	26.07.2010	2424	2485	61	2159	2187	28
	09.11.2010	2402	2399	-3	2302	2310	8
E	03.03.2010	2379	2393	14	2313	2328	15
	07.04.2010	2346	2342	-4	2068	2082	14
	17./18.05.2011	2445	2451	6	2209	2221	12
	20.08.2002	2377	2414	37	2010	2030	20
	01.11.2010	2423	2439	16	2293	2298	5

830 \*: This value was estimated.

831

832 **Table 2: Daily Wadden Sea runoff to the North Sea at different export areas.**

Position	wad_exc [ $10^6 \text{ m}^3 \text{ d}^{-1}$ ]
N1	273
N2	1225
N3	1416
N4	1128
N5	4038
N6	18
J1 - J3	251
E1	380
E2	634
E3	437
E4	857

833

834

835

836 **Table 3: Examples for the carbonate system composition of small fresh water inlets**  
 837 **draining into the Jade Bay and the backbarrier tidal area of Spiekeroog Island, given in**  
 838 **( $\mu\text{mol kg}^{-1}$ ). Autumn results (A) (October 31<sup>st</sup>, 2010) are taken from Winde et al. (2014);**  
 839 **spring sampling (S) took place on May 20<sup>th</sup>, 2011.**

Site	Position	DIC(A)	TA(A)	DIC(S)	TA(S)
Neuharlingersiel	53°41.944 N 7°42.170 E	2319	1773	1915	1878
Harlesiel	53°42.376 N 7°48.538 E	3651	3183	1939	1983
Wanger- /Horumersiel	53°41.015 N 8°1.170 E	5405	4880	6270	6602
Hooksiel	53°38.421 N 8°4.805 E	2875	3105	3035	3302
Maade	53°33.534 N 8°7.082 E	5047	4448	5960	6228
Mariensiel	53°30.895 N 8°2.873 E	6455	5904	3665	3536
Dangaster Siel	53°26.737N 8°6.577 E	1868	1246	1647	1498
Wappelersiel	53°23.414 N 8°12.437 E	1373	630	1358	1152
Schweiburger Siel	53°24.725 N 8°16.968 E	4397	3579	4656	4493
Eckenwarder Siel	53°31.249 N 8°16.527 E	6542	6050	2119	4005

840

841

842

843

844

845 **Table 4: Averages ( $\mu\text{mol kg}^{-1}$ ), standard deviations ( $\mu\text{mol kg}^{-1}$ ), RMSE ( $\mu\text{mol kg}^{-1}$ ), and**  
846 **correlation coefficients  $r$  for the observed TA concentrations and the corresponding**  
847 **scenarios A and B within the validation area.**

TA	Average	Stdv	RMSE	$r$
Obs 2008	2333.52	32.51		
Obs 2005	2332.09	21.69		
Obs 2001	2333.83	33.19		
Sim A 2008	2327.64	6.84	27.97	0.77
Sim A 2005	2322.16	5.21	22.05	0.45
Sim A 2001	2329.79	5.32	31.89	0.24
Sim B 2008	2338.60	22.09	18.34	0.86
Sim B 2005	2339.48	26.81	31.81	0.18
Sim B 2001	2342.96	17.28	30.07	0.47

848

849

850

851

852

853

854

855

856

857

858

859

860

861 **Table 5: Averages ( $\mu\text{mol kg}^{-1}$ ), standard deviations ( $\mu\text{mol kg}^{-1}$ ), RMSE ( $\mu\text{mol kg}^{-1}$ ), and**  
862 **correlation coefficients  $r$  for the observed DIC concentrations and the corresponding**  
863 **scenarios A and B within the validation area.**

864

DIC	Average	Stdv	RMSE	$r$
Obs 2008	2107.05	24.23		
Obs 2005	2098.20	33.42		
Obs 2001	2105.49	25.21		
Sim A 2008	2080.93	14.24	43.48	-0.64
Sim A 2005	2083.53	21.94	26.97	0.73
Sim A 2001	2077.53	17.61	38.89	0.22
Sim B 2008	2091.15	9.25	25.87	0.55
Sim B 2005	2101.26	10.97	33.96	0.10
Sim B 2001	2092.69	11.71	25.33	0.48

865

866

867

868

869

870

871

872

873

874

875 **Table 6: Annual TA budgets in the validation area of the years 2001 to 2009, annual**  
876 **averages and seasonal budgets of January to March, April to June, July to September and**  
877 **October to December [Gmol]. Net Flow is the annual net TA transport across the**  
878 **boundaries of the validation area. Negative values indicate a net export from the**  
879 **validation area to the adjacent North Sea.  $\Delta$ content indicates the difference of the TA**  
880 **contents between the last and the first time steps of the simulated year or quarter.**

	Wadden Sea export Gmol/yr	internal processes Gmol/yr	river loads Gmol/yr	Riv <sub>eff</sub> Gmol/yr	net flow Gmol/yr	$\Delta$ content Gmol
2001	39	13	87	-5	38	177
2002	39	19	152	-7	-223	-13
2003	39	16	91	-3	-98	48
2004	39	13	78	-5	-8	122
2005	39	12	89	-5	-98	42
2006	39	12	88	-4	-56	83
2007	39	12	110	-5	-132	29
2008	39	14	93	-5	-71	75
2009	39	10	83	-5	-151	-19
Average	Gmol/yr 39	Gmol/yr 14	Gmol/yr 101	Gmol/yr -5	Gmol/yr -89	Gmol 65
t = 3 mon	Gmol/t	Gmol/t	Gmol/t	Gmol/t	Gmol/t	Gmol
Jan - Mar	7	-1	38	-1	-49	-5
Apr - Jun	10	15	23	-2	6	54
Jul - Sep	17	-2	15	-2	13	43
Oct - Dec	4	1	25	0	-56	-26

881 **6. Figure Captions**

882

883 Figure 1: Upper panel: Map of the south-eastern North Sea and the bordering land. Lower  
884 panel: Model domains of ECOHAM (red) and FVCOM (blue), positions of rivers 1 – 16 (left,  
885 see Table 2) and the Wadden Sea export areas grid cells (right). The magenta edges identify  
886 the validation area, western and eastern part separated by the magenta dashed line.

887 Figure 2: Monthly Wadden Sea export of DIC and TA [ $\text{Gmol mon}^{-1}$ ] at the North Frisian  
888 coast (N), East Frisian coast (E) and the Jade Bay in scenario B. The export rates were  
889 calculated for DIC and TA based on measured concentrations and simulated water fluxes.

890 Figure 3: Surface TA ~~concentrations~~ [ $\mu\text{mol TA kg}^{-1}$ ] in August 2008 observed (a) and simulated  
891 with scenario A (b) and B (c). The black lines indicate the validation box.

892 Figure 4: Differences between TA surface summer observations and results from  
893 scenario A (a) and B (b) and the differences between DIC surface observations and results  
894 from scenario A (c) and B (d), all in  $\mu\text{mol kg}^{-1}$ . The black lines indicate the validation box.

895 Figure 5: Surface DIC concentrations [ $\mu\text{mol DIC kg}^{-1}$ ] in August 2008 observed (a) and  
896 simulated with scenario A (b) and B (c). The black lines indicate the validation box.

897 Figure 6: Flushing times in the validation area in summer (June to August) and winter (January  
898 to March). The whole validation area is represented in blue, green is the western part of the  
899 validation area ( $4.5^\circ \text{ E}$  to  $7^\circ \text{ E}$ ) and red is the eastern part (east of  $7^\circ \text{ E}$ ).

900 Figure 7: Monthly mean simulated streamlines for summer months 2003 and 2008.

901 Figure 8: Simulated monthly mean ~~concentrations of~~ TA (scenario A (a), scenario B (b))  
902 [ $\mu\text{mol TA kg}^{-1}$ ] and DIC (scenario A (c), scenario B (d)) [ $\mu\text{mol DIC kg}^{-1}$ ] in the validation area for  
903 the years 2001-2009.

904 Figure 9: Temporally interpolated TA/DIC ratio of the export rates in the North Frisian, East  
905 Frisian, and Jade Bay. These ratios are calculated using the  $\Delta$ -values of Table 1.

906



907 **7. References**

908

909 Akam, S.A., Coffin, R.B., Abdulla, H.A.N., and Lyons T.W.: Dissolved inorganic carbon pump in  
910 methane-charged shallow marine sediments: State of the art and new model perspectives.

911 *Frontiers in Marine Sciences* 7, 206, DOI: 10.3389/FMARS.2020.00206, 2020.

912 Al-Raei, A.M., Bosselmann, K., Böttcher, M.E., Hespeneide, B., and Tauber, F.: Seasonal  
913 dynamics of microbial sulfate reduction in temperate intertidal surface sediments: Controls  
914 by temperature and organic matter. *Ocean Dynamics* 59, 351-370, 2009.

915 Amann, T., Weiss, A., and Hartmann, J.: Inorganic Carbon Fluxes in the Inner Elbe Estuary,  
916 Germany, *Estuaries and Coasts* 38(1), 192-210, doi:10.1007/s12237-014-9785-6, 2015.

917

918 Artioli, Y., Blackford, J. C., Butenschön, M., Holt, J. T., Wakelin, S. L., Thomas, H., Borges, A.  
919 V., and Allen, J. I.: The carbonate system in the North Sea: Sensitivity and model validation,  
920 *Journal of Marine Systems*, 102-104, 1-13, doi:10.1016/j.jmarsys.2012.04.006, 2012.

921

922 Backhaus, J.O.: A three-dimensional model for the simulation of shelf sea dynamics, *Ocean*  
923 *Dynamics*, 38(4), 165–187, doi:10.1016/0278-4343(84)90044-X, 1985.

924

925 Backhaus, J.O., and Hainbucher, D.: A finite difference general circulation model for shelf  
926 seas and its application to low frequency variability on the North European Shelf, Elsevier  
927 *Oceanography Series*, 45, 221–244, doi:10.1016/S0422-9894(08)70450-1, 1987.

928

929 Ben-Yaakov, S.: pH BUFFERING OF PORE WATER OF RECENT ANOXIC MARINE SEDIMENTS,  
930 *Limnology and Oceanography*, 18, doi: 10.4319/lo.1973.18.1.0086, 1973.

931

932 Berner, R. A., Scott, M. R., and Thomlinson, C.: Carbonate alkalinity in the pore waters of  
933 anoxic marine sediments. *Limnology & Oceanography*, 15, 544–549,  
934 doi:10.4319/lo.1970.15.4.0544, 1970.

935

936 Billerbeck, M., Werner, U., Polerecky, L., Walpersdorf, E., de Beer, D., and Hüttel, M.:  
937 Surficial and deep pore water circulation governs spatial and temporal scales of nutrient

938 recycling in intertidal sand flat sediment. *Mar Ecol Prog Ser* 326, 61-76, 2006.  
939

940 Böttcher, M.E., Al-Raei, A.M., Hilker, Y., Heuer, V., Hinrichs, K.-U., and Segl, M.: Methane and  
941 organic matter as sources for excess carbon dioxide in intertidal surface sands:  
942 Biogeochemical and stable isotope evidence. *Geochimica et Cosmochim Acta* 71, A111,  
943 2007.  
944

945 Böttcher, M.E., Hespeneheide, B., Brumsack, H.-J., and Bosselmann, K.: Stable isotope  
946 biogeochemistry of the sulfur cycle in modern marine sediments: I. Seasonal dynamics in a  
947 temperate intertidal sandy surface sediment. *Isotopes Environ. Health Stud.* 40, 267-283,  
948 2004.  
949

950 Borges, A. V.: Present day carbon dioxide fluxes in the coastal ocean and possible feedbacks  
951 under global change, In *Oceans and the atmospheric carbon content* (P.M. da Silva Duarte &  
952 J.M. Santana Casiano Eds), Chapter 3, 47-77, doi:10.1007/978-90-481-9821-4, 2011.  
953

954 Borges, A. V. and Gypens, N.: Carbonate chemistry in the coastal zone responds more  
955 strongly to eutrophication than to ocean acidification. *Limn. Oceanogr.* 55(1): 346-353, 2010.  
956

957 Brasse, J., Reimer, A., Seifert, R., and Michaelis, W.: The influence of intertidal mudflats on  
958 the dissolved inorganic carbon and total alkalinity distribution in the German Bight,  
959 southeastern North Sea, *J. Sea Res.* 42, 93-103, doi: 10.1016/S1385-1101(99)00020-9, 1999.  
960

961 Brenner, H., Braeckman, U., Le Guitton, M., and Meysman, F. J. R.: The impact of  
962 sedimentary alkalinity release on the water column CO<sub>2</sub> system in the North Sea,  
963 *Biogeosciences*, 13(3), 841-863, doi:10.5194/bg-13-841-2016, 2016.  
964

965 Burt, W. J., Thomas, H., Pätsch, J., Omar, A. M., Schrum, C., Daewel, U., Brenner, H., and de  
966 Baar, H. J. W.: Radium isotopes as a tracer of sediment-water column exchange in the North  
967 Sea, *Global Biogeochemical Cycles* 28, pp 19, doi:10.1002/2014GB004825, 2014.  
968

969 Burt, W. J., Thomas, H., Hagens, M., Pätsch, J., Clargo, N. M., Salt, L. A., Winde, V., and  
970 Böttcher, M. E.: Carbon sources in the North Sea evaluated by means of radium and stable  
971 carbon isotope tracers, *Limnology and Oceanography*, 61(2), 666-683,  
972 doi:10.1002/lno.10243, 2016.

973

974 Cadée, G. C., and Hegeman, J.: Phytoplankton in the Marsdiep at the end of the 20<sup>th</sup> century;  
975 30 years monitoring biomass, primary production, and *Phaeocystis* blooms, *J. Sea Res.* 48,  
976 97-110, doi:10.1016/S1385-1101(02)00161-2, 2002.

977

978 Cai, W.-J., Hu, X., Huang, W.-J., Jiang, L.-Q., Wang, Y., Peng, T.-H., and Zhang, X.: Surface  
979 ocean alkalinity distribution in the western North Atlantic Ocean margins, *Journal of*  
980 *Geophysical Research*, 115, C08014, doi:10.1029/2009JC005482, 2010.

981

982 Carvalho, A. C. O., Marins, R. V., Dias, F. J. S., Rezende, C. E., Lefèvre, N., Cavalcante, M. S.,  
983 and Eschrique, S. A.: Air-sea CO<sub>2</sub> fluxes for the Brazilian northeast continental shelf in a  
984 climatic transition region, *Journal of Marine Systems*, 173, 70-80,  
985 doi:10.1016/j.jmarsys.2017.04.009, 2017.

986

987 Chambers, R. M., Hollibaugh, J. T., and Vink, S. M.: Sulfate reduction and sediment  
988 metabolism in Tomales Bay, California, *Biogeochemistry*, 25, 1–18, doi:10.1007/BF00000509,  
989 1994.

990

991 Chen, C.-T. A., and Wang, S.-L.: Carbon, alkalinity and nutrient budgets on the East China Sea  
992 continental shelf. *Journal of Geophysical Research*, 104, 20,675–20,686,  
993 doi:10.1029/1999JC900055, 1999.

994

995 Chen, C., Liu, H., and Beardsley, R. C.: An Unstructured Grid, Finite-Volume, Three-  
996 Dimensional, Primitive Equations Ocean Model: Application to Coastal Ocean and Estuaries, *J*  
997 *Atmos Oceanic Technol*, 20 (1), 159-186,  
998 doi:10.1175/1520-0426(2003)020<0159:AUGFVT>2.0.CO;2, 2003.

999

1000 CPSL. Final Report of the Trilateral Working Group on Coastal Protection and Sea Level Rise.

1001 Wadden Sea Ecosystem No. 13. Common Wadden Sea Secretariat, Wilhelmshaven,  
1002 Germany. 2001.  
1003  
1004 de Beer, D., Wenzhöfer, F., Ferdelman, T.G., Boehme, S., Huettel, M., van Beusekom, J.,  
1005 Böttcher, M.E., Musat, N., Dubilier, N.: Transport and mineralization rates in North Sea sandy  
1006 intertidal sediments (Sylt-Rømø Basin, Waddensea). *Limnol. Oceanogr.* 50, 113-127, 2005.  
1007  
1008 Dickson, A.G., Afghan, J.D., Anderson, G.C.: Reference materials for oceanic CO<sub>2</sub> analysis: a  
1009 method for the certification of total alkalinity. *Marine Chemistry* 80, 185-197, 2003.  
1010  
1011 Dollar, S. J., Smith, S. V., Vink, S. M., Obrebski, S., and Hollibaugh, J.T.: Annual cycle of  
1012 benthic nutrient fluxes in Tomales Bay, California, and contribution of the benthos to total  
1013 ecosystem metabolism, *Marine Ecology Progress Series*, 79, 115–125,  
1014 doi:10.3354/meps079115, 1991.  
1015  
1016 Duarte, C. M., Hendriks, I. E., Moore, T. S., Olsen, Y. S., Steckbauer, A., Ramajo, L.,  
1017 Carstensen, J., Trotter, J. A., and McCulloch, M. Is Ocean Acidification an Open-Ocean  
1018 Syndrome? Understanding Anthropogenic Impacts on Seawater pH. *Estuaries and Coasts*  
1019 36(2): 221-236. 2013.  
1020  
1021 Ehlers, J.: Geomorphologie und Hydrologie des Wattenmeeres. In: Lozan, J.L., Rachor, E., Von  
1022 Westernhagen, H., Lenz, W. (Eds.), *Warnsignale aus dem Wattenmeer*. Blackwell  
1023 Wissenschaftsverlag, Berlin, pp. 1–11. 1994.  
1024  
1025 Faneca Sánchez, M., Gunnink, J. L., van Baaren, E. S., Oude Essink, G. H. P., Siemon, B.,  
1026 Auken, E., Elderhorst, W., de Louw, P. G. B.: Modelling climate change effects on a Dutch  
1027 coastal groundwater system using airborne electromagnetic measurements. *Hydrol. Earth*  
1028 *Syst. Sci.* 16(12), 4499-4516, 2012.  
1029  
1030 Flemming, B. W., and Davis, R. A. J.: Holocene evolution, morphodynamics and  
1031 sedimentology of the Spiekeroog barrier island system (southern North Sea). *Senckenb.*

1032 Marit. 25, 117-155, 1994.

1033

1034 Große, F., Kreuz, M., Lenhart, H.-J., Pätsch, J., and Pohlmann, T.: A Novel Modeling Approach  
1035 to Quantify the Influence of Nitrogen Inputs on the Oxygen Dynamics of the North Sea,  
1036 *Frontiers in Marine Science* 4(383), pp 21, doi:10.3389/fmars.2017.00383, 2017.

1037

1038 Grashorn, S., Lettmann, K. A., Wolff, J.-O., Badewien, T. H., and Stanev, E. V.: East Frisian  
1039 Wadden Sea hydrodynamics and wave effects in an unstructured-grid model, *Ocean*  
1040 *Dynamics* 65(3), 419-434, doi:10.1007/s10236-014-0807-5, 2015.

1041

1042 Gustafsson, E., Hagens, M., Sun, X., Reed, D. C., Humborg, C., Slomp, C. P., Gustafsson, B. G.:  
1043 Sedimentary alkalinity generation and long-term alkalinity development in the Baltic Sea.  
1044 *Biogeosciences* 16(2): 437-456, 2019.

1045 HASEC: OSPAR Convention for the Protection of the Marine Environment of the North-East  
1046 Atlantic. Meeting of the Hazardous Substances and Eutrophication Committee (HASEC), Oslo  
1047 27 February – 2 March 2012.

1048

1049 Hild, A.: Geochemie der Sedimente und Schwebstoffe im Rückseitenwatt von Spiekeroog  
1050 und ihre Beeinflussung durch biologische Aktivität. *Forschungszentrum Terramare Berichte*  
1051 5, 71 pp., 1997.

1052 Höpner, T., and Michaelis, H.: Sogenannte ‚Schwarze Flecken‘ – ein Eutrophierungssymptom  
1053 des Wattenmeeres. In: L. Lozán, E. Rachor, K. Reise, H. von Westernhagen und W. Lenz.  
1054 *Warnsignale aus dem Wattenmeer*. Berlin: Blackwell, 153-159, 1997.

1055

1056 Hoppema, J. M. J.; The distribution and seasonal variation of alkalinity in the southern bight  
1057 of the North Sea and in the western Wadden Sea, *Netherlands Journal of Sea Research*, 26  
1058 (1), 11-23, doi: 10.1016/0077-7579(90)90053-J, 1990.

1059

1060 Hu, X. and Cai, W.-J.: An assessment of ocean margin anaerobic processes on oceanic  
1061 alkalinity budget. *Global Biogeochemical Cycles* 25: 1-11, 2011.

1062

1063 Johannsen, A., Dähnke, K., and Emeis, K.-C.: Isotopic composition of nitrate in five German  
1064 rivers discharging into the North Sea, *Organic Geochemistry*, 39, 1678-1689  
1065 doi:10.1016/j.orggeochem.2008.03.004, 2008.

1066

1067 Johnson, K.M., Wills, K.D., Buttler, D.B., Johnson, W.K., and Wong, C.S.: Coulometric total  
1068 carbon dioxide analysis for marine studies: maximizing the performance of an automated  
1069 gas extraction system and coulometric detector. *Marine Chemistry* 44, 167-187, 1993.

1070

1071 Kalnay, E., Kanamitsu, M., Kistler, R., Collins, W., Deaven, D., Gandin, L., Iredell, M., Saha S.,  
1072 White, G., Woollen, J., Zhu, Y., Chelliah, M., Ebisuzaki, W., Higgins, W., Janowiak, J., Mo, K.C.,  
1073 Ropelewski, C., Wang, J., Leetmaa, A., Reynolds, R., Jenne, R., and Joseph, D.: The  
1074 NCEP/NCAR 40-year reanalysis project, *Bulletin of The American Meteorological Society*,  
1075 77(3), 437–471, doi: 10.1175/1520-0477(1996)077<0437:TNYRP>2.0.CO;2, 1996.

1076

1077 Kempe, S. and Pegler, K.: Sinks and sources of CO<sub>2</sub> in coastal seas: the North Sea, *Tellus* 43 B,  
1078 224-235, doi: 10.3402/tellusb.v43i2.15268, 1991.

1079

1080 Kerimoglu, O., Große, F., Kreuz, M., Lenhart, H.-J., and van Beusekom, J. E. E.: A model-based  
1081 projection of historical state of a coastal ecosystem: Relevance of phytoplankton  
1082 stoichiometry, *Science of The Total Environment* 639, 1311-1323,  
1083 doi:10.1016/j.scitotenv.2018.05.215, 2018.

1084

1085 Kohlmeier, C., and Ebenhöf, W.: Modelling the biogeochemistry of a tidal flat ecosystem  
1086 with EcoTiM, *Ocean Dynamics*, 59(2), 393-415, doi: 10.1007/s10236-009-0188-3, 2009.

1087

1088 Kowalski, N., Dellwig, O., Beck, M., Gräwe, U., Pierau, N., Nägler, T., Badewien, T., Brumsack,  
1089 H.-J., van Beusekom, J.E., and Böttcher, M. E. Pelagic molybdenum concentration anomalies  
1090 and the impact of sediment resuspension on the molybdenum budget in two tidal systems of  
1091 the North Sea. *Geochimica et Cosmochimica Acta* 119, 198-211, 2013.

1092

1093 Kühn, W., Pätsch, J., Thomas, H., Borges, A. V., Schiettecatte, L.-S., Bozec, Y., and Prowe, A. E.

1094 F.: Nitrogen and carbon cycling in the North Sea and exchange with the North Atlantic-A  
1095 model study, Part II: Carbon budget and fluxes, *Continental Shelf Research*, 30, 1701-1716,  
1096 doi:10.1016/j.csr.2010.07.001, 2010.  
1097

1098 Laruelle, G. G., Lauerwald, R., Pfeil, B., and Regnier, P.: Regionalized global budget of the CO<sub>2</sub>  
1099 exchange at the air-water interface in continental shelf seas, *Global Biogeochemical Cycles*,  
1100 28 (11), 1199-1214, doi: 10.1002/2014gb004832, 2014.  
1101

1102 Lenhart, H.-J., Radach, G., Backhaus, J. O., and Pohlmann, T.: Simulations of the North Sea  
1103 circulation, its variability, and its implementation as hydrodynamical forcing in ERSEM, *Neth.*  
1104 *J. Sea Res.*, 33, 271–299, doi:10.1016/0077-7579(95)90050-0, 1995.  
1105

1106 Lettmann, K. A., Wolff, J.-O., and Badewien, T.H.: Modeling the impact of wind and waves on  
1107 suspended particulate matter fluxes in the East Frisian Wadden Sea (southern North Sea),  
1108 *Ocean Dynamics*, 59(2), 239-262, doi: 10.1007/s10236-009-0194-5, 2009.  
1109

1110 Lipinski, M.: Nährstoffelemente und Spurenmetalle in Wasserproben der Hunte und Jade.  
1111 Diploma thesis, C.v.O. University of Oldenburg, 82 pp., 1999.  
1112

1113 Lorkowski, I., Pätsch, J., Moll, A., and Kühn, W.: Interannual variability of carbon fluxes in the  
1114 North Sea from 1970 to 2006 – Competing effects of abiotic and biotic drivers on the gas-  
1115 exchange of CO<sub>2</sub>, *Estuarine, Coastal and Shelf Science*, 100, 38-57,  
1116 doi:10.1016/j.ecss.2011.11.037, 2012.  
1117

1118 Łukawska-Matuszewska, K. and Graca, B.: Pore water alkalinity below the permanent  
1119 halocline in the Gdańsk Deep (Baltic Sea) - Concentration variability and benthic fluxes.  
1120 *Marine Chemistry* 204: 49-61, 2017.  
1121

1122 Mayer, B., Rixen, T., and Pohlmann, T.: The Spatial and Temporal Variability of Air-Sea CO<sub>2</sub>  
1123 Fluxes and the Effect of Net Coral Reef Calcification in the Indonesian Seas: A Numerical  
1124 Sensitivity Study. *Frontiers in Marine Science* 5(116), 2018.  
1125

1126 McQuatters-Gollop, A., Raitzos, D. E., Edwards, M., Pradhan, Y., Mee, L. D., Lavender, S. J.,  
1127 and Attrill, M. J.: A long-term chlorophyll data set reveals regime shift in North Sea  
1128 phytoplankton biomass unconnected to nutrient trends, *Limnology & Oceanography*, 52,  
1129 635-648, doi:10.4319/lo.2007.52.2.0635, 2007.

1130

1131 McQuatters-Gollop, A., and Vermaat, J. E.: Covariance among North Sea ecosystem state  
1132 indicators during the past 50 years e contrasts between coastal and open waters, *Journal of*  
1133 *Sea Research*, 65, 284-292, doi:10.1016/j.seares.2010.12.004, 2011.

1134

1135 Moore, W.S., Beck, M., Riedel, T., Rutgers van der Loeff, M., Dellwig, O., Shaw, T.J.,  
1136 Schnetger, B., and Brumsack, H.-J.: Radium-based pore water fluxes of silica, alkalinity,  
1137 manganese, DOC, and uranium: A decade of studies in the German Wadden Sea, *Geochimica*  
1138 *et Cosmochimica Acta*, 75, 6535 – 6555, doi:10.1016/j.gca.2011.08.037, 2011.

1139

1140 Neal, C.: Calcite saturation in eastern UK rivers, *The Science of the Total Environment*, 282-  
1141 283, 311-326, doi:10.1016/S0048-9697(01)00921-4, 2002.

1142

1143 Neira, C., and Rackemann, M.: Black spots produced by buried macroalgae in intertidal sandy  
1144 sediments of the Wadden Sea: Effects on the meiobenthos. *J. Sea Res.*, 36, 153 - 170, 1996.

1145

1146 Onken, R., and Riethmüller, R.: Determination of the freshwater budget of tidal flats from  
1147 measurements near a tidal inlet, *Continental Shelf Research*, 30, 924-933,  
1148 doi:10.1016/j.csr.2010.02.004, 2010.

1149

1150 Otto, L., Zimmerman, J.T.F., Furnes, G.K., Mork, M., Saetre, R., and Becker, G.: Review of the  
1151 physical oceanography of the North Sea, *Netherlands Journal of Sea Research*, 26 (2-4), 161–  
1152 238, doi:10.1016/0077-7579(90)90091-T, 1990.

1153

1154 Pätsch, J., and Kühn, W.: Nitrogen and carbon cycling in the North Sea and exchange with  
1155 the North Atlantic – a model study Part I: Nitrogen budget and fluxes, *Continental Shelf*  
1156 *Research*, 28, 767–787, doi: 10.1016/j.csr.2007.12.013, 2008.

1157



1158 Pätsch, J., and Lenhart, H.-J.: Daily Loads of Nutrients, Total Alkalinity, Dissolved Inorganic  
1159 Carbon and Dissolved Organic Carbon of the European Continental Rivers for the Years  
1160 1977–2006, Berichte aus dem Zentrum für Meeres- und Klimaforschung  
1161 ([https://wiki.cen.uni-hamburg.de/ifm/ECOHAM/DATA\\_RIVER](https://wiki.cen.uni-hamburg.de/ifm/ECOHAM/DATA_RIVER)), 2008.  
1162

1163 Pätsch, J., Serna, A., Dähnke, K., Schlarbaum, T., Johannsen, A., and Emeis, K.-C.: Nitrogen  
1164 cycling in the German Bight (SE North Sea) - Clues from modelling stable nitrogen isotopes.  
1165 *Continental Shelf Research*, 30, 203-213, doi:10.1016/j.csr.2009.11.003, 2010.  
1166

1167 Pätsch, J., Kühn, W., and Six, K. D.: Interannual sedimentary effluxes of alkalinity in the  
1168 southern North Sea: model results compared with summer observations, *Biogeosciences*  
1169 15(11), 3293-3309, doi: 10.5194/bg-15-3293-2018, 2018.  
1170

1171 Pätsch, J., Burchard, H., Dieterich, C., Gräwe, U., Gröger, M., Mathis, M., Kapitza, H.,  
1172 Bersch, M., Moll, A., Pohlmann, T., Su, J., Ho-Hagemann, H.T.M., Schulz, A., Elizalde, A., and  
1173 Eden, C.: An evaluation of the North Sea circulation in global and regional models relevant  
1174 for ecosystem simulations, *Ocean Modelling*, 116, 70-95,  
1175 doi:10.1016/j.ocemod.2017.06.005, 2017.  
1176

1177 Pohlmann, T.: Predicting the thermocline in a circulation model of the North Sea – Part I:  
1178 model description, calibration and verification, *Continental Shelf Research*, 16(2), 131–146,  
1179 doi:10.1016/0278-4343(95)90885-S, 1996.  
1180

1181 Provoost, P., van Heuven, S., Soetaert, K., Laane, R. W. P. M., and Middelburg, J. J.: Seasonal  
1182 and long-term changes in pH in the Dutch coastal zone, *Biogeoscience*, 7, 3869-3878,  
1183 doi:10.5194/bg-7-3869-2010, 2010.  
1184

1185 Raaphorst, W., Kloosterhuis H. T., Cramer, A., and Bakker, K. J. M.: Nutrient early diagenesis  
1186 in the sandy sediments of the Dogger Bank area, North Sea: pore water results, *Neth. J. Sea.*  
1187 *Res.*, 26(1), 25-52, doi: 10.1016/0077-7579(90)90054-K, 1990.  
1188

1189 Radach, G. and Pätsch, J.: Variability of Continental Riverine Freshwater and Nutrient Inputs  
1190 into the North Sea for the Years 1977-2000 and Its Consequences for the Assessment of  
1191 Eutrophication, *Estuaries and Coasts* 30(1), 66-81, doi: 10.1007/BF02782968, 2007.  
1192

1193 Rassmann, J., Eitel, E. M., Lansard, B., Cathalot, C., Brandily, C., Taillefert, M., and Rabouille,  
1194 C.: Benthic alkalinity and dissolved inorganic carbon fluxes in the Rhône River prodelta  
1195 generated by decoupled aerobic and anaerobic processes. *Biogeosciences*, 17, 13-33,  
1196 doi:10.5194/bg-17-13-2020, 2020.

1197

1198 Reimer, S., Brasse, S., Doerffer, R., Dürselen, C. D., Kempe, S., Michaelis, W., and Seifert, R.:  
1199 Carbon cycling in the German Bight: An estimate of transformation processes and transport,  
1200 *Deutsche Hydr. Zeitschr.* 51, 313-329, doi: /10.1007/BF02764179, 1999.  
1201

1202 Riedel, T., Lettmann, K., Beck, M., and Brumsack, H.-J.: Tidal variations in groundwater  
1203 storage and associated discharge from an intertidal coastal aquifer. *Journal of Geophysical*  
1204 *Research* 115, 1-10, 2010.  
1205

1206 Rullkötter, J.: The back-barrier tidal flats in the southern North Sea—a multidisciplinary  
1207 approach to reveal the main driving forces shaping the system, *Ocean Dynamics*, 59(2), 157-  
1208 165, doi: 10.1007/s10236-009-0197-2, 2009.  
1209

1210 Salt, L. A., Thomas, H., Prowe, A. E. F., Borges, A. V., Bozec, Y., and de Baar, H. J. W.:  
1211 Variability of North Sea pH and CO<sub>2</sub> in response to North Atlantic Oscillation forcing, *Journal*  
1212 *of Geophysical Research*, *Biogeosciences*, 118, pp 9, doi:10.1002/2013JG002306, 2013.  
1213

1214 Santos, I. R., Eyre, B. D., and Huettel, M.: The driving forces of porewater and groundwater  
1215 flow in permeable coastal sediments: A review, *Estuarine, Coastal and Shelf Science*, 98, 1-  
1216 15, doi:10.1016/j.ecss.2011.10.024, 2012.  
1217

1218 Santos, I. R., Beck, M., Brumsack, H.-J., Maher, D.T., Dittmar, T., Waska, H., and Schnetger,  
1219 B.: Porewater exchange as a driver of carbon dynamics across a terrestrial-marine transect:

1220 Insights from coupled <sup>222</sup>Rn and pCO<sub>2</sub> observations in the German Wadden Sea, *Marine*  
1221 *Chemistry*, 171, 10-20, doi:10.1016/j.marchem.2015.02.005, 2015.  
1222

1223 Schott, F.: Der Oberflächensalzgehalt in der Nordsee, *Deutsche Hydr. Zeitschr.*, Reihe A Nr. 9,  
1224 SUPPL. A9, pp 1-29, 1966.  
1225

1226 Schwichtenberg, F.: Drivers of the carbonate system variability in the southern North Sea:  
1227 River input, anaerobic alkalinity generation in the Wadden Sea and internal processes,  
1228 (Doktorarbeit/PhS), Universität Hamburg, Hamburg, Germany, 161 pp, 2013.  
1229

1230 Seibert, S.L., Greskowiak J., Prommer H., Böttcher M.E., Waska H., and Massmann G.:  
1231 Modeling biogeochemical processes in a barrier island freshwater lens (Spiekeroog,  
1232 Germany). *J. Hydrol.*, 575, 1133-1144, 2019.  
1233

1234 Seitzinger, S., and Giblin, A.E.: Estimating denitrification in North Atlantic continental shelf  
1235 sediments, *Biogeochemistry*, 35, 235–260, doi: 10.1007/BF02179829, 1996.  
1236

1237 Shadwick, E. H., Thomas, H., Azetsu-Scott, K., Greenan, B. J. W., Head, E., and Horne, E.:  
1238 Seasonal variability of dissolved inorganic carbon and surface water pCO<sub>2</sub> in the Scotian Shelf  
1239 region of the Northwestern Atlantic, *Marine Chemistry*, 124 (1–4), 23-37,  
1240 doi:10.1016/j.marchem.2010.11.004, 2011.  
1241

1242 Sippo, J.Z., Maher, D.T., Tait, D.R., Holloway, C., Santos, I.R.: Are mangroves drivers or  
1243 buffers of coastal acidification? Insights from alkalinity and dissolved inorganic carbon export  
1244 estimates across a latitudinal transect. *Global Biogeochemical Cycles*, 30, 753-766, 2016.  
1245

1246 Smith, S. V., and Hollibaugh, J. T.: Coastal metabolism and the oceanic organic carbon  
1247 balance, *Reviews of Geophysics*, 31, 75–89, doi:10.1029/92RG02584, 1993.  
1248

1249 Streif, H.: Das ostfriesische Wattenmeer. Nordsee, Inseln, Watten und Marschen. Gebrüder  
1250 Borntraeger, Berlin, 1990.  
1251

1252 Su, J. and Pohlmann, T.: Wind and topography influence on an upwelling system at the  
1253 eastern Hainan coast. *Journal of Geophysical Research: Oceans* 114(C6), 2009.  
1254

1255 Sulzbacher, H., Wiederhold, H., Siemon, B., Grinat, M., Igel, J., Burschil, T., Günther, T.,  
1256 Hinsby, K.: Numerical modelling of climate change impacts on freshwater lenses on the  
1257 North Sea Island of Borkum using hydrological and geophysical methods." *Hydrol. Earth Syst.*  
1258 *Sci.* 16(10): 3621-3643, 2012.

1259

1260 Thomas, H., Bozec, Y., Elkalay, K., and de Baar, H. J. W.: Enhanced open ocean storage of CO<sub>2</sub>  
1261 from shelf sea pumping, *Science*, 304, 1005-1008, doi:10.1126/science.1095491, 2004.  
1262

1263 Thomas, H., Schiettecatte, L.-S., Suykens, K., Kone, Y. J. M., Shadwick, E. H., Prowe, A. E. F.,  
1264 Bozec, Y., De Baar, H. J. W., and Borges, A. V.: Enhanced ocean carbon storage from  
1265 anaerobic alkalinity generation in coastal sediments, *Biogeosciences*, 6, 267-274,  
1266 doi:10.5194/bg-6-267-2009, 2009.  
1267

1268 van Beusekom, J. E. E., Carstensen, J., Dolch, T., Grage, A., Hofmeister, R., Lenhart, H.-J.,  
1269 Kerimoglu, O., Kolbe, K., Pätsch, J., Rick, J., Rönn, L., and Ruitter, H.: Wadden Sea  
1270 Eutrophication: Long-Term Trends and Regional Differences. *Frontiers in Marine Science*  
1271 6(370), 2019  
1272

1273 van Beusekom, J. E. E., Loebel, M., and Martens, P.: Distant riverine nutrient supply and local  
1274 temperature drive the long-term phytoplankton development in a temperate coastal basin,  
1275 *J. Sea Res.* 61, 26-33, doi:10.1016/j.seares.2008.06.005, 2009.  
1276

1277 van Beusekom, J. E. E., Buschbaum, C., and Reise, K.: Wadden Sea tidal basins and the  
1278 mediating role of the North Sea in ecological processes: scaling up of management? *Ocean &*  
1279 *Coastal Management*, 68, 69-78, doi:10.1016/j.ocecoaman.2012.05.002, 2012.  
1280

1281 van Goor, M. A., Zitman, T. J., Wang, Z. B., and Stive, M. J. F.: Impact of sea-level rise on the  
1282 equilibrium state of tidal inlets, *Mar. Geol.* 202, 211-227, doi:10.1016/S0025-3227(03)00262-  
1283 7, 2003.

1284  
1285 van Koningsveld, M., Mulder, J. P. M., Stive, M. J. F., Van der Valk, L., and Van der Weck,  
1286 A.W.: Living with sea-level rise and climate change: a case study of the Netherlands, *J. Coast.*  
1287 *Res.* 24, 367-379, doi:10.2112/07A-0010.1, 2008.  
1288  
1289 Wang, Z. A., and Cai, W.-J.: Carbon dioxide degassing and inorganic carbon export from a  
1290 marsh-dominated estuary (the Duplin River): A marsh CO<sub>2</sub> pump, *Limnology &*  
1291 *Oceanography*, 49, 341–354, doi:10.4319/lo.2004.49.2.0341, 2004.  
1292  
1293 Winde, V.: Zum Einfluss von benthischen und pelagischen Prozessen auf das Karbonatsystem  
1294 des Wattenmeeres der Nordsee. Dr.rer.nat. thesis, EMA University of Greifswald, 2012.  
1295  
1296 Winde, V., Böttcher, M. E., Escher, P., Böning, P., Beck, M., Liebezeit, G., and Schneider, B.:  
1297 Tidal and spatial variations of  $\delta^{13}\text{C}$  and aquatic chemistry in a temperate tidal basin during  
1298 winter time, *Journal of Marine Systems*, 129, 396-404, doi:10.1016/j.jmarsys.2013.08.005,  
1299 2014.  
1300  
1301 Wolf-Gladrow, D. A., Zeebe, R. E., Klaas, C., Kortzinger, A., and Dickson, A. G.: Total alkalinity:  
1302 The explicit conservative expression and its application to biogeochemical processes, *Marine*  
1303 *Chemistry*, 106, 287–300, doi:10.1016/j.marchem.2007.01.006, 2007.  
1304  
1305 Wurgaft E., Findlay A.J., Vigderovich H., Herut B., and Sivan O.: Sulfate reduction rates in the  
1306 sediments of the Mediterranean continental shelf inferred from combined dissolved  
1307 inorganic carbon and total alkalinity profiles. *Marine Chemistry*, 211,64-74, 2019.  
1308  
1309 Zhai, W.-D., Yan, X.-L., and Qi, D.: Biogeochemical generation of dissolved inorganic carbon  
1310 and nitrogen in the North Branch of inner Changjiang Estuary in a dry season. *Estuarine,*  
1311 *Coastal and Shelf Science* 197: 136-149, 2017.  
1312  
1313 Zeebe, R.E., and Wolf-Gladrow, D. 2001. CO<sub>2</sub> in seawater: Equilibrium, Kinetics, Isotopes.  
1314 Elsevier Science Ltd., 2001.

1315

1316

1317

1318

1319

1320

1321

1322

1323

1324

1325

1326 **8. Appendix**

1327

1328 **Table A1: Annual riverine freshwater discharge [km<sup>3</sup> yr<sup>-1</sup>]. The numbering refers to Fig. 1.**

	2001	2002	2003	2004	2005	2006	2007	2008	2009
1) Elbe	23.05	43.38	23.95	19.56	25.56	26.98	26.61	24.62	24.28
2) Ems	3.47	4.48	3.15	3.52	2.99	2.54	4.32	3.32	2.58
3) Noordzeekanaal	3.21	2.98	2.49	3.05	3.03	2.96	1.55	3.05	2.46
4) IJsselmeer (east)	9.55	9.94	6.27	7.97	7.35	7.30	9.10	8.23	6.59
5) IJsselmeer (west)	9.55	9.94	6.27	7.97	7.35	7.30	9.10	8.23	6.59
6) Nieuwe Waterweg	50.37	51.33	34.72	42.91	41.61	44.21	49.59	49.76	44.69
7) Haringvliet	33.10	35.18	17.92	10.77	12.36	16.02	24.00	15.70	11.06
8) Scheldt	7.28	2.74	4.31	3.64	3.59	3.74	4.63	4.57	3.63
9) Weser	11.43	18.97	11.80	10.52	10.37	9.72	16.21	12.59	9.58
10) Firth of Forth	2.72	3.76	2.06	3.01	3.00	2.84	2.85	3.59	3.66
11) Tyne	1.81	2.25	1.18	2.04	1.92	1.78	2.09	2.70	2.05
12) Tees	1.33	1.78	0.94	1.59	1.27	1.45	1.49	1.99	1.55
13) Humber	10.76	12.10	7.16	10.51	7.68	11.11	12.03	13.87	9.60
14) Wash	5.46	4.39	3.08	3.91	1.96	2.72	5.24	4.77	3.21
15) Thames	4.47	3.23	2.41	2.13	0.96	1.57	3.52	3.20	2.38
16) Eider	0.67	0.97	0.47	0.70	0.68	0.67	0.63	0.58	0.57
Sum	178.2	207.4	128.1	133.7	131.6	142.9	172.9	160.7	134.4

1329

1330

1331

1332

1333

1334

1335

1336

1337

1338 **Table A2: River numbers in Fig. 1, their positions and source of data**

Number in Fig. 1	Name	River mouth position	Data source
1	Elbe	53°53'20"N 08°55'00"E	Pätsch & Lenhart (2008); TA-, DIC- and nitrate- concentrations by Amann (2015)
2	Ems	53°29'20"N 06°55'00"E	Pätsch & Lenhart (2008)
3	Noordzeekanaal	52°17'20"N 04°15'00"E	Pätsch & Lenhart (2008); TA-, DIC- and nitrate-

			concentrations from waterbase.nl
4	Ijsselmeer (east)	53°17'20"N 05°15'00"E	As above
5	Ijsselmeer (west)	53°05'20"N 04°55'00"E	As above
6	Nieuwe Waterweg	52°05'20"N 03°55'00"E	As above
7	Haringvliet	51°53'20"N 03°55'00"E	As above
8	Scheldt	51°29'20"N 03°15'00"E	As above
9	Weser	53°53'20"N 08°15'00"E	Pätsch & Lenhart (2008)
10	Firth of Forth	56°05'20"N 02°45'00"W	HASEC (2012)
11	Tyne	55°05'20"N 01°25'00"W	HASEC (2012)
12	Tees	54°41'20"N 01°05'00"W	HASEC (2012)
13	Humber	53°41'20"N 00°25'00"W	HASEC (2012)
14	Wash	52°53'20"N 00°15'00"E	HASEC (2012): sum of 4 rivers: Nene, Ouse, Welland and Witham
15	Thames	51°29'20"N 00°55'00"E	HASEC (2012)
16	Eider	54°05'20"N 08°55'00"E	Johannsen et al, 2008

1339

1340 **Table A3: Monthly values of TA, DIC and NO<sub>3</sub> concentrations [ $\mu\text{mol kg}^{-1}$ ] of rivers, the annual**  
1341 **mean and the standard deviation**

River parameter	Jan	Feb	Mar	Apr	May	Jun	Jul	Aug	Sep	Oct	Nov	Dec	Mean	SD
Elbe TA	2380	2272	2293	2083	2017	1967	1916	1768	1988	2156	2342	2488	2139	218
Noordzeekanaal TA	3762	3550	3524	3441	4748	3278	3419	3183	3027	3299	3210	3413	3488	441
Nieuwe Waterweg TA	2778	2708	2765	3006	2883	2658	2876	2695	2834	2761	2834	2927	2810	102
Haringvliet TA	2588	2635	2532	3666	2826	2829	2659	2660	2496	2816	2758	2585	2754	309
Scheldt TA	3781	3863	3708	3725	3758	3626	3722	3514	3367	3666	3825	3801	3696	140
Ijsselmeer TA	2829	3005	2472	2259	2611	1864	1672	1419	1445	2172	2286	2551	2215	521
Elbe DIC	2415	2319	2362	2179	2093	2025	1956	1853	2018	2200	2428	2512	2197	211
Noordzeekanaal DIC	3748	3579	3470	3334	3901	3252	3331	3136	2977	3214	3183	3405	3378	264
Nieuwe Waterweg DIC	2861	2794	2823	2991	2879	2657	2886	2706	2828	2773	2907	3036	2845	108
Haringvliet DIC	2673	2735	2600	3661	2850	2846	2687	2681	2512	2859	2803	2670	2798	292
Scheldt DIC	3798	3909	3829	3737	3704	3592	3705	3490	3316	3648	3733	3868	3694	167
Ijsselmeer DIC	2824	3008	2458	2234	2576	1826	1636	1369	1399	2134	2285	2565	2193	538
Elbe NO <sub>3</sub>	247	330	277	225	193	161	129	103	112	157	267	164	197	72
Noordzeekanaal NO <sub>3</sub>	150	168	190	118	79	71	64	73	78	92	107	137	111	42
Nieuwe Waterweg NO <sub>3</sub>	232	243	231	195	150	140	132	135	113	145	201	220	178	47
Haringvliet NO <sub>3</sub>	233	252	218	200	143	144	133	117	128	127	143	228	172	50
Scheldt NO <sub>3</sub>	320	341	347	345	243	221	219	215	189	202	190	274	259	63
Ijsselmeer NO <sub>3</sub>	136	159	190	192	135	46	20	14	7	18	20	79	85	73

1342